TESI DOCTORAL

Identification of microcrystalline phases in Lead Glazes of ceramics from 17th-19th centuries: archaeometric implications

Dra. Roberta Di Febo

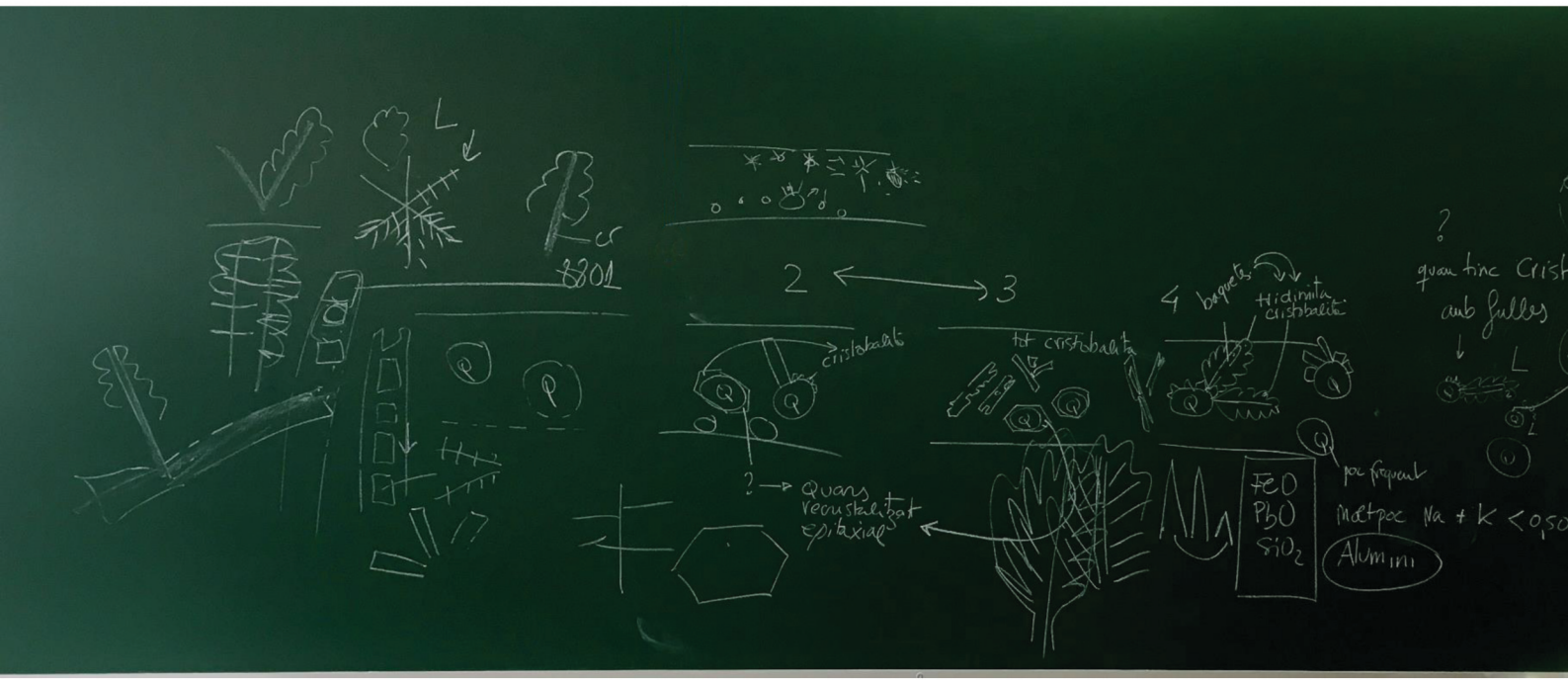

Thesis Directors: **Dra. Judit Molera** and **Dra.Trinitat Pradell**

PhD in Experimental Sciences and Technology

Universitat de Vic - Universitat Central de Catalunya

Vic, September 2019

UNIVERSITAT DE VIC
UNIVERSITAT CENTRAL DE CATALUNYA
Escola de Doctorat

TESI DOCTORAL

Identification of microcrystalline phases in Lead Glazes of ceramics from 17th-19th centuries: archaeometric implications

Dra. Roberta Di Febo

Thesis Directors: Dra. Judit Molera i Dra.Trinitat Pradell

PhD in Experimental Sciences and Technology

Universitat de Vic - Universitat Central de Catalunya

2019

UNIVERSITAT DE VIC
UNIVERSITAT CENTRAL DE CATALUNYA
Escola de Doctorat

Acknowledgments

Per la realizzazione di questa tesi si ringraziano:

Le Relatrici Dra. Judit Molera e Dra. Trinitat Pradell per aver accettato la direzione di questa tesi, per le proficue e pazienti correzioni, osservazioni e suggerimenti.

I Gruppi di Ricerca GCM (Universitat Politècnica de Catalunya) e MECAMAT (Universitat de Vic) per aver contribuito al finanziamento del presente dottorato di ricerca.

L'Universitat de Vic per la concessione di una borsa predottorale (Ajut Predoctoral Uvic, 2015-2016).

Il Dott. Claudio Capelli per la sua ospitalità presso il DISTAV di Genova e per la donazione di alcuni campioni ceramici che sono stati oggetto di studio della presente tesi.

Il Prof. Joan Carles Melgarejo i Draper per i suoi commenti e revisioni degli articoli presentati in questa tesi.

Abstract

Crystalline phases inside ancient glazes can have different origins: unreacted compounds (thus already formed before the glaze formation), crystallites developed during the glaze production or devitrification crystals formed after the glaze production (during burial by weathering processes). This study deals with the identification of the crystalline phases developed during the firing of lead glazes in ceramics from the 17th to 19th centuries. The formation of the crystallites during firing and their distribution depends on the original composition of the glaze and body (clay, stonepastes, etc.), the use of raw or pre-fired materials and on the firing conditions (temperature and atmosphere of the furnace, single or double firing, etc.). Therefore, the detailed investigation of the crystal inclusions and the microstructural heterogeneities in the glazes yield information on the nature of the objects, the raw materials used, their thermal history as well as other important aspects of the glass making technology.

This research develops a methodological approach to study of ceramic glaze microstructures based on the thin section. Starting from its present role as an accessory identification technique, thin-section petrography turns here into a pivotal tool to characterize micro-crystals embedded in ceramic glazes and hence characterize the glazes themselves. Firstly, the crystallites are located and described using thin-section petrographic methods. Special attention is paid to the description of the morphologies and the optical features of the crystallites. Then, the thin section petrography data are linked to compositional and structural data obtained from other analytical tools, such as SEM (scanning electron microscopy), EPMA (electron probe micro-analyser), µ-Raman (micro-Raman) and SR-µXRD (synchrotron-radiation X-ray micro-diffraction). For each mineral phase identified, chemical, mineralogical and structural data are collected in such a way to obtain a correlation between morphological and analytical data. Once established, this correlation could allow a quick and easy identification of the crystallites using a petrographic microscope and therefore avoiding the repetition of an exhaustive identification protocol involving the use of expensive characterization techniques.

Contents

1. Introduction 1
1.1 Crystalline phases related with decoration of glazes 2
1.2 Experimental techniques to identify crystals in glazes 8
2. Objectives 12
3. Cases of study 14
3.1 Misfired lead glazes 14
3.2 Lead glazes and iron brown decorations 17
3.3 Lead glazes and manganese brown decorations 20
4. Methodology 22
4.1 Sample preparation 22
4.1.2 Optical microscopy: transmitted light (TL) and reflected (RL) modes 22
4.1.3 Choice of analytical techniques that can best implement the studies on ceramic glazes by thin section 23
4.2 SEM 23
4.3 FIB 23
4.4 EPMA 24
4.5 µ-XRD ALBA BL04 24
4.6 µ-Raman 24
5. Results 25
5.1 *The production of a lead glaze with galena: Thermal transformations in the PbS–SiO_2 systems* 25
5.1.2 Introduction 25
5.1.3 Results 25
5.2 *Technological implications of neo-formed hematite crystals in ceramic lead glazes* 27
5.2.1 Introduction 27
5.2.2 Results 27
5.3 *Thin-section petrography and SR-µXRD for the identification of micro-crystallites in the brown decorations of ceramic lead glazes* 29
5.3.1 Introduction 29
5.3.2.Results 29
6. Discussion 31
7. Conclusions 36

8. References 37
Annex 1 50
Glossary of terms 50
Annex 2. 53
Petrography features of crystalline phases identified in this Thesis 53
Annex 3 68
Other related articles published by R. Di Febo 68

1 Introduction

Crystalline phases inside ancient glazes can have different origins: unreacted compounds, crystallization processes during the firing cycle or degradation phenomena such as devitrification during burial (Pradell et al., 2010). The unreacted compounds and crystals formed into glazes modify their colour, shine, and opacity, besides being the most important relicts of the technology used to produce them. Their presence depends on the original composition of the glaze, composition of the body (clay, stonepastes, etc.), use of raw or pre-fired materials and firing conditions (temperature and atmosphere of the furnace, single or double firing, etc.). Furthermore, crystallites can grow inside glazes due to partial or total insolubility of some colorants and opacifiers such as those formed at the interaction zone between the melt and the ceramic surface (Molera et al., 1993; Tite et al., 1998; Molera et al., 2004; Molera et al., 2013; Pradell et al., 2013).

Detailed investigation of the crystalline phases and the microstructural heterogeneities in glazes yield information on the nature of the objects and the raw materials used to manufacture them, on their thermal history and on several other important aspects of the glaze making technology. Therefore, the micro-crystallites are excellent ceramic markers of technology and/or provenance. They can be associated to a specific ceramic workshop, to the method of application of the pigment (underglaze or overglaze), composition (pre-fritted or raw initial pigment mixture) and firing process. From the materials science point of view, both the starting materials and the applied process play important roles and much information about technology remains imprinted in the glaze microstructure. For this reason, the study of the technological processes is crucial to understand behavioural attributes related to particular social groups that perform handicraft. The interpretation of the manufacturing technology can be used to address a range of very different archaeological questions. These include the knowledge and technical skills of artisans and their awareness of the physical behaviour of raw materials, transmission of technology across space and time, standardization and specialization, craft tradition up to the style and expression of the identity trough ceramic practice (Quinn, 2009).

Several authors identified and described crystals formed in the glaze-body interface (Molera et al., 1993; Molera et al., 1996; Tite et al., 1998; Molera et al., 2001) and their presence has been related to a specific kind of glaze and/or ceramic body used. In particular, Molera et al. (1993) described the formation of lead feldspars at the interface between high lead glazes and iron rich clays. Molera (1996) has shown that, due to the greater surface area and to reactivity of unfired clay, the concentration of lead feldspar crystals formed at the glaze/body interface tends to be greater when the glazing mixture is applied to a raw clay body than to a biscuit-fired body (Tite et al., 1998; Molera,

et al. 2001). However, since the concentration of formed crystals depends on many other factors - in particular the glaze thickness -, it is not possible to use only this criterion for distinguishing between application to a raw clay or to a biscuit-fired body (Molera, personal communication). Among the series of feldspar, anorthite needles are another kind of crystals that can give bonding between glaze and body. In this case, the presence of anorthite between glaze and body is probably related to high temperatures with a long firing and /or slow cooling time (Jiazhi, 1984; Vandiver and Kingery, 1986; Yang et al., 2009; Reedy 2016). The presence of precipitates of anorthite in ceramic glazes, sometimes in association with wollastonite ($CaSiO_3$), is thought to be responsible for the jade-like translucency macroscopically observed. Precipitates of $CaSiO_3$ together with diopside crystals were found at the ceramic interface in both pre and earlier Islamic glazes -alkali-lime type -, (Mason and Tite, 1997).

1.1 Crystalline phases related with decoration of glazes

Neo-formed crystalline phases related with glaze decorations have been studied by different authors. In **yellow decorations**, lead stannate and lead antimoniate have been used in different sites and epochs. For instance, lead-antimonate ($Pb_2Sb_2O_7$), the well-known *Giallo di Napoli*- was frequently used in the manufacturing of Italian renaissance ceramics, as reported by Piccolpasso (Kingery and Aronson, 1990; Dik et al., 2005; Sandalinas et al., 2006; Lightbown and Caiger-Smith, 2007; Tite, 2009; Carratoni and Di Santo, 2015). This artificial pigment has been manufactured in various periods as early as the Eighteenth Dynasty in Egypt and it was the only yellow colorant and opacifier used in ancient Egyptian and Mesopotamian glasses and glazes (Molina et al., 2014). One of the original recipes from the "Calabranci Codice" mentioned the use of "ghetta" (probably PbO or PbO_2) and "antimonio" (probably Sb_2O_3) for its preparation (Wainwright and Harley, 1986; Ashok, 1997; Dik et al., 2005). Components such as "ferraccia" or "ferrugine" (iron oxides or hidroxides) were added to the yellow pigment in order to produce the colour called *Zallo* (Lightbown and Caiger-Smith, 2007). In the Renaissance yellow decorations of Deruta and Gubbio pottery, lustre was used overlapped to yellow decorations (Borgia et al., 2002). In such case, that has been found was very informative: the large antimonite crystals hindered lustre formation, avoiding the initial penetration of silver and copper ions into the glaze. In addition, yellow lead-antimonate even inhibited the crystallization of tin dioxide, which is normally present in the glaze as opacifier in the volume surrounding the pigmented region. The Naples Yellow pigment was also detected both in the majolica altar of St Mary of the Angels (Assisi, Italy) made by Andrea della Robbia and in the analogous synthesized pigments products (Sakellariou et al., 2004). In this specific case, meaningful results have been obtained when the samples were in the form of mineralogical thin sections. In fact, the optical

observation of thin section revealed the presence in the yellow region of regular hexagonal crystals. The comparison with the analogous final products from the synthesized pigments suggested that the firing temperature for similar morphologies was about 1100 °C and the firing time did not seem to be important for the final forms of the crystalline pigment. Analogous yellow hexagonal crystals have been found in 17th century Portuguese azulejos by Coentro et al. (2012).

In respect to the **blue decorations**, when a arsenic-rich *zaffre* is used, calcium-lead arsenate particles can form during firing by the reaction among the arsenic, calcium and lead from the glaze (Borgia et al., 2002; Viti et al., 2003; Zucchiatti et al., 2006; Pérez-Arantegui et al., 2009; Tite, 2009; Pradell et al., 2013). According to historical sources, zaffre, which is an impure cobalt oxide prepared by roasting cobalt minerals such as cobaltite (CoAsS), skutterudite (CoAs3) and erythrite ($Co_3(AsO_4)_2$ $8H_2O$), was invented in the Erzgebirge region of Saxony in about 1520 AD by Peter Weidenhammer. Studying cobalt blue glazes from the Della Robbia and Buglioni workshops, Zucchiatti et al., (2006) found that the differences in chemical composition of the cobalt blue glazes are due to the different treatment of the cobalt ore. Particularly, before 1520 AD, the cobalt pigment was obtained as a by-product of silver smelting during which the volatile arsenic was lost. In contrast, after 1520 AD, cobalt minerals were excavated from rich veins and not collected together with ores for silver production. These cobalt-rich minerals were then roasted in reverberatory furnaces allowing a partial recuperation of the arsenic during the cooling process. Beside calcium-lead arsenates, some authors also detected the presence of Co-olivines into glaze blue layers (Padeletti et al., 2006; Waal, 2009; Coentro et al., 2012; Carratoni and Di Santo, 2015). The presence of Co-olivines might be ascribed to a supersaturation phenomenon that leads to the precipitation of this crystalline phase (Colomban et al., 2004; Colomban, 2013). However, according to Vieira, who analysed ceramic sherds of Portuguese production dated back to early 16th and 17th centuries, this phenomenon occurs when the temperature of the kiln is high enough to allow the formation of the cobalt silicate (Vieira et al., 2013a, b). In support of this theory, it has been stated by Pishch and Rotman (1989) that orthorhombic structure of cobalt olivine starts to form in the range of about 1000 – 1100 °C. Dendritic cobalt and nickel olivines (α-Co_2SiO_4, α-Ni_2SiO_4) were detected in dark blue decorations of Portuguese azulejos by Coentro et al. (2012). Cobalt olivines were used as ceramic pigments and studies show that Co^{2+} ions dissolve and diffuse in the glaze matrix, giving a dark-indigo colour (Llusar et al., 2001; Padeletti et al., 2006; Waal 2009). On the contrary, nickel olivines are not mentioned as traditional ceramic pigments, but as modern synthetic inorganic pigments and designated as nickel green olivines (Herbst and Hunger, 2004). A probable cause of the presence of nickel olivines might be the metallurgical procedure used to refine the blue pigment. In fact, the use of a cobalt source with nickel excess, may boost the formation of a nickel olivine along with the cobalt olivine.

In **green decorations** and monochrome green glazes is not common to found crystals associated to the copper pigment. The colouring agent usually employed for this kind of tonality is based on copper compounds, which tend to be completely dissolved into the glaze. However, the colour associated with copper oxide depends on the composition of the glaze. In soda-lime glazes, the colour observed is normally a turquoise blue (Tite and Shortland, 2008) whereas, in high lead glazes, such as those used in Roman lead glazed pottery, the colour is green (Weyl, 1976; Greene, 2007). Similarly, in lead-alkali glazes, the colour is again green but with a slight bluish tint. Piccolpasso describes both a ‘‘burnt copper’’ and a ‘‘mixed green’’ (Lightbown and Caiger-Smith, 2007). The former also called *ramina*, was made from oxidized copper metal which, after milling, was used directly without further additions. In contrast, the ‘‘mixed green’’ which consisted of a prefired mixture of copper oxide with lead oxide and antimony oxide, was green without any bluish tint. Copper in combination with lead antimonite particles has been observed in Italian majolica (Padeletti et al., 2006; Tite, 2009) and in the Della Robbia's workshop (Sendova et al., 2007).

In **red and lustre decorations** nano-crystals of copper and silver have been determined by several authors (Kingery and Vandiver, 1986; Spitzer-Aronson, 1986, Pérez-Arantegui et al 2001, Molera et al., 2001, Padeletti and Fermo, 2003; Pradell et al., 2006; Roqué et al., 2006; Pradell et al., 2008; Gutiérrez et al., 2010; Padeletti et al., 2010). Lustre consists of a thin metallic film containing silver, copper and other substances like iron oxide and cinnabar applied in a reducing atmosphere on a previously glazed ceramic. In this way, beautiful iridescent reflections of different colours are obtained. These decorations are produced by ionic exchange between the alkalis of the glass and the copper and silver of the lustre paint (Pradell et al., 2007). The optical properties, in particular colour and metal-like shine shown by lustre, are linked to the density of nanoparticles present in the layer, although the size and nature also affect them. In particular, metal-like reflectivity is achieved for lead-containing glazes, while for alkaline glazes red decorations are achieved without the lustre shine (Molera et al, 2007, Pradell et al. 2007). The lustre technique was introduced to the Mediterranean basin from Islamic potters, in order to deceive the religious prohibition of using gold and silver vessels at the table. The technique was first made in Iraq in the 9th century (Caiger-Smith, 1985), then spread to Egypt, Persia and Spain, following the expansion of Arabian culture during the medieval times (Caiger-Smith, 1985). The first examples of lustre that was made in Spain were found in Murcia and date back to the 12th century AD (Navarro, 1986). Later, during the 14th and 15th centuries, luster pottery was produced largely in Manises, Paterna, and other centers (Amigues and Mesquida, 1993). From Spain, lustre was introduced to the Italian peninsula, where it was used mostly in central Italy to decorate majolicas. Important centres for this activity, were Gubbio and Deruta, located in Umbria (Mattei and Cecchetti, 1995; Fiocco and Gherardi, 1998). Concerning the Italian production, it has to

be pointed out that the artisans developed their own style for the decorative motifs, as well as for the metallic colours obtained. Recent works demonstrated that a peculiar characteristic of the Italian lustre decorations is the presence of cosalite ($Pb_2Bi_2S_5$), a compound containing bismuth combined with lead and sulphur (Padeletti and Fermo, 2003). Since cosalite is not observed in the Hispano-Moresque lustre decorations, it might be considered as a discriminating element in order to differentiate the Italian lustre productions from the Hispano-Moresque ones (Padeletti and Fermo, 2003). Several recipes were used to obtain different lustre colours that ranged from goldlike to copperlike. Under different firing conditions, the same recipe gave different colours. In particular, tin opacified lead-alkali glazes were preferred in order to obtain a good quality lustre decoration (Tite el al., 1998). EDX analyses found that ruby-red lustres show Cu/Ag ratios > 1, whereas the gold ones, are characterised by Cu/Ag < 1 (Pérez-Arantegui, et al, 2001). On the other hand, Molera et al. (2001) found that gold-brown lustre decorations show a higher Ag content compared with red ones. However, because of the difficulties to produce the lustre decoration, this technique was only used for valuable objects and it soon becomes an exhibition of the personal skilfulness of the master.

Regarding the **brown and black decorations** that have been studied in two articles of the present research work, different iron, manganese or chromium compounds were employed to obtain them. As far as Fe compounds are concerned, hematite has been detected in brown decorations of majolica from Mission San Luis (Florida, US). In these decorations, the use of high amounts of iron oxide (35 to 40 wt% of Fe_2O_3) led to the growth of large hematite crystallites responsible of the metallic black colour macroscopically observed (Iñañez et al., 2013). In general, iron oxides are the most sensitive to temperature and the red is a particularly difficult colour to achieve for decorations. If the red hematite is in contact with an alkaline glass matrix turns into a dark brown because the surface iron ions change their chemical coordination environment from 6-fold to 4-fold (Vogel, 1985). The methods used to achieve red decorations on faience shards (18^{th} and 19^{th} centuries) from different French manufactories have been investigated by De Lucas et al. (2006). The results showed as only in one case the red colour was obtained thanks to a particular reddish sandstone containing α-quartz grains and goethite that produced red hematite during the firing process. In other cases, manufactures used the Naples yellow together with hematite in order to obtain a suitable red colour. Hematite used alone or in combination with other components has been detected on enamelled glass objects of the second half of the 19^{th} century (Caggiani et al., 2014). In such instance, the Raman study allowed to understand the enamelling technology of fine art objects providing guidelines to discriminate between different genuine productions and/or copies. The Raman signature of hematite was found in all the red enamels, both of medieval and of modern objects. On the opposite, the orange colour was obtained by adding some hematite to an arsenate-based white enamel, while the brown enamel was attributable

to the presence of hematite and magnetite with traces of carbon likely added to control the Fe^{2+}/Fe^{3+} ratio. Besides the pigments, hematite is one of the principal components found in ceramic glazes such as the aventurine glazes and so called hematite crystalline glazes (Orlova, 1999). The latter, were already known in the early 12th century and particularly suitable to coat porcelain and faience. The typical chemical composition of the hematite glazes consists of SiO_2 (60-70 wt%), Al_2O_3 (12-20 wt%), Fe_2O_3 (5-8 wt%), CaO (5-10 wt%), K_2O+ Na_2O (< 5 wt%), MgO (< 3 wt%) and slight quantities of TiO_2 and P_2O_5. The structure of such glazes has been investigated by using electron microscope and electron microprobe by Chen et al. (1984). According to the mentioned study, the glass structure is formed as a result of the double phase separation of the glaze glass. In the primary phase separation, small drops enriched with iron are formed which later enlarge or aggregate to become a continuous phase. After the secondary phase separation in an oxidizing medium, hematite crystals emerge whose agglomerates form a red or a brown pattern, and the iron-deficient phase is formed. Sizes and quantities of the hematite crystals depend on the glass composition and firing conditions. Moreover, due to the high content of Al_2O_3 and CaO that these glazes can be contain, anorthite crystals could also be expected in hematite glazes.

Hematite in association with melanotekite has been found in grisailles, which are brown blackish paints used to draw on stained glass windows (Pradell et al., 2015). The presence of melanotekite in such lead aluminosilicate glasses shows as this lead–iron silicate may crystallise in a large range of compositions (8.8 - 45.1 wt% Fe_2O_3).

In respect to the Mn compounds, braunite and kentrolite have been widely identified in medieval glazed potteries (Molera, et al 2013; Pradell et al., 2013). Braunite ($Mn^{2+}Mn^{3+}{}_6SiO_{12}$) along with hausmannite ($Mn^{2+}Mn^{3+}{}_2O_4$) were detected in Hispano Moresque tiles (15th – 16th century) by Coentro et al. (2018). According to the phase diagram, at a temperature of about 550-600° C, the original $Mn^{4+}O_2$ pigment (pyrolusite) starts to decompose to $(Mn^{3+},Fe^{3+})_2O_3$ (bixbyite). Later, at about 870-900° C, or a higher temperature, it converts into $Mn^{2+}Mn^{3+}{}_2O_4$ (hausmannite) (Muan 1959; Muan and Somiya, 1962; Dent Glasser and Smith, 1968; Roy, 1968). In this case, braunite probably formed from the reaction of pyrolusite with a silica-rich glaze at temperatures above 1000°C. The coexistence with hausmannite would suggest an incomplete transformation to braunite, which may be due to either the temperature being barely above 1000°C or to a not long enough firing time. Braunite and hausmannite have been also found in 17th century Hungarian tin glazed faience artefacts (Bajnóczi et al., 2014). In this case, braunite was observed both as rhombic crystals and as aggregates of particles. The idiomorphic morphology of crystals clearly indicated that braunite crystallized *in situ* during firing (and subsequent cooling). The presence of braunite in brown decorations has been also documented in 17th century Portuguese tiles (Coentro et al., 2012), in 17th century Italian majolica (Pradell et al., 2013), in 19th century Portuguese polychrome relief tiles (Coutinho et al., 2016), in

11th century Almohade tin glazed ceramics and in 13th century Catalan tin glazed ceramics (Molera et al., 2013; Pradell et al., 2013). On the other hand, kentrolite ($Pb_2Mn_2Si_2O_9$) has been identified around braunite and hausmannite crystals in Islamic ceramics (Molera et al., 2013; Pradell et al., 2013). Since the stability domain of kentrolite ranges between 650 and 840°C, its presence in such ceramics allowed to suggest a firing temperature below 850°C. Later, Coentro et al. (2018) found kentrolite in association with braunite and/or hausmannite in Hispano-Moresque tiles (15th–16th century). The presence of braunite and/or hausmannite along with kentrolite in the same glaze could suggest that the manganese-bearing pigment suffered the first firing at a temperature of ca. 1000°C, during which hausmannite and/or braunite were formed. A second and final firing should be followed at temperatures lower than ca. 850°C (Molera et al., 2013). However, other possibility would be that the manganese-brown glaze was fired at a temperature of ca. 1000°C, when hausmannite and/or braunite were formed, followed by a slow cooling which allowed the formation of kentrolite between 850° and 650°C. More recently, kentrolite has been identified in brown decorations of Catalan imitations of the Ligurian Taches Noires pottery (Di Febo et al., 2018). The presence of kentrolite in association with neo-formed hematite crystallites, can be considered as a fingerprint of temperature and their coexistence in the glaze matrix suggested a firing temperature < 925 °C.

Finally, chromite used as black underglaze pigment was first identified in pre-Islamic ceramics (Hatcher et al. 1994), in Early Islamic Glaze productions from Uzbekistan (Henshaw, 2010) and in Iznik pottery glazes (Colomban et al., 2004). Pure chromite ore has a spinel crystalline structure and the theoretical chemical composition is $FeCr_2O_4$.. Chromite is characterized by high thermal and chemical stability compared with other minerals oxides and can be used as inexpensive natural raw material to produce pigments. However, when raw chromite is used as colouring agent in glaze, brown spots may be produced and colour changes from yellow to brown depending on glaze composition.

1.2 Experimental techniques to identify crystals in glazes

Microscopy is an essential tool to analyse glaze features, including thickness of glaze layer, presence of cracks and bubbles, shape and distribution of the different crystalline phases as well as devitrification phenomena due to weathering processes (Quinn, 2013). Under the **Optical Microscopy** (OM), thin sectioning reveals general details such as the nature of finishing methods that were performed before the "overglazing" technique (e.g. slip or paint) and they have been thus covered up by the enamelling layer. Along this line, the studies of coatings by using thin section petrography, have demonstrated that their optical observation by thin section represent an easy and approachable tool to confirm or improve archaeological classifications. Using this basic tool it is possible to discriminate among different productions and to associate to a same production or provenance area samples of different typology (Fukang, 1987; Berti and Mannoni, 1990; Capelli and Marescotti, 2000; Capelli and Cabella, 2012, 2013; Reedy, 2013). However, if the glazes are well formed and no crystalline phases are present, little compositional information can be gained by using thin sections (Quinn, 2013).

Scanning Electron Microscopy (SEM) combined with energy dispersive X-ray analysis (EDS) is normally used in the studies of ceramic glazes (Freestone and Middleton, 1987; Olsen, 1988; Tite, 1992; Goldstein et al., 2003; Nigra et al., 2015). In fact, SEM has the advantage of better resolution than optical microscopy under a polarising microscope and its sensitivity to the mean atomic number of individual phases allows, at least, a rough identification. Furthermore, information on the firing temperature can be obtained from the presence or absence of vitrification in ceramic matrices. Using SEM plastic pictures can be obtained, which can easily be interpreted in terms of structural details. When combined with the analysis of characteristic X-rays emitted from the sample, it also provides information on the element distribution in the sample surface. To obtain a scanning electron micrograph, the sample surface is scanned line by line with a well-focussed beam of electrons having an energy somewhere in the range between about 0.5 and 30 keV. The interactions of these primary electrons with the specimen give rise to the emission of electrons and photons, most importantly of secondary electrons (SEs), backscattered electrons (BSEs) and X-rays. SEs have low energies and they are sensitive to the specimen's topography and are useful for imaging surface details. Backscattered electrons (BSEs) offer another way to image a specimen. The dependence on atomic number is used to produce images that show compositional contrast. BSE images have bright areas where the mean atomic number is higher and dark areas where it is lower. Contrast in BSE images, though, reveals only relative differences in composition. The elements present cannot be identified without measuring their X-ray emissions. Characteristic X-rays have wavelengths and energies

unique to the elements from which they are emitted and they are measured using X-ray spectrometers to determine a specimen's elemental composition. SEMs are commonly outfitted with energy-dispersive spectrometers (EDS) that measure such X-rays. EDS spectra, though, suffer from overlapping X-ray peaks for some elements, and the system is usually not sensitive enough to measure the tiny signals produced by trace elements.

A closely related technique, which developed alongside SEM, is **Electron Microprobe** analysis (EPMA). An electron microprobe (Birks, 1963; Freestone, 1982) is outfitted with several wavelength-dispersive spectrometers (WDS). EPMA-WDS differentiates X-rays by wavelength, rather than energy, giving rise to more precise measurements. Like an SEM, a microprobe has also EDS, and it can acquire highly magnified images of a specimen. SEM-EDS and EPMA-WDS are both spot techniques, meaning that the electron beam is focused on a spot and elemental composition is measured for only a small volume, just a few cubic micrometers, not the full specimen. This permits to obtain highly localized data and to analyse specimens so small that they cannot be studied using other techniques. Applications of scanning electron microscopy to pottery and ceramics are manifold. The impact of SEM and X-ray microprobe analysis on ceramic studies has been reviewed by Tite (1992), who mentions mainly three types of information that can be obtained from SEM: information on the raw materials used, information on firing procedures and information on surface decoration (i.e. the application and nature of slips and glazes). However, SEM-EDS and WDS have some limitations identifying minute crystallites (below 0.5 micrometres) that are smaller than the electron beam probe volume. Other difficulties concern the possibility to identify polymorphs or mineral phases present in oxide scale. In such cases, meaningful results can be obtained by combining SEM with X-ray diffraction and particularly **micro-X-ray Diffraction using Synchrotron Radiation** (μ-XRD), (Pradell et al., 2010; Iñañez et al., 2013; Molera et al., 2013; Pradell et al., 2013; Di Febo et al., 2018). In fact, the detection of the crystallites present in glazes may be difficult using conventional diffractometers because of the small sizes and low volume fraction of the crystallite phases investigated. In addition, the shallow penetration of the X-rays into glazes - in particular lead-rich glazes- limits the identification of the compounds present. The advantage of using synchrotron radiation is its high brilliance, ideal to get diffraction intensity even in samples with very low amount of crystalline material, as it is the case of crystallites embedded in glazes. Micro-XRD allows the identification of phases which have similar contrast in SEM (similar atomic weight and composition such as nepheline, carnegieite, analcime, albite), even if they are very small (smaller than 0.5 micrometer) and, when there exist different polymorphs (such as quartz and cristobalite; nepheline and carnegieite; calcite, aragonite and vaterite). High temperature X-ray diffraction (HT-XRD) is also very useful to understand the reactions of crystalline phases during firing glazes. Pradell and Molera

group had used this technique since 1999 in their pioneer work about the recrystallization of tin oxide in lead glazes (Molera et al. 1999). Later, the same technique has been employed to investigate both the role of cinnabar in luster ceramics (Pradell et al. 2004) and to study the temperature reactions in the decoration paint while the luster layer is formed (Pradell et al., 2008).

Imaging, chemical and structural information are functions that **Raman spectroscopy** is capable to provide. The use of Raman spectroscopy to identify and study archaeological materials, has flourished in recent years in addition to other standard analytical techniques (Smith and Clarck, 2001; Colomban and Truong, 2004; Casadio et al., 2016). Some advantages of the Raman spectroscopy include the specificity of the signal, no destructiveness, high spatial and spectral resolution and the possibility to perform *in situ* analysis. It can be considered as a fingerprint technique since the materials are identified by comparing their characteristic vibrational spectra with those in a database. In the case of ceramics, the Raman analysis is mainly aimed at investigating raw materials and production procedures in order to study the technological choices and the cultural models within the same context, as well as contaminations and circulations among different cultural groups (Zuo et al., 1998; Wopenka et al., 2002; Leon et al., 2010; Raskovska et al., 2010). The huge development of the Raman spectrometry in the study of glass, glazes and enamels relies on the possibility to use the SiO_4 tetrahedron bands as a fingerprint of the glass composition, structure and processing temperature. In this way, each glass type has a specific Raman signature and different procedures have been developed for the identification of soda, soda-lime, alumina or lead-containing compositions (Colomban, 2003; Colomban and Prinsloo, 2009; Colomban and Slodzyck, 2009; Ricciardi et al., 2009). As far the studies on ceramic glazes and their decorations are concerned, the best way to perform deep investigations on glaze microstructures is certainly the Raman microscopy. The coupling of a Raman spectrometer to a high-magnification optical microscope (x100 objective) allows to record the Raman signature of each phase individually, to analyse selectively components of heterogeneous samples, to avoid and/or limit fluorescence by the selection of a specific spot where its intensity is minimal and reduce the amount of sample required (Casadio et al., 2016; Caggiani and Colomban, 2018). However, the more and more widespread Raman applications on glazed ceramics and tiles are normally carried out on archaeological samples, in the form of shards or intact items. These procedures have both the advantage to preserve the samples from the sectioning and to cut on time and costs. Sometimes, the samples are prepared in the form of cross-cut pieces of several millimetres for the Raman study (Colomban et al., 2001; Colomban and Treppoz, 2001; Colomban et al., 2003; Kock and De Waal, 2008; Ricciardi et al., 2009; Caggiani et al., 2013). The use of thin sections for the Raman investigations within the frame of Cultural Heritage studies is quite rare, despite what happens in other research areas such as mineralogy and petrology (Ghiribelli, et al.,

2002; Kaindl et al., 2006; Acosta-Maeda et al., 2010; Fries and Steele, 2010). Notwithstanding that, we must take into account that the optical examination of the glaze microstructures by thin sections, should never be neglected in the Raman studies, particularly in case integrated studies on glaze microstructures are not provided (e.g. by using SEM). Micro-Raman systems can be easily used in combination with thin sections, and with an appropriate coupled microscope, the samples can be visualized using both transmition light (TL) and reflection light (RL) modes. An important remark is that by using TL, it is possible to focus on crystals that lie under the polished glaze surface getting the corresponding Raman spectra. The use of TL allows an accurate inspection of the glaze matrix, localizing the crystallites below and above the polished surface and avoiding the overlapping signals corresponding to other mineral phases.

2 Objectives

From the foregoing, it is quite clear that a full identification of glaze microstructures, nucleation processes and composition of the glazes cannot be fully collected with only one technique. This research develops a methodological approach to study of ceramic glaze microstructures based on the polished thin section that is to say without to protect the thin section with a cover glass. At first, the crystallites are located, described and characterised using thin-section petrographic methods. Special attention is paid on the description of the morphologies and optical features of the crystallites. Detailed data about the morphology is crucial to identify the symmetry of the crystals and to understand nucleation processes and conditions of formation. Then, the thin section petrography data are linked to compositional and structural data obtained from other analytical tools, such as SEM (scanning electron microscopy), EPMA (electron microprobe analysis), μ-Raman (micro-Raman) and SR-μXRD (synchrotron-radiation X-ray micro-diffraction), always using the same thin section specimen. For each mineral phase identified, chemical, mineralogical and structural data are collected to have a solid base making it possible a mineralogical identification. Once this correlation is well established, it should allow everybody to perform quick and easy identifications of the crystallites as viewed in thin section under an optical microscope avoiding the need to repeat all the integrated analyses necessary for an unambiguous characterization.

All the samples chosen to investigate correspond to lead glazed pottery, from different places and periods, which have in common the presence in their glazes of micro-crystallites that are difficult to determine by more conventional methods. In respect to the crystallites identified in this work, it is worthy of note that some of them have already been documented in archaeological potteries or historic tiles, but OM reference data useful for their identification in thin section were not available. In two cases, the analyses have been complemented by replications of the glaze recipes based on the written sources and the data obtained from the analyses of the archaeological bulk glaze mixtures. The case studies here allow to demonstrate that a combination of different analytical techniques is crucial in order to obtain meaningful results capable to answer to the archaeological questions. At the same time, they are excellent examples of the value added by the use of our methodology for the study of the glaze microstructures.

Therefore, the aim of this research is two-fold: methodologic and archaeometric:

1. From a methodological point of view, this research develops an experimental approach to study ceramic glaze microstructures based on the thin section. The different micro-analytical techniques used are adapted to thin-section specimens and the crystallites are analysed regardless of their orientation and position within the glaze matrix. Furthermore, the OM data obtained from the thin section analyses are linked to the compositional and structural data to provide a solid base for a mineralogical identification.
2. From an archaeometric point of view, the crystallites found inside the glazes are identified in order to get information about ancient technological processes. In fact, there is a direct relationship between the quality of final products and each step at the production time. The same technology applied to different materials or different processing of raw materials can give different products. Nevertheless, much information about technology remains imprinted in the glaze microstructure. For this reason, using the crystallites as technological markers, we expect to obtain information about the behaviour of the ceramic technologies, knowledge and technical skills of artisans, awareness of the physical behaviour of raw materials as well as transfer of knowledge between cultures and regions.

3 Cases of study

3.1 Misfired lead glazes

The starting point of this investigation was an historical misfired lead glazed ware from 18th century. The glaze exhibits three different colours: opaque green, opalescent yellow and transparent honey (Fig. 1a, b). Each glaze colour contains different types of crystals that had never been seen before in ancient ceramics (Fig.1c-f). These crystals seemed to be related with some relicts of galena no completely decomposed and could be technological markers in future investigations on lead glazes made by using lead sulphide. The identification of these crystals by SEM-EDS was difficult because all of them contain mainly Pb and S but also some Cl and minor amounts of Si and Ca. Because the large overlapping of S-Kα, Pb-Mα and Cl-Kα X-ray fluorescent peaks, the proper identification by SEM-EDS was not possible. Consequently, the chemical composition of the crystallites and the glaze were obtained by EPMA, while the appropriated identification of crystals was obtained by micro-XRD at the ALBA Synchrotron. In order to understand the condition of formation of such crystals, laboratory replicas at European Synchrotron Radiation Facility (ESRF) were obtained and studied in high temperature x-ray diffraction using $PbO\text{-}SiO_2$ and $PbS\text{-}SiO_2$.

The sample investigated was found during the rehabilitation works of the Casa de Convalescència in Vic (Catalonia, Spain, Fig. 2) in 2014. The edifice was built in the 18th century, outside the walls of the city and next to the reformed hospital and the new "dels Dolors" church. The Casa de Convalescència was built around a central courtyard square, in two stages; the first one was started on 17 February, 1772 (Gómez et al. 2015). Once it was built, it was stopped until 1798. The architectural complex was a civil building that provided medical assistance. The restoration works of the Casa de Convalescència begun in February 2012, uncovered a large number of whole vessels that were used as architectural filling material in the vaults (Fig. 3). A reference on the use of waste ceramics to fill vaults is found in a document of 28 February 1774. The written source refers to the presence of pieces - we understand that they may be ceramic- deposited in the vaults with the aim of lessening their weight. Such practice was very widespread during the Medieval and Modern times for civil and religious buildings as documented in many buildings in Barcelona (e.g. Cathedrals of Santa Maria del Mar and Santa Maria del Pi, Monastery of Pedralbes and the Convent of Sant Agustí).

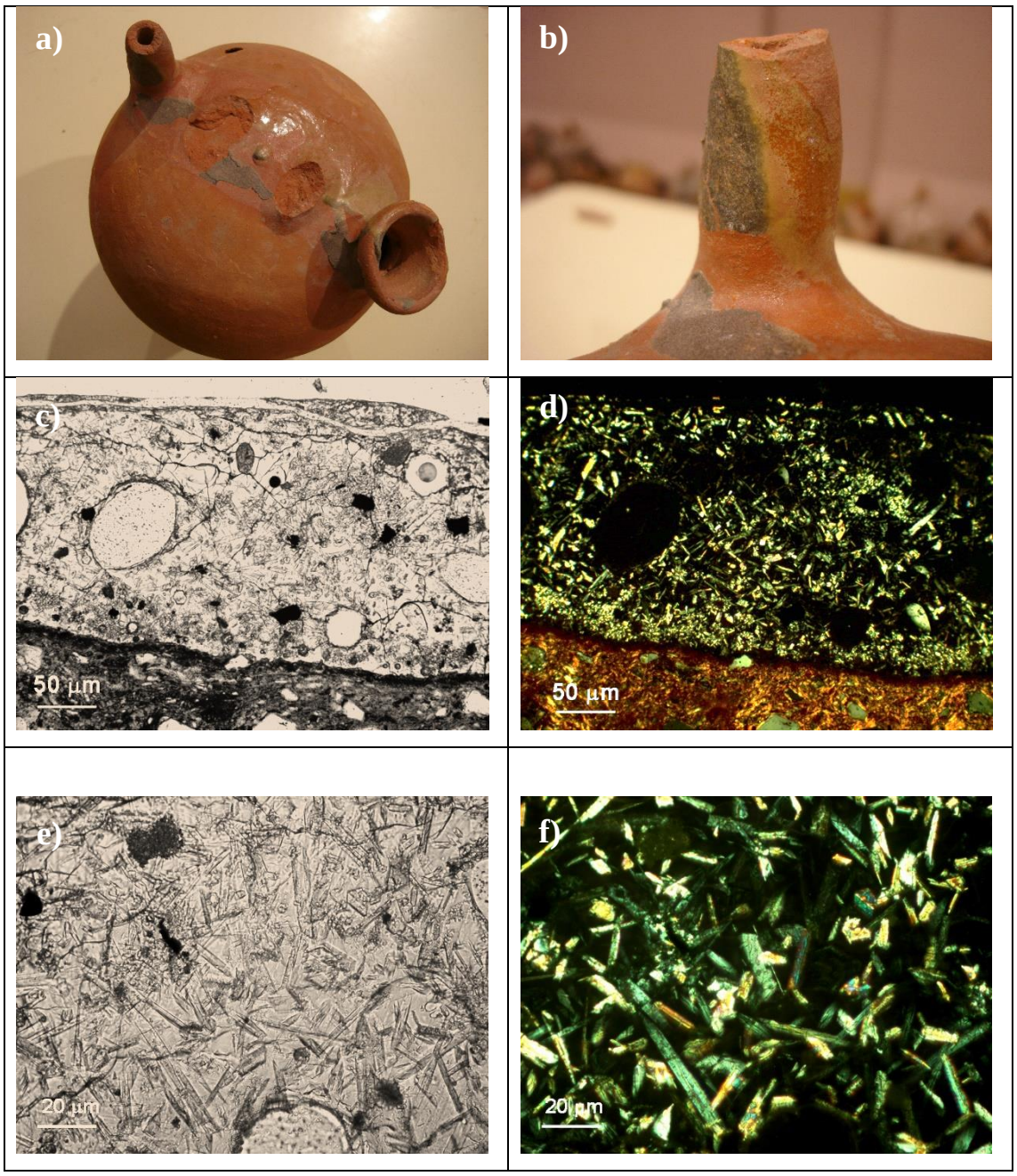

Fig. 1. (a) Picture of the misfired lead glazed ware from the Casa de Convalescència. (b) Detail of the misfired region of the glaze which exhibits three different colours: opaque green, opalescent yellow and transparent honey. (c) Optical image of the green glaze in plane polarized light (PPL). Bubbles, opaque relict grains and small transparent crystallites are visible. (d) The same image as picture (c) in crossed polarized light (XPL). (e) Detail at higher magnification of the ceramic glaze. Opaque grains and many transparent crystallites are visible (PPL). (f) The same image as picture (e) in crossed polarized light (XPL). The transparent crystallites show 1st / 2nd and 3rd order interference colours in XPL

Fig. 2. Above: The location of Vic in the Comarca of Osona (on the left side) and the position of the Casa de Convalescència in the city of Vic (marked with a blue square on the right side of the picture). Below: the modern building of the Casa de Convalescència (on the left side) and a sketch of the building (on the right side). Source: Ajuntament de Vic, Fons ACOS80-23-T2-713

Other documents from the Hospital de la Santa Creu (Barcelona) that focused on the day-to-day management of the Hospital show the presence of ceramic materials purchased or donated. The records provide evidence of the purchase of vases that had been made both for the use of the Hospital and for patients care (Ylla-Català, 2002).

The set of 229 pieces from the Casa de Convalescència is mainly characterized by containers of globular type, associated to the main activities of the time. The presence of basins, jars, and pots for the transformation of liquids and semi-liquids of different sizes stands out (Fig. 3). The Casa de Convalescència collection also includes glazed ceramics, mainly with reddish or orange bodies due to oxidizing conditions. The most represented glazing colours are honey, green, brown and to a lesser extent yellow and black. The remaining material corresponds to pots fired in reduced atmosphere. Most of the pieces are wastes of kiln, that is to say pieces that have been deformed or broken during the manufacturing or cooking process or that present technical imperfections such as cracks or loss of applied elements.

Fig. 3. Images of the uncovered vessels from the Casa de Convalescència. Source: Ajuntament de Vic, J. Molera.

3.2 Lead glazes and iron brown decorations

Regarding this kind of decorations, three different crystallites have been observed in thin section: honey acicular crystals, transparent euhedral/subhedral tabular crystals and red hexagonal crystallites. The first and second type of crystallites have been identified in lead glazes of the French imitations of the Ligurian Taches Noires ware from the 18th Joques workshop (France, Fig. 4a). The acicular crystals were present only in the decorated areas (Fig. 4b and c), while the transparent crystals were found all over the glazes and they were particularly abundant in the undecorated areas (Fig. 4d).
On the other hand, the red hexagonal crystallites (Fig. 4e) have been observed in thin sections of different Medieval and Post-Medieval lead glazed ceramics, also including the above mentioned French imitations of the Ligurian Taches Noires ware (Di Febo, 2016). Despite of their dissimilarity in chronology and provenance, the Medieval and Post-Medieval glazed ceramics share some common technical features: a moderately developed interface, red/orange Fe-rich bodies and transparent high lead glazes with a relatively low content of FeO. The potteries taken into account for our study are again Taches Noires imitations from the Jouques workshop: they contain abundant red hexagonal crystals clearly visible in thin section and therefore they are suitable parallels for our investigation.
The three different types of crystals found in the iron brown decorations have been investigated and discussed in terms of glaze and pigment composition as well as firing conditions. Furthermore, in the

case of the red hexagonal crystals, replicas were obtained in controlled conditions to determine if their presence could be a fingerprint of firing temperatures.

The first evidence of the production of the Taches Noires ware (from this point onwards it will be called TNW) trace back to the first half of the 18th century as a reaction to the decrease of the Majolica production and to the competition of the English cream ware (Cameirana 1970, 1977; Milanese et al., 1994, Fig. 4f). The TNW is characterized by a fine, hard, deep red fabric and brown transparent glazes decorated with wavy black bands (Fig. 4g and h). The common documented forms are plates, bowls and, to a lesser extent, kitchen wares (Blake 1981). The TNW manufacturing technology can be found in the technical report of the Napoleonic Prefect Chabrol de Volvic (Assereto 1994). According to him, the paste recipe involved the use of local available raw materials, such as red clay and marl, which were mixed in different proportions (2/3 of red clay and 1/3 of marl). The pottery was fired in two stages; in the second one, saggars were used to guarantee sufficient oxidising conditions. Lead, used in glazing mixture, was purchased in Genoa or imported from Almeria (Spain) and mixed with sand from Antibes (France) or ground quartz from Noli (Liguria). The addition of one twelfth of iron oxide gave an orange-brown colour to the glazes, while manganese decorations were applied under the glazed coat before the second firing.

The strategic position of Albisola, not far from the port of Genoa, and the existence of large clay outcrops, certainly favoured a large-scale production. By 1798, 48 workshops produced about 24 million pieces a year, most of these were exported to Piedmont, Tuscany, Sardinia, and outside Italy to Corsica, France, Spain, Greece, Africa, Canada, Caribbean Islands and Mexico (Barton 1970; Petrucci 1977; Foy et al. 1986; Cavaletto 1989; Long and Richez 1993; Moussette ,1993; Dadea 1994; Milanese et al. 1994). The supremacy of Albisola products and Ligurian trade in the western Mediterranean caused the reaction of the Provençal and Spanish potters. Spain (1809) and France (1820) imposed import duties on Ligurian pottery. This ended the Albisola pottery industry and forced many potters to emigrate to those countries to locally produce the TNW (Cameirana 1970; Amourich and Vallauri 1993; Milanese et al. 1994).


a)
1 cm

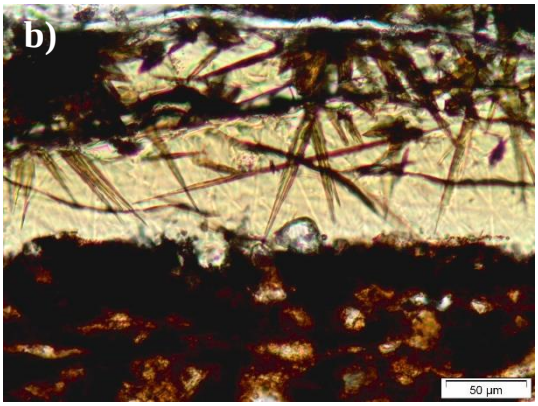
b)
50 µm

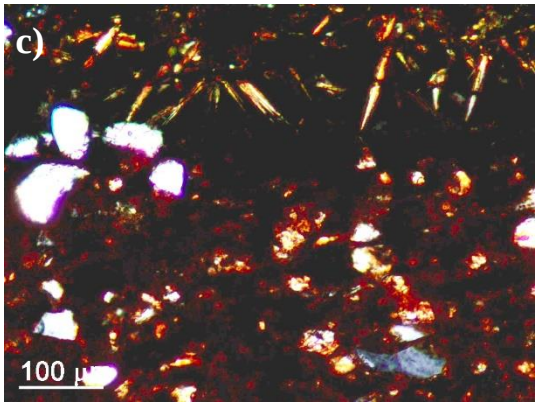
c)
100 µ

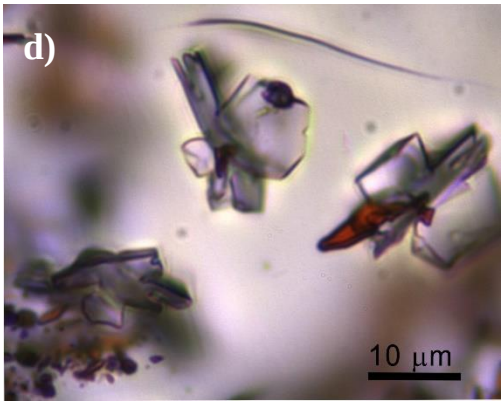
d)
10 µm

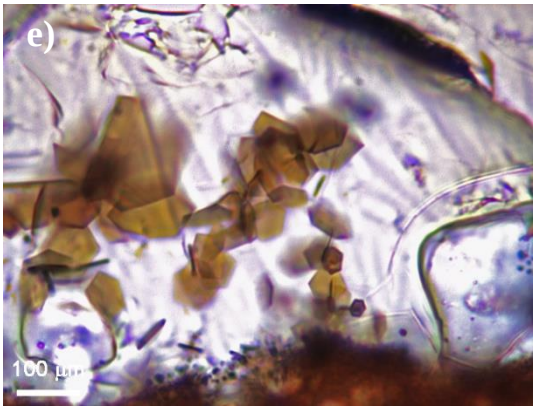
e)
100 µm


f)
1 cm

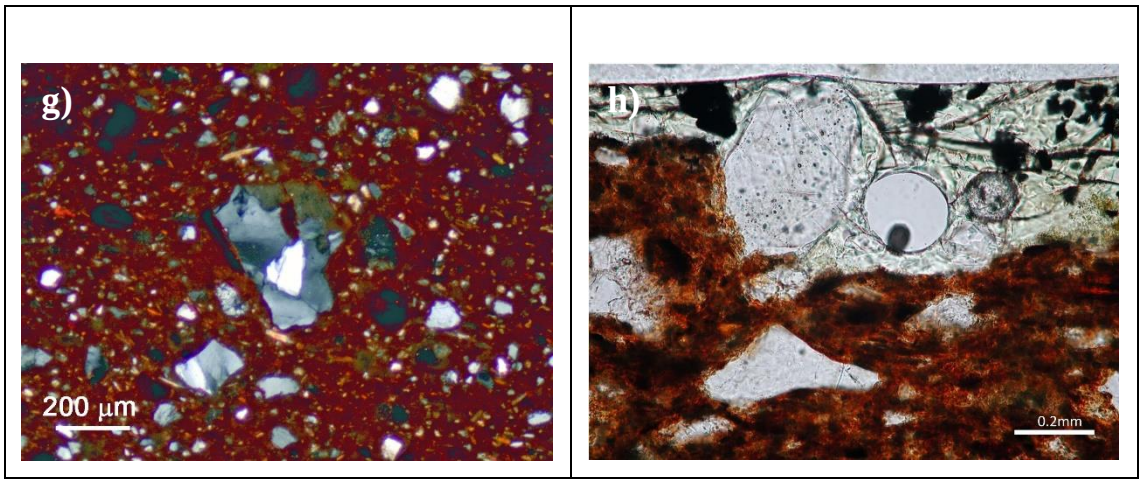

Fig. 4. (a) French imitation of the Ligurian Taches ware (sample 9703) from Jouques (first half of 19th century). (b-c) Optical image of the sample 9703: honey acicular crystals can be observed in in plane polarized light (PPL) and in crossed polarized light (XPL) respectively. (d) Optical image of the sample 9703: transparent euhedral/subhedral tabular crystals are visible in plane polarized light (PPL). (e) Optical image of the glaze of the sample 9703: hexagonal neo-formed crystallites are visible in plane polarized light (PPL). (f) Ligurian Taches Noires ware (sample 9619) from Albisola (first half of 18th century). (g) Optical image of the ceramic body of the sample 9619 in plane polarized light (PPL). A gneiss fragment is visible in the ceramic matrix. (h) Optical image of the ceramic body and glaze (sample 9619). Relict hexagonal grains are visible inside the glaze (XPL).

3.3 Lead glazes and manganese brown decorations

For the study of the manganese brown decorations, one sherd of a bowl decorated in brown colour has been selected (sample SBG 10, Fig. 5a). In this case, the decoration is related to the presence of euhedral crystallites that have been previously identified by Molera et al (2013) as braunite. In this contribution, we provide new data about braunite and we also identify and discus the presence of two types of dendritic crystals associated to braunite (Fig. 5b and c). The occurrence of these crystalline phases in the decoration is explained in term of glaze and pigment composition and their petrographic features are studied. Finally, we show how the different morphologies can be explained by the firing processes.

According to its decoration and typology, the sample studied was a cheaper version of the Catalan blue majolica pottery dating back to the end of the 16th -18th centuries. The ceramic shard came from the excavations of the old Church of Sant Bartomeu del Grau (Catalonia), which is a small town located 90 km North of Barcelona. A Romanesque church built before the 11th century was used until 1787, when a new church was constructed 700 m north of the old one. In 1810, the older church roof fell in and it was definitively abandoned. The archaeological works at the Medieval church recovered fragments of tin glazed pottery that correspond to a common Catalan ceramic production dating back to the end of the 16th - 18th centuries.

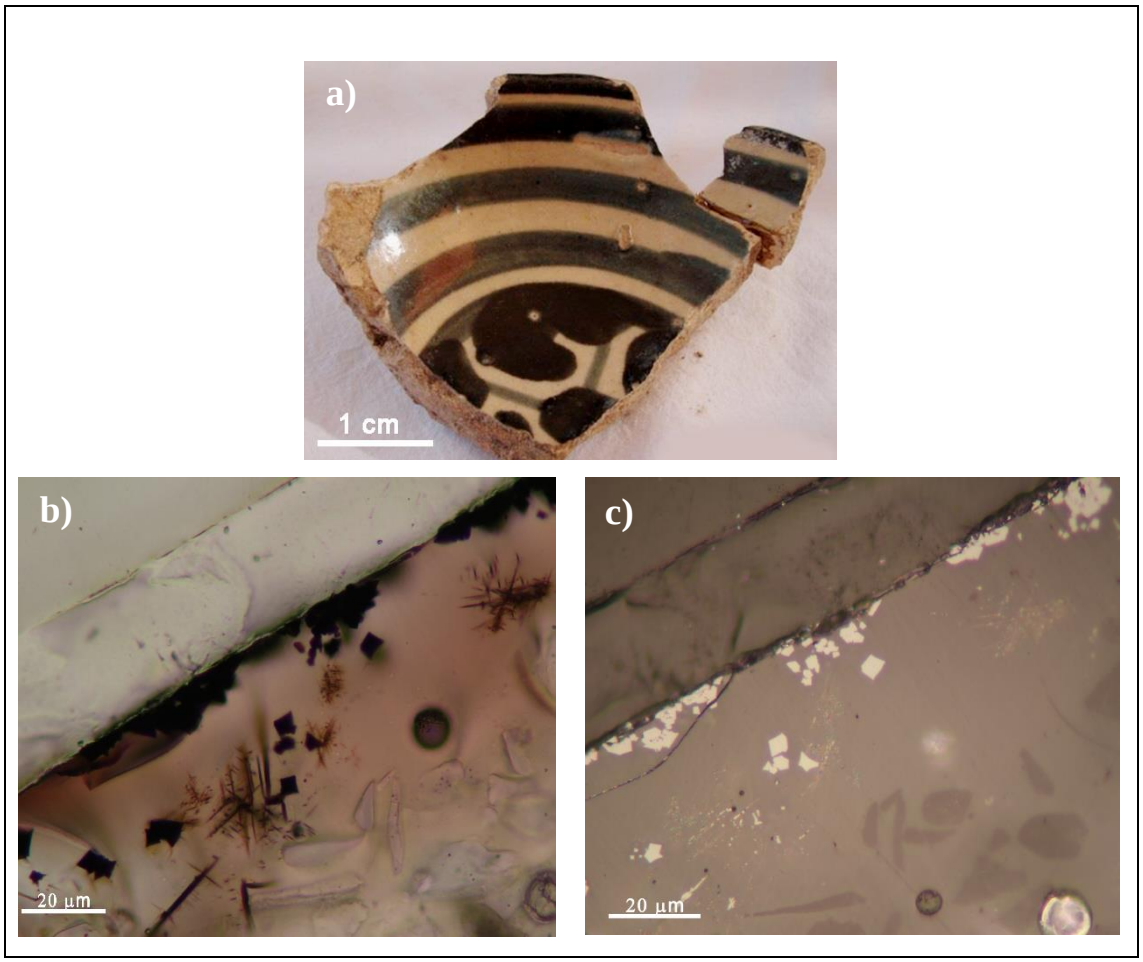

Fig. 5. (a) Brown decorated Catalan tableware (sample SBG10) from the old Church of Sant Bartomeu del Grau (17th century). (b) Optical image of the brown decoration in plane polarized light (PPL). Crystallites with euhedral and dendritic habits can be observed. (c) The same image as picture (b) in reflected light (RL).

4 Methodology

This thesis develops a protocol to study ceramic glaze microstructures by using polished thin section in order to allow the systematic recording of data in a number of techniques. Detailed procedures include: sample preparation, observations under the optical microscope and choice of analytical techniques that can best implement the studies on ceramic glazes samples prepared as polished thin sections.

4.1 Sample preparation

In the studies of archaeological ceramic glazes, the most commonly procedure employed consists in using two different sample preparations: covered thin sections (30 µm thickness) for the study of ceramic pastes and polished cross sections of few millimetres thick for the investigation of ceramic glazes. Instead of using different kinds of laboratory preparations, our protocol uses only polished thin sections for both ceramic and glaze analyses. The use of the same sample preparation - that is to say the polished thin section- during all the steps of the analysis, from the optical observation to the multi-analytical stage, represents a huge improvement. This enables continuity in analysis and the possibility to check, at each step of the investigation, the crystals on which the analyses are performed.

4.1.2 Optical microscopy: transmitted light (TL) and reflected (RL) modes

The observation of crystallites using OM requires thin sections with a good finish and a petrographic microscope with enough magnification power. The advantages of using the common transmitted light mode (TL) are manifold. In TL, the light passes through the ceramic glaze and the crystallites can be seen even if they are below the surface. Therefore, through different focus positions, it is possible to get an overall idea of the 3D morphology and distribution of the crystallites (both single crystals and aggregates) embedded in the glaze. Another important aspect concerns the use of the reflected light mode (RL). Although it is scarcely used for the ceramic pastes, RL is essential in the study of the glaze microstructures. In fact, observations in RL are necessary to obtain optical images comparable to those from SEM or similar techniques. This step allows to understand which crystallites will be visible on the polished surface and how. This makes possible to choose the best analytical strategy and save time. Furthermore, some optical properties that can be observed in RL mode, such as polishing relief and reflectance, can be very useful to identify glaze phases of similar composition often indistinguishable from one another using SEM.

4.1.3 Choice of analytical techniques that can best implement the studies on ceramic glazes by thin section

Besides OM, the choice of analytical techniques that could best complement the studies on ceramic glazes should be based on two main criteria: the information that they can give and the capacity to perform the measurement directly on the petrographic thin section. Within these analytical techniques, SEM – along with associated techniques like FIB and spectroscopies like EDX or WDX – can for sure have a place of its own. In addition, SR-μXRD and μ-Raman are two powerful techniques that have been tested on ceramic glaze thin sections.

4.2 SEM

The crystallites and the glazes were analysed by SEM-EDS to ascertain their chemical composition. The analyses were carried out at the Research Center in Multiscale Science and Engineering of Barcelona (UPC). The bulk chemical composition of the glazes was determined by analysing areas and avoiding the glaze–body interface as well as mineral inclusions. A crossbeam workstation (Zeiss Neon 40) equipped with SEM (Shottky FE) column and EDS (INCAPentaFETx3 detector, 30 mm2, ATW2 window) was employed. The microscope was operated at 20 kV, with 100 s measuring time, and BSE images were obtained. Quantitative analysis calibration was accomplished with mineral and synthetic standards.

4.3 FIB

Focus Ion Beam (FIB) technique was used to modify polished thin sections of the glazes at the Research Center in Multiscale Science and Engineering of Barcelona. The instrument was used to produce polished cross sections of the crystallites directly on the thin section. A crossbeam workstation (Zeiss Neon 40) equipped with SEM (Shottky FE) and Ga + FIB columns, was used to prepare cross sections of the crystals. First, the sample surface was coated with a thin protective Pt layer (1 μm) by ion-beam-assisted deposition; then the cross section was cut and polished and a thin layer of Pt deposited to enhance conductivity. Subsequently secondary electrons SEM images of the inclusions were obtained at 5 kV.

4.4 EPMA

Electron microprobe (EPMA, JEOL JXA-8230; JEOL Ltd, Akishima, Tokyo, Japan) analyses were carried out directly on the polished thin sections of glazes at the Centres Científics i Tecnològics, University of Barcelona. They were used to quantify the chemical composition of the micro-crystallites that contained both Pb and S which requires the high-energy resolution provided by the WDS (wavelength dispersive spectroscopy) detector instead of EDX. A minimum of three analyses on the crystallites were acquired and the average and standard deviations were obtained. The operating conditions were 20 kV and 15nA with a focused beam (spot analysis). The standards used were PbS for galena and Pb, $SrSO_4$ for S, $CaSiO_3$ for Si and Ca, and AgCl for Cl. Finally, the chemical composition of the glaze was determined avoiding the glaze-ceramic interface as well as the crystallites.

4.5 μ-XRD ALBA BL04

Synchrotron-radiation micro-X-ray diffraction (SR-μ-XRD) was performed on the focused-beam station of the beamline BL04 at the ALBA Synchrotron of Barcelona. The areas of interest from the polished thin sections were selected using an on-axis visualization system and measured in transmission geometry with a focused beam of 15×15 μm^2 (FWHM). The energy used was 29.2 keV ($\lambda = 0.4246$ Å) and the diffraction patterns were recorded with a Rayonix SX165 CCD detector (active area of 165 mm diameter, frame size 2048 x 2048 pixels, 79 μm pixel size, dynamic range 16 bit). The calibration of the sample–to-detector distance and beam centre (from a LaB6 sample measured at the same conditions) and the radial integration of the images were performed with the Fit2D software (Hammersley et al., 1996). Identification of the compounds has been performed based on the Powder Diffraction File (PDF) database from the International Centre for Diffraction Data (ICDD).

4.6 μ-Raman

Micro-Raman analyses were carried out directly on the polished thin sections of the glazes at the Centres Científics i Tecnològics, University of Barcelona. Spectra were obtained with a HORIBA Jobin Yvon LabRam HR 800 dispersive spectrometer, equipped with an Olympus BXFM optical microscope, using a 600 g/mm grating and a Synapse CCD detector cooled at -70ºC. The Raman spectra reported in this study were recorded with the 532 nm excitation line of a solid state laser.

5 Results

5.1. *The production of a lead glaze with galena: Thermal transformations in the PbS–SiO_2 system*

Journal of the American Ceramic Society, 101, 2119-2129 (2017)
DOI: 10.1111/jace.15346
Di Febo, R., Molera, J., Pradell, T., Melgarejo, J.C., Madrenas, J., Vallcorba, O.

5.1.2 Introduction

Galena has been widely used in the production of lead glazes. A mixture of galena and sand was applied to the surface of the ceramic body and fired. The decomposition of galena and further reaction with the sand gives rise to the development of a lead glaze. The starting point of the present investigation was an historical misfired lead glaze that retains galena relic grains. Due to uncontrolled and unequal temperature conditions in the kiln, the glaze exhibits three different colours: opaque green, opalescent yellow and transparent honey. The presence of different macroscopic colours was related to the existence of three different crystalline phases inside the glaze. These phases were determined and discussed in terms of both the composition of the galena mineral used and the firing conditions. Later, also the firing conditions were investigated in light of the high-temperature transformations previously obtained in the PbS-SiO_2 system, for which no information was available in literature. Two mixtures of the eutectic composition 70% PbO: 30% SiO_2 were prepared using PbO in one case and galena (PbS) in the second case. The phase transformations and thermal stability of the compounds formed were determined and the results obtained compared to the available data for the PbO-SiO_2 and PbO-$PbSO_4$ systems.

5.1.3 Results

The green, yellow and honey coloured areas of the misfired lead glaze were analysed by SEM-EDS at first. The chemical analyses revealed the presence of three different crystallites, which contained mainly Pb and S and in one case also Cl and minor amounts of Si and Ca. Due to the large overlapping of S-Kα, Pb-Mα and Cl-Kα X-ray fluorescent peaks the chemical composition of the crystallites and glaze could not be obtained by using an EDS detector. For this reason, both glaze and crystallites were again analysed, this time using EPMA and micro-XRD. The crystallites identified correspond to galena, PbS, lanarkite, $PbO{\cdot}PbSO_4$ and mattheddleite, $(Ca,Pb)_{10}(SiO_4)_{3.5}(SO_4)_2Cl_2$.
EPMA results were integrated and compared with the high-temperature diffraction data taken during the heating of the PbO-SiO_2 and PbS-SiO_2 mixtures.

In respect to the PbO-SiO_2 mixture, the appearance of the new crystalline compounds and the disappearance of the initial one can be summarized as follow:

- At 600ºC, PbO begin to decrease until it disappeared completely at 722 ºC. At this temperature a melt coexisting with other crystalline compounds is formed.
- The reaction of PbO with SiO_2 is responsible for the formation of Pb_2SiO_4, which is stable up to 715 ºC, then starts to destabilize and when it disappears completely at 727 ºC.
- At 670°C, Pb_4SiO_6 is formed and it disappeared at 722°C.
- At 625°C, $PbSiO_3$ is formed and it disappeared completely at 727°C.

On the other hand, the high-temperature diffraction data obtained for the PbS-SiO_2 mixture (75 wt% of galena plus 30 wt% of quartz) showed the appearance and disappearance of the following phases:

- Galena is stable up to 315°C and disappears completely at 795°C.
- A melt coexisting with other crystalline compounds appears at about 775°C.
- Cerussite and anglesite, the two weathering compounds of galena, are respectively stable up to 275°C and 575°C and they disappear respectively at 315°C and 860°C.
- At 315°C, Massicot (PbO) appears and it disappears at 595°C.
- Above 315°C, $PbO{\cdot}PbSO_4$ (lanarkite) appears when galena decreases. This lead oxysulfate disappears at 795°C.
- At 795°C a lead dioxy-sulfate $2PbO{\cdot}PbSO_4$ is formes which is stable up to 950°C when a sulphate melt is formed.
- After the cooling, two lead oxysulfates, $2PbO{\cdot}PbSO_4$ and $4PbO{\cdot}PbSO_4$ which crystallized from the melt are present.

Received: 21 July 2017 | Accepted: 10 November 2017

DOI: 10.1111/jace.15346

ORIGINAL ARTICLE

Journal of the American Ceramic Society

The production of a lead glaze with galena: Thermal transformations in the PbS–SiO_2 system

Roberta Di Febo[1] | **Judit Molera**[1] | **Trinitat Pradell**[2] | **Joan C. Melgarejo**[3] | **Josep Madrenas**[4] | **Oriol Vallcorba**[5]

[1]U. Science Tech, MECAMAT Group, University of Vic—Central University of Catalonia, Vic, Spain

[2]Physics Department, UPC-BarcelonaTech, Castelldefels, Spain

[3]Department of Mineralogia, Petrologia i Geologia Aplicada, University of Barcelona, Barcelona, Spain

[4]Escola d'Art i Superior de Disseny de Vic, Vic, Spain

[5]ALBA Synchrotron Light Source, Barcelona, Spain

Correspondence
Judit Molera, U. Science Tech, MECAMAT Group, University of Vic—Central University of Catalonia-, Vic, Spain.
Email: judit.molera@uvic.cat

Funding information
Generalitat de Catalunya, Grant/Award Number: 2014SGR-1585, 2014SGR-1661, 2014SGR-581; University of Vic—Central University of Catalonia.; Ministerio de Ciencia e Innovación (Spain), Grant/Award Number: MAT2016-77753-R; ALBA Synchrotron Light Facility, Grant/Award Number: 2014060905 (BL04)

Abstract

Galena, also known as PbS, was widely used in the production of lead glazes from the beginning of the 18th century to the second half of the 20th century. Although the PbO-SiO_2 system has been studied for years, the PbS–SiO_2 phase diagram, involved in the formation of a glaze with galena, has not yet been investigated. Temperature transformations for the system 75 wt% PbS-25 wt% SiO_2 are investigated in a high-temperature resolved X-ray diffraction experiment with synchrotron radiation and compared to those of the equivalent system 70 wt% PbO-30 wt% SiO_2. Lanarkite, $PbO{\cdot}PbSO_4$, is the phase predominantly formed as soon as galena decomposes during the heating. The results show that the system melts at a temperature higher than the PbO–SiO_2 system, but far lower than those expected for the PbO–$PbSO_4$–PbS system. A historical misfired lead glaze produced with galena is also studied. The presence of galena, lanarkite, and mattheddleite, $Pb_{10}(SiO_4)_{3.5}(SO_4)_2Cl_2$, is determined and discussed in terms of the composition of the galena mineral used and the firing conditions in light of the high-temperature transformations previously obtained.

KEYWORDS

$2PbO{\cdot}PbSO_4$, $4PbO{\cdot}PbSO_4$ mattheddleite, galena, high lead glazes, $PbO{\cdot}PbSO_4$ lanarkite, PbO–SiO_2 system, PbS–SiO_2 system, thermal stability

1 | INTRODUCTION

Lead glazes are among the earliest glazes used to coat earthenware, stoneware, and porcelain to make them waterproof. Lead glazes have a wide processing range, low melting point, low viscosity and surface tension, and a thermal expansion coefficient which match those of earthenware giving them good adherence (minimal flaking and crazing) and excellent covering capability. They also have a high refraction index that confers brilliance to the glaze.[1]

The first lead-containing glazes were produced in China (Warring States period, 475–221 BC), to cover large jars, but were comprised of relatively low quantities of lead (<20 wt% PbO). High lead glazes (with composition close to the eutectic mixture 70 wt% PbO, 30 wt% SiO_2, which melts at 717°C) were not produced until the 1st century BC (Han dynasty and Greco-Roman world).[2,3] All these glazes show green, yellow, and brown colors and imitated metal forms.[4]

There were two primary methods of applying lead glazes to ceramic surfaces: either using lead compounds alone or a mixture of lead compounds plus powdered quartz or sand.[2] The former method was used between the 1st and 3rd centuries AD and the latter between the 2nd and 4th centuries AD.[4] One further variation was the

 © 2017 The American Ceramic Society

fritting of the lead compounds-plus-quartz mixture before its application to the ceramic surface.[1] A frit is any glassy or partially glassy material obtained after firing a mixture of sand with flux materials (lead compounds, plant ashes, alkaline salts, etc.).[5] This method was widely used in the Medieval period until modern times.

Galena, PbS, is the most important lead ore and known to have been widely exploited by the Romans to extract silver and to obtain metallic lead, but there is no archeological evidence or literature demonstrating the use of galena or roasted galena (PbO) in the production of the lead glaze in Roman times. The use of galena would have the advantage of eliminating one stage (the roasting of galena to obtain lead oxide) in the process of producing a lead glaze. However, the use of galena was not documented until the 18th century.[6] At the same time as Ramazzini, an Italian physician linked the diseases shared by potters, guilders, and glassmakers to lead poisoning.[7]

Although there is a detailed phase diagram for the PbO–SiO_2 system,[8-10] there is no information about the transformations that take place in the PbS–SiO_2 system. However, complementary information of the Pb–PbS, PbS–O, and PbO–$PbSO_4$ systems is available.[11-14] The use of *galena* implies the oxidation of PbS, but as PbS and PbO do not have a common boundary in the phase diagram, it will always involve the formation of lead sulfates and oxysulfates; $PbO{\cdot}PbSO_4$, $2PbO{\cdot}PbSO_4$, and $4PbO{\cdot}PbSO_4$ which are known to have a limited solubility in the silica melt. Therefore, the use of galena implies oxidation of the PbS into $PbSO_4$ and progressively more oxidized oxysulfates, sulfate anion breakdown (above 880°C), and the reaction with SiO_2 to obtain the melt. The main advantage of the PbO–SiO_2 system in the production of glazes is its low melting point (717°C[10]). The large compositional range, between 20 and 60 mol% SiO_2, for which a melt forms at a relatively low temperature, below 760°C[10], is also an advantage. This does not occur in the PbS–SiO_2 system. The PbS–$PbSO_4$–PbO phase diagrams show higher melting temperatures, the lowest for the more oxidized species at 916°C.

The production of a lead glaze with *galena*, PbS–SiO_2 system, and the equivalent PbO–SiO_2 system are investigated in a time-resolved high-temperature X-ray diffraction experiment with synchrotron radiation (HT-SR-XRD). Although the equilibrium phase diagram of the PbO–SiO_2 system is well known, equilibrium conditions are not necessarily reached during the time-resolved experiment. Therefore, the data obtained for the PbO–SiO_2 mixture will reveal any shift in the phase transformation and melting temperatures due to nonequilibrium conditions.

A historical misfired lead glaze ware that retains *galena* relic grains is also studied. The crystalline phases present in the glaze vestiges from an incomplete glaze firing are identified, and their presence is discussed in terms of the data obtained from the high-temperature experiment and of the composition of the glaze. Finally, the reasons for the use of galena in the production of lead glazes and its limitations are discussed in light of the results obtained.

2 | EXPERIMENTAL PROCEDURE

2.1 | High-temperature resolved XRD experiment (HT-SR-XRD)

Two mixtures of the eutectic composition 70 wt% PbO:30 wt% SiO_2 were prepared using PbO in one case and using galena in the second case. Chemical reagents for both the PbO (Fluka ref. 11526) and SiO_2 (Merck ref. 107536) were selected. Galena is of mineral origin, and the sample obtained was from the Molar mine (Catalonia).

The in situ high-temperature X-ray diffraction measurements were obtained on the high-brilliance, high-energy (90 keV) (HT-SR-XRD) synchrotron beamline ID15B at the ESRF (Grenoble, France). The experimental setup consisted of a small cylindrical furnace with the raw powders contained in unsealed 0.5-mm-diameter MgO capillaries mounted on a goniometer for alignment. An image-plate detector (Model MAR345; Marresearch, Norderstedt, Germany) was used to collect the XRD patterns with an exposure time of 1 min, and rotation of the sample was sufficient to ensure good data quality.

The furnace temperature was controlled by a previously calibrated external regulator. An initial drying stage was programmed, consisting of a slow heating rate (1°C/min) between 90 and 110°C and then maintaining the temperature for 5 min. The sample was afterward heated at a constant heating rate of 5°C/min up to the maximum temperature with data being recorded during this slow ramping. The measuring time took only 1 min and consequently a variation of 5°C existed between the beginning and the end of the data collection. The data collection, readout, and erasure of the image plate took 4 min in total. The whole cycle for each dataset took 5 min (measuring time, readout, and then erasure of the image plate), resulting in images being taken every 25°C. Finally, the sample was cooled down to room temperature at a rate of 10°C/min. The whole measurement cycle took 3 h.

The calibration of the sample to detector distance, beam center, and orthogonality of the detector was determined using a silicon standard measured under the same conditions. The radial integration of the images was performed using the Fit2D software.[15] Identification of the compounds was performed based on the powder diffraction file (PDF) database from the International Centre for Diffraction Data (ICDD). Figures 2 and 3 represent high-temperature XRD patterns (HT-SR-XRD) obtained during the firing of the mixtures. Thermal stability ranges of the crystalline phases

identified for (a) $PbO–SiO_2$ and (b) $PbS–SiO_2$ are shown in Figure 4. The ordinate axis is obtained from the intensity of the principal peak of each crystalline phase relative to the intensity of the MgO crucible and gives a qualitative temperature evolution of each compound.

2.2 | Analysis of a misfired lead glaze

A misfired storage jar (CCV050) dating from the 18th century was investigated.[6] The jar was part of an assemblage of coarse wares found in the garret of *Casa Convalescència*, an ancient hospital building that provided medical assistance, in Vic. Due to uncontrolled and unequal temperature conditions in the kiln, the glaze exhibits three different colors: opaque green, opalescent yellow, and transparent honey (Figure 1).

A polished thin section of glaze and ceramic body to a standard thickness of 30 μm was obtained. The thin section was studied by optical microscopy (OM) with transmitted and reflected light using a petrographic microscope (LEICA DM 2700 P; Leica Microsystems, Wetzlar, Germany) and scanning electron microscopy with an energy dispersive spectroscopy detector attached (SEM-EDS) to identify the crystalline compounds present. A crossbeam workstation (Zeiss Neon 40; Carl Zeiss AG, Oberkochen, Germany) equipped with a Schottky field emitter column with an EDS detector (INCAPentaFETx3 detector, 30 mm^2, ATW2 window, Oxford Instruments, Abingdon, UK) attached was employed for the SEM investigation. Backscattered electron (BSE) images were obtained and analyses of the crystallites were carried out to ascertain the composition at 20 kV acceleration voltage.

Electron microprobe (EPM, JEOL JXA-8230; JEOL Ltd, Akishima, Tokyo, Japan) was also used to quantify the chemical composition of the different microcrystallites present that contained both Pb and S which requires the high-energy resolution provided by the WDS (wavelength dispersive spectroscopy) detector. A minimum of three analyses of the crystallites and of the glaze were acquired, and the average and standard deviation were obtained. The operating conditions were 20 kV and 15nA with a focused beam (spot analysis). The standards used were PbS for galena and Pb, $SrSO_4$ for S, $CaSiO_3$ for Si and Ca, and AgCl for Cl. Finally, the chemical composition of the glaze was determined avoiding the glaze-ceramic interface as well as the crystallites.

The crystalline structure of the microcrystallites was determined by synchrotron radiation micro-X-ray diffraction

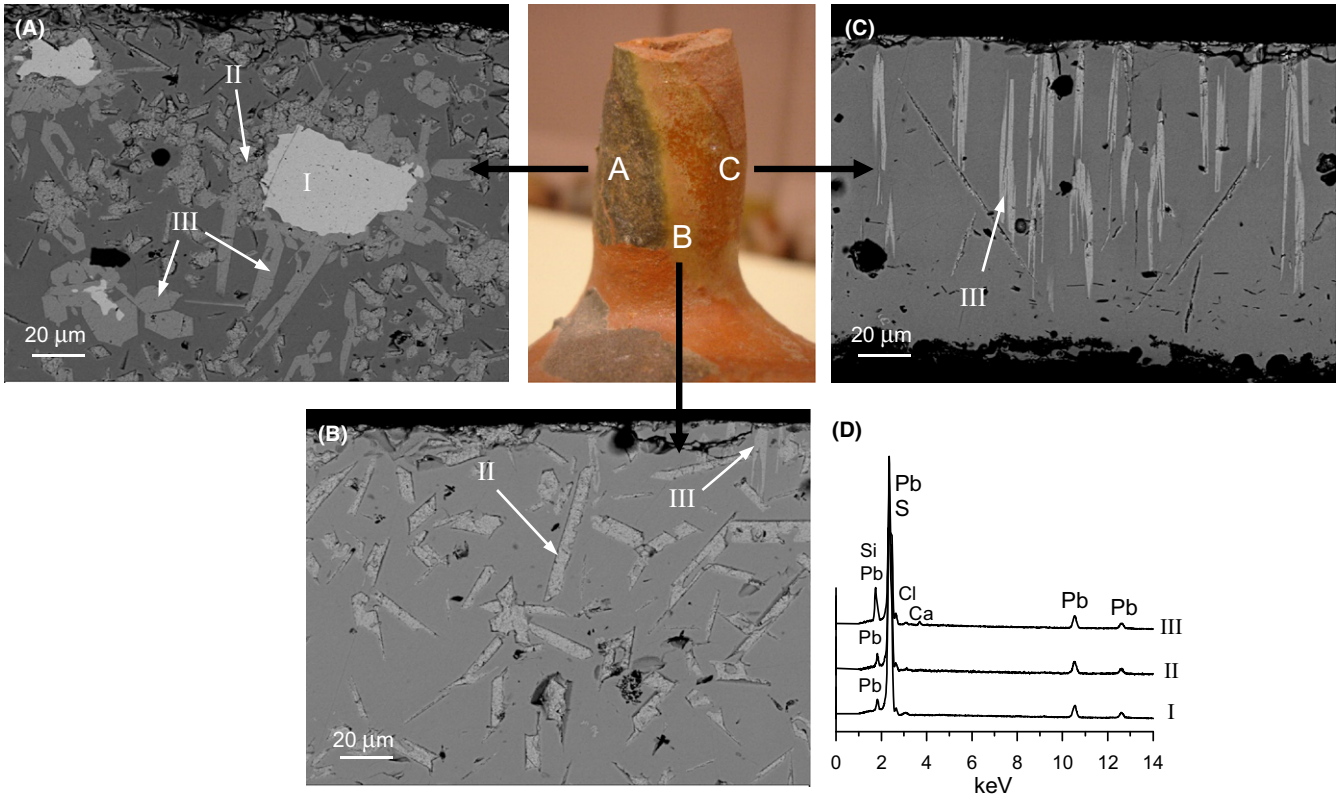

FIGURE 1 The neck of a 18th-century jar, which exhibit a misfired glaze showing three color glaze areas. Scanning electron microscopy backscattering images of (A) the opaque green area which contains relics of galena (I) and neoformed crystallites II and III, (B) the translucent yellow area containing crystallites II and III, and (C) the honey transparent area containing only crystallites III. (D) EDS spectra of the three types of crystallites

(SR-μXRD) on the same polished thin section in the focused beam station of beamline BL04[16] at the ALBA Synchrotron (Spain). The areas of interest from the polished thin section were selected using an on-axis visualization system and measured in transmission geometry with a 15 × 15 μm^2 (FWHM) focused beam of 29.2 keV (λ = 0.4246 Å). The diffraction patterns were recorded with a Rayonix SX165 CCD detector (active area of 165 mm diameter, frame size 2048 × 2048 pixels, 79 μm pixel size, and dynamic range 16 bit). The calibration of the sample to detector distance, beam center, and orthogonality of the detector were performed using a LaB_6 standard, and the radial integration of the images was performed with the Fit2D software.[15] Identification of the compounds was performed based on the powder diffraction file (PDF) database from the ICDD.

3 | RESULTS

The corresponding high-temperature diffraction data taken during the heating of PbO–SiO_2 and PbS–SiO_2 mixtures are shown in 2D images in Figures 2 and 3, respectively. The HT-SR-XRD patterns taken before heating and after cooling are also shown. Apart from the initial and new crystalline compounds formed during the heating, the XRD pattern corresponding to the periclase (MgO) from the crucible is also seen.

3.1 | PbO–SiO_2 high-temperature resolved XRD experiment

The high-temperature diffraction data taken during the heating of a mixture 70 wt% PbO: 30 wt% SiO_2 is shown in Figure 2 and the appearance and disappearance of the phases marked. The initial compounds are massicot (PbO, orthorhombic, Pbcm) and α-quartz (SiO_2, trigonal). The thermal stability range of the different compounds identified is summarized in Figure 4A.

The reversible transformation between α-SiO_2 and β-SiO_2 at 573°C is observed in Figure 2. PbO was stable up to 560°C. At 600°C, PbO began to decrease until it disappeared completely at 722°C. A melt coexisting with other crystalline compounds (a melt is expected to form at 717°C[10] in the system 70 wt% PbO-30 wt% SiO_2) was clearly found at about 722°C. As soon as PbO reacted with SiO_2, Pb_2SiO_4 was formed increasing until 690°C; it decreased quickly at 715°C and completely disappeared at 727°C. At 670°C, Pb_4SiO_6 was formed and disappeared at 722°C. Finally, $PbSiO_3$ was formed at 625°C and

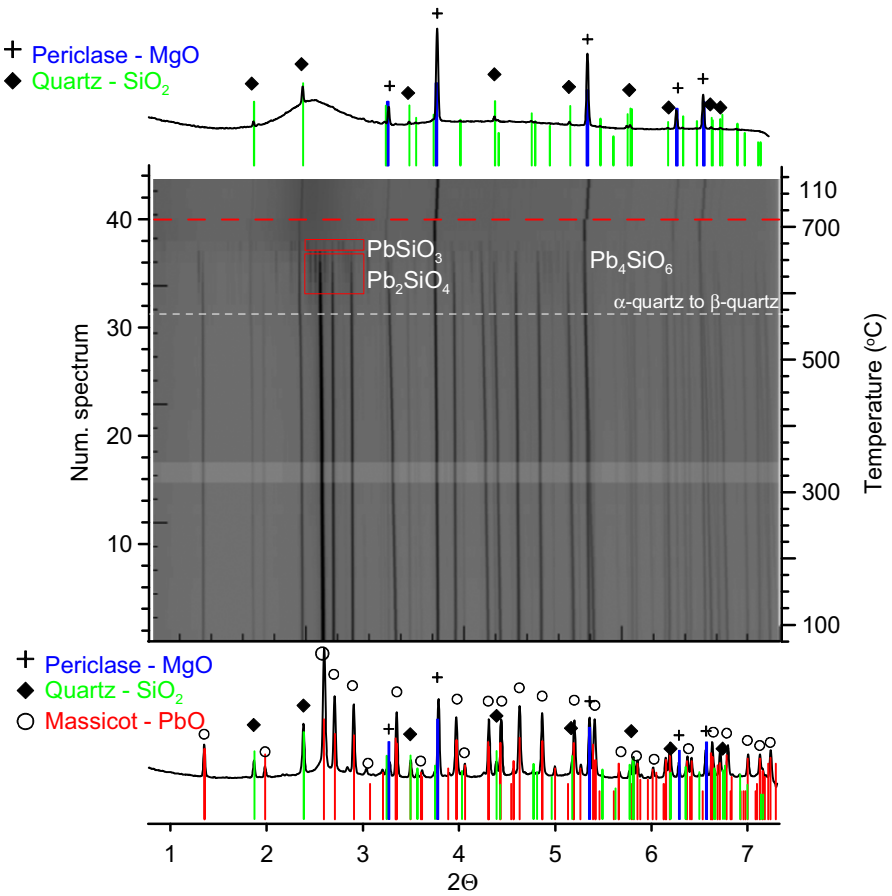

FIGURE 2 High-temperature XRD patterns (HT-SR-XRD) obtained during the firing of 70 wt% PbO-30 wt% SiO_2. The XRD patterns corresponding to the initial mixture before heating (bottom) and after cooling (top) are also shown

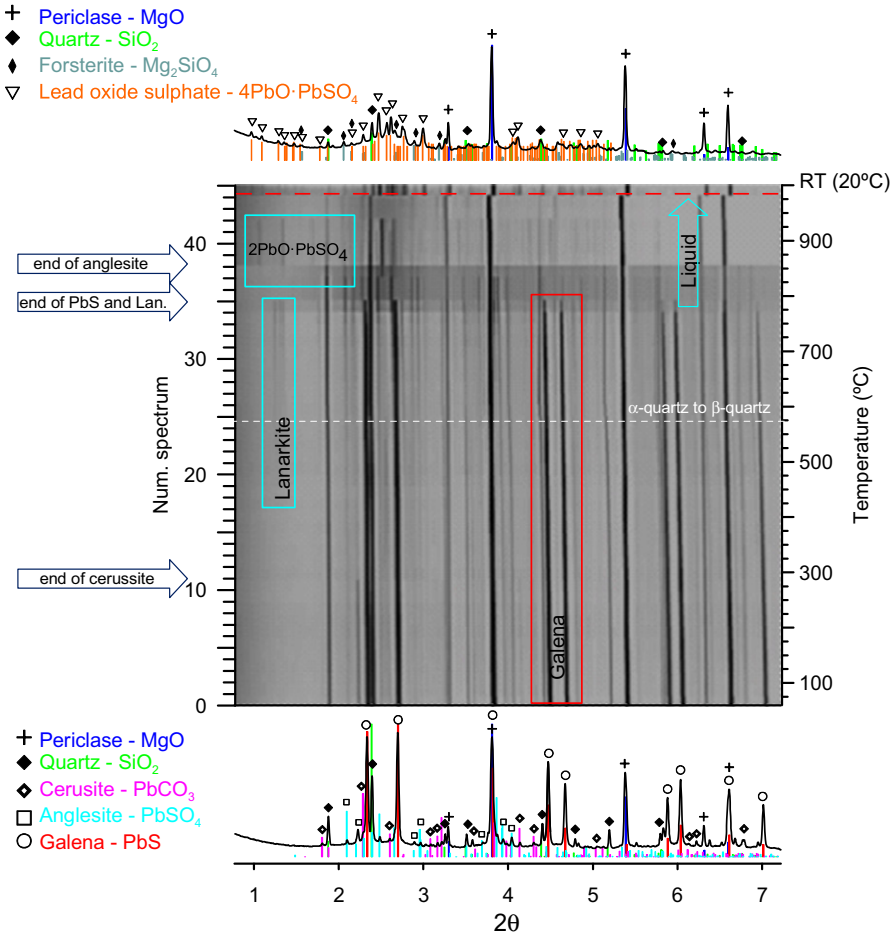

FIGURE 3 High-temperature XRD patterns (HT-SR-XRD) obtained during the firing of the mixture 75 wt% PbS-30 wt% SiO_2. The XRD patterns corresponding to the initial mixture before heating (bottom) and after cooling (top) are also shown

disappeared completely at 727°C with an increase in the range 715-722°C, just when Pb_4SiO_6 decomposed incongruently into Pb_2SiO_4 and $PbSiO_3$.

3.2 | High-temperature resolved XRD experiment PbS–SiO_2

The high-temperature diffraction data obtained for a mixture of 75 wt% of galena plus 30 wt% of quartz with a composition equivalent to the eutectic composition 70 wt% PbO:30 wt% SiO_2 are shown in Figure 3. The appearance and disappearance of the phases are also marked. The initial compounds determined were galena (PbS), α-quartz, anglesite ($PbSO_4$), cerussite ($PbCO_3$), as well as periclase (MgO) from the crucible. Both anglesite and cerussite are weathering compounds of the natural galena deposit and were present in a very small amount. The thermal stability ranges of the crystalline phases identified are summarized in Figure 4B.

Galena was stable up to 315°C and then began to slowly decrease until it disappears completely at 795°C. A melt coexisting with other crystalline compounds appeared at about 775°C (a melt is expected at 717°C in the system 70 wt% PbO-30 wt% SiO_2).[10] With regard to the galena weathering compounds, cerussite was stable up to 275°C decreasing from 275°C upwards and disappearing at 315°C. Massicot (PbO) appeared at 315°C increasing up to 475°C and completely disappearing at 595°C. Anglesite was stable up to 575°C, increasing between 575 and 775°C and afterward decreasing when it completely disappeared at 860°C. The reversible transformation between α-$PbSO_4$ and β-$PbSO_4$ at 883°C did not occur because the anglesite had already fully decomposed at a lower temperature (≈860°C) in our system. The appearance of lead oxysulfate, PbO·$PbSO_4$ (lanarkite),[17] followed the decrease in galena (above 315°C) increasing progressively, but more quickly between 595 and 775°C. Lanarkite suddenly disappeared at 795°C, and a lead dioxy-sulfate, 2PbO·$PbSO_4$, formed. The lead dioxy-sulfate, 2PbO·$PbSO_4$, began to decrease at 900°C completely disappearing at 950°C. Minium (Pb_3O_4) formed between 810 and 860°C and was not found at 900°C. Meanwhile, a second melt developed; in fact, according to the PbO–$PbSO_4$ phase diagram, a sulfate melt should appear at this temperature.[13] At 900°C, forsterite (Mg_2SiO_4) was also formed due to the reaction of the silica melt with the magnesia crucible. After cooling, the crystalline phases found were 2PbO·$PbSO_4$ and 4PbO·$PbSO_4$ crystallizing from the sulfate melt, quartz, and forsterite (Mg_2SiO_4).

In summary, the oxidation of galena (Figures 4 and 5) gave rise mainly to the formation of lanarkite, anglesite, and $2PbO{\cdot}PbSO_4$. In theory, anglesite is the first phase formed during the oxidation of galena.[11] However, this is only true at very low temperatures. According to other studies,[14] lanarkite is actually the phase predominantly formed during the roasting of galena at 600°C.[6] In our case, the anglesite determined was, in fact, already present in the original galena ore although some was also formed during the decomposition of galena between 600 and 800°C. The $PbO–PbSO_4$ phase diagram[11] indicates that both $PbSO_4$ and $PbO{\cdot}PbSO_4$ are stable at temperatures below 928°C when a sulfate liquid is formed. In contrast, in our case, a $PbO–SiO_2$ melt already developed at a lower temperature ~775°C and anglesite disappeared completely at ~860°C. In addition, the $PbO–PbSO_4$ phase diagram also indicates that, on further oxidation, lanarkite and $2PbO{\cdot}PbSO_4$ should coexist. However, in our case, lanarkite decomposed completely at 795°C, while the lead dioxysulfate, $2PbO{\cdot}PbSO_4$, was formed which in turn decomposed at 950°C when a melt was formed. During the cooling, two lead oxysulfates, $2PbO{\cdot}PbSO_4$ and $4PbO{\cdot}PbSO_4$, recrystallized from the melt; this is consistent with the $PbO–PbSO_4$ phase diagram where both compounds are stable below 863°C.[11] In fact, the presence of these lead oxysulfates indicates that a complete oxidation of galena into PbO was not obtained during the heating.

3.3 | Analysis of a misfired lead glaze

The misfired lead glaze exhibits three distinctive areas of different colors: opaque green, opalescent yellowish, and transparent honey, Figure 1. Figure 1A-C shows SEM BSE images corresponding to the green, yellow, and honey-colored areas, respectively. Three types of crystallites are observed in the three areas, and all of them contain mainly Pb and S (Figure 1D). Type I crystals appearing light gray are found only in the green glaze, Figure 1A. Type II crystals, which appear slightly darker in the SEM BSE images, show tabular or elongated sections of euhedral crystals. They also have a similar composition to Type I crystals, Figure 1D, and are found in both the green and the yellow glazes, Figure 1A,B. Type III crystals show a similar light gray color and share the tabular or elongated sections of

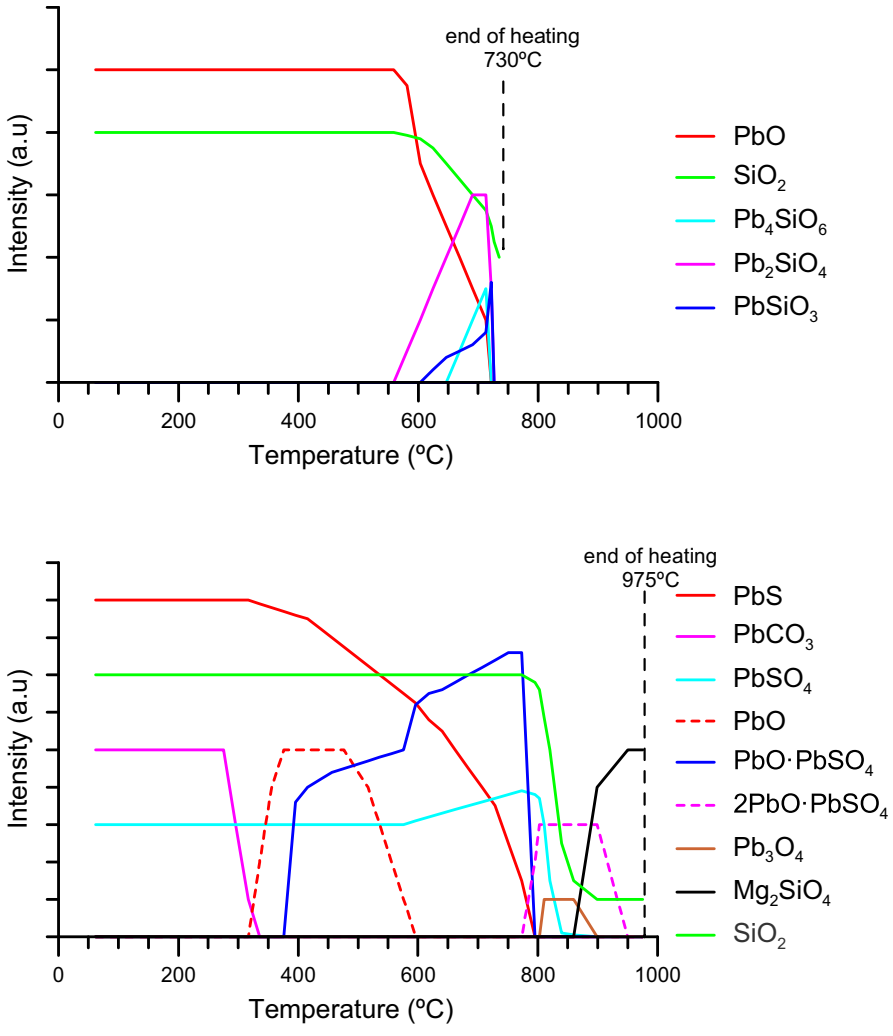

FIGURE 4 Thermal stability ranges of the crystalline phases identified for (A) $PbO–SiO_2$ and (B) $PbS–SiO_2$. The ordinate axis is obtained from the intensity of the principal peak of each crystalline phase relative to the intensity of the MgO crucible and gives a qualitative temperature evolution of each compound

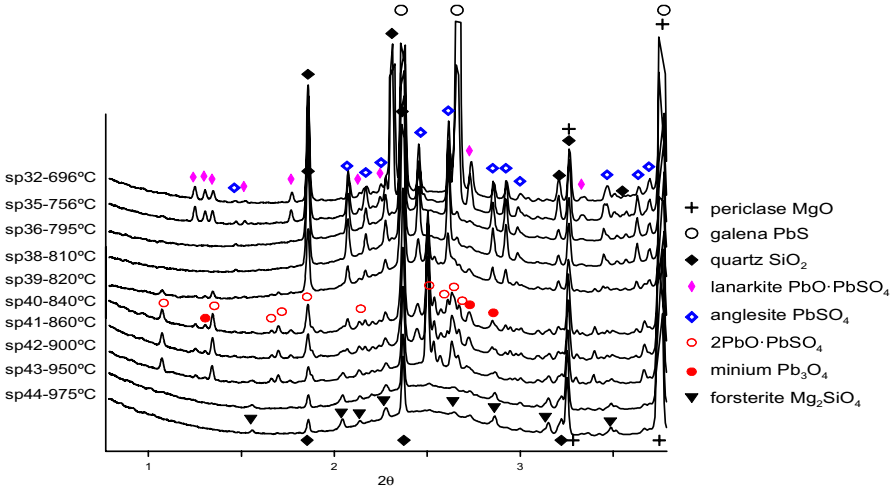

FIGURE 5 Selection of HT-SR-XRD patterns of the final firing stage for the mixture PbS–SiO_2

euhedral crystals as found in Type II. They are present in the three colored areas of the glaze, Figure 1. However, the chemical composition of Type III crystals is slightly different to those of Type II; they contain mainly Pb and S, but also some Cl, and minor amounts of Si and Ca, Figure 1D. Crystallites, Type II and Type III, show a similar atomic contrast in the BSE images. Quantitative chemical analysis of the crystallites is not possible with the EDS detector because of the large overlapping of S-Kα, Pb-Mα, and Cl-Kα X-ray fluorescent peaks. Consequently, the chemical composition of the crystallites and the glaze is obtained by EPM, using a wavelength dispersive X-ray spectroscopy detector system (WDS) with a superior X-ray peak resolution and greater peak to background ratio. The chemical composition of the glaze in wt% is 73.5% PbO, 19.6% SiO_2, 1.5% Al_2O_3, 1.5% SO_3, 1.2% ZnO, 1.1% FeO, 0.5% Na_2O + K_2O, 0.2% CaO, and 0.05% Cl. The average and standard deviation of the various analyses made on the crystallites are shown in Table 1. Type I crystals contain 86.1 wt% Pb and 13.6 wt% S and no O, corresponding to galena. Type II and Type III crystallites are identified by SR-μXRD as lanarkite, $PbO{\cdot}PbSO_4$, and mattheddleite, a lead silicate sulfate chloride[18-20] of composition $Pb_{10}(SiO_4)_{3.5}(SO_4)_2Cl_2$, respectively, as shown in Figure 6. The chemical composition obtained for the Type II crystals is also in good agreement with those of lanarkite, $PbO{\cdot}PbSO_4$. Conversely, the chemical composition determined for the Type III crystallites $(Ca_{0.04},Pb_{0.96})_{10}(SiO_4)_4(SO_4)_2Cl_{0.8}$ differs from the theoretical composition; contains less Cl, some unexpected Ca, and unbalanced Si and S. In fact, mattheddleite is a rare mineral of the apatite supergroup (ellestadite) of theoretical composition $Pb_5(SiO_4)_{1.5}(SO_4)_{1.5}(Cl,OH)$[21]; the other endmembers of this group are hydroxylellestadite and fluorellestadite of theoretical composition $Ca_5(SiO_4)_{1.5}(SO_4)_{1.5}(OH)$ and $Ca_5(SiO_4)_{1.5}(SO_4)_{1.5}F$, respectively.[20] Consequently, calcium may also be incorporated in the structure. The unbalanced Si and S measured by EPM were already noticed and associated to large and inaccurate absorption corrections occurring when celestite is used as S standard.[21] In fact, our data are in good agreement with other mattheddleite EPM analysis. In our case, the neoformed inclusions of mattheddleite integrated available elements from the surrounding environment (glaze) during crystallization and, particularly, incorporated some calcium. The gangue also included some sphalerite grains that explain the presence ZnO in the glaze.

Under the optical microscope (Figure 7), galena is easily recognizable in reflected light, Figure 7C, by its high reflectance and because of the fractures along the cubic planes of exfoliation of some grains. Lanarkite and mattheddleite can be distinguished with crossed polarized light (XPL); lanarkite displays 2nd/3rd-order interference colors and inclined extinction (birefringence = 0.108), while mattheddleite has straight extinction and 1st and low 2nd-order interference colors (birefringence = 0.018), Figure 7B. In addition, some tabular sections of lanarkite show polysynthetic twins. In reflected light, lanarkite

TABLE 1 Average and standard deviation (in parenthesis) of the chemical composition of the crystallites measured by electron microprobe

wt%	N	Pb	S	Si	Cl	Ca	O	Sum
Type I	6	86.1 (0.3)	13.6 (0.1)	—	—	—	—	99.7 (0.3)
Type II	8	78.1 (0.8)	5.5 (0.1)	0.2 (0.2)	—	0.1 (0.1)	14.6 (0.2)	98.5 (1.1)
Type III	9	75.1 (0.5)	2.5 (0.1)	4.5 (0.3)	1.2 (0.2)	0.7 (0.1)	14.9 (0.2)	98.8 (0.3)

The oxygen is calculated by stoichiometry.
N, number of crystallites measured.

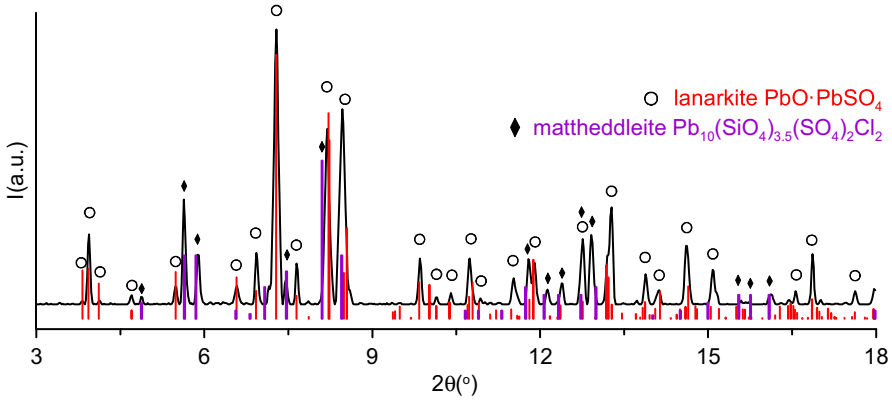

FIGURE 6 Synchrotron radiation micro-X-ray diffraction pattern of the crystallites in the misfired glazes. The reference patterns marked correspond to the JPDF database patterns 01-071-2069 for lanarkite and 00-041-0610 for mattheddleite

shows relief and a darker contrast than mattheddleite, Figure 7C.

The presence of different crystallites in the glaze is responsible for the various appearances and colors of the three areas: opaque green, translucent yellow, and transparent honey. The occurrence of galena grains accounts for the opacity, and the presence of Fe^{2+} ions dissolved in the glaze is most probably responsible for the green color. The concurrence of galena and Fe^{2+} is explained by the glaze exposure to a reducing atmosphere during the firing. The shortage of oxygen is responsible for both the delayed decomposition of galena and the reduction in the iron ions. A possible cause for this reducing atmosphere might be the exposure of the glazed surface to the flame. The opalescent yellow and the transparent honey areas would not have been exposed and, consequently, show the yellow tinge characteristic of Fe^{3+} and of lead glazes. Although both lanarkite and mattheddleite crystallites are present in the opalescent yellow area, lanarkite crystallites are responsible for the opalescence, as they have a pearly luster appearing macroscopically translucent. The transparent honey area, however, contains only mattheddleite crystallites, which are transparent and show an adamantine luster.

4 | DISCUSSION

Although the first experimental studies of the $PbO–SiO_2$ system[9] indicated that a series of compounds with PbO: SiO_2 mole ratios of 4:1, 3:1, 2:1, 1:1, and 5:8 were formed; only $PbSiO_3$, Pb_2SiO_4, and Pb_4SiO_6 were confirmed by other research.[8,22] Moreover, Jak et al[23] found that $PbSiO_3$ and Pb_2SiO_4 melt congruently, while Pb_4SiO_6 decomposes incongruently. Our high-temperature experiment is in perfect agreement with this. Moreover, the temperatures at which the different compounds form and decompose match our data, supporting the validity of our kinetic data.

On the other hand, based on the PbO-$PbSO_4$ phase diagram[13] for temperatures lower than 860°C, anglesite ($PbSO_4$) and lanarkite ($PbO·PbSO_4$) are the two stable

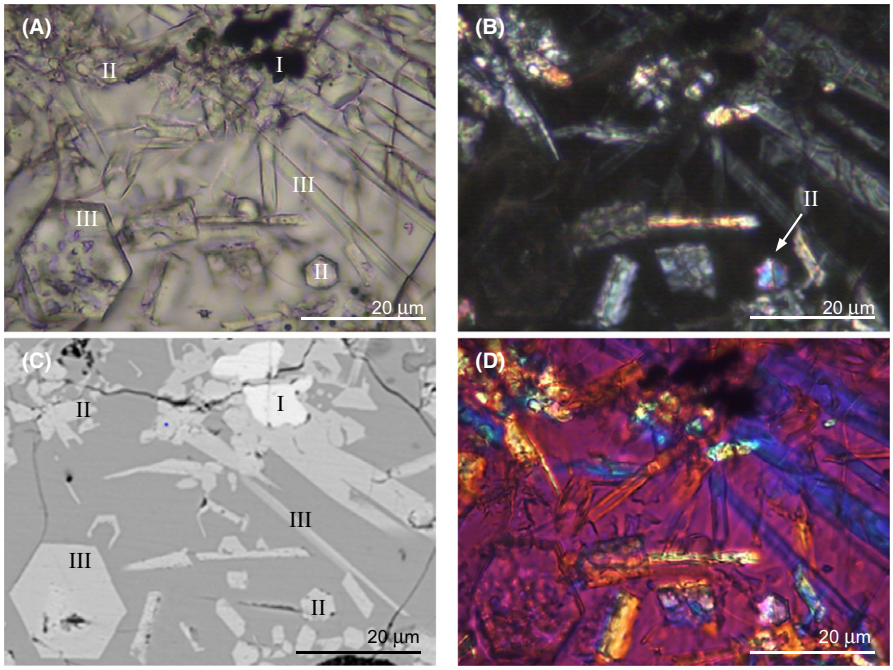

FIGURE 7 Optical microscopy images of the green area glaze. (A) PPL transmitted light showing opaque grains of galena (I), transparent crystals of lanarkite (II), and mattheddleite (III); (B) XPL transmitted light where the elongated section of the mattheddleite crystals shows a 1st-order gray color, and the hexagonal basal sections are extinguished: the elongated and prismatic sections of lanarkite exhibit 2nd/3rd-order interference colors; marked with an arrow, a twin; (C) reflected light, galena (I) appears very reflectant, mattheddleite (III) exhibits lower relief than lanarkite (II); (D) XPL transmitted light with ¼ lambda compensator

phases. Further oxidation tends to form lanarkite which leads to the subsequent development of first $2PbO{\cdot}PbSO_4$ and then $3PbO{\cdot}PbSO_4$.[24]

In the $PbS–SiO_2$ system studied, lead silicates are not formed. The lack of lead silicates is probably due to remaining sulfates in the glaze mixture that handicapped the crystallization of the PbO/SiO_2 compounds. The oxidation of galena gives rise mainly to the formation of lanarkite ($PbO{\cdot}PbSO_4$) at a temperature as low as ~315°C disappearing suddenly at 795°C. The sudden disappearance of lanarkite in the $PbS–SiO_2$ system happens at lower temperatures than in the $PbO–PbSO_4$ system. This can be related to the presence of SiO_2, which certainly plays a role, giving rise to a $PbO–SiO_2$ melt at ~775°C. The green and yellow areas of the misfired glaze also show the presence of a silica melt and lanarkite, but not the compounds formed at higher temperatures. Anglesite is often present in the original galena ore as a weathering product and, considering that it is stable up to ~860°C, it should be found in the misfired glaze. Therefore, the absence of anglesite could be an indicative that it was not present in the galena used by ancient potters.

The two basic lead sulfates, $2PbO{\cdot}PbSO_4$ and $4PbO{\cdot}PbSO_4$ which are formed after the lanarkite decomposition in the high-temperature experiment, are not found in the honey area of the historical lead glaze. In fact, the presence of both galena and lanarkite in the misfired glaze indicates not only a low firing temperature (below 795°C) but also a short firing. Moreover, the flame also produces a reducing atmosphere, which delays sulfur oxidation and sulfate decomposition. The green and yellow colors of the misfired areas also indicate the presence of reduced and oxidized iron, respectively. Therefore, we can also suppose that the lack of oxygen due to the direct hit of the flame in the area affected the oxidation of galena and lanarkite and the formation of the glaze. Conversely, the transparent honey glaze shows neither galena nor lanarkite. However, mattheddleite $Pb_5(SiO_4)_{1.5}(SO_4)_{1.5}(Cl,OH)$, with some calcium substituting the lead atoms, is identified. Mattheddleite occurs in oxidized zones of lead deposits, associated with lanarkite and anglesite, and its formation is driven by the presence of chlorine. The thin cross section shows the sequence of formation of the sulfate compounds in the glaze. Galena is found surrounded by lanarkite crystals, Figure 7A, while lanarkite is found inside mattheddleite crystals in the green area of the glaze, Figure 8. Therefore, the sequence of compounds formed during the oxidation of galena is, first lanarkite and then mattheddleite, provided chlorine is available in the surrounding glaze.

There are two possible sources for the chlorine found in the glazes; it formed part of the galena mineral or there was contamination during the firing. A very popular lead mineral extraction site in Catalonia is the Begur Coast, also known as the coast of the six lead mines.[25] The mines are often flooded by seawater, which could explain the presence of chlorine in the galena gangue. On the other hand, the ashes generated burning halophyte type plants[26,27] during the firing could also provide chlorine to the surface of the glazes. In fact, the presence of ashes on the glaze surface during the firing could also explain the preferential direction of growth shown by the mattheddleite crystals—from the glaze surface toward the ceramic body—observed in the yellowish and honey areas of the glaze, Figure 1B,C.

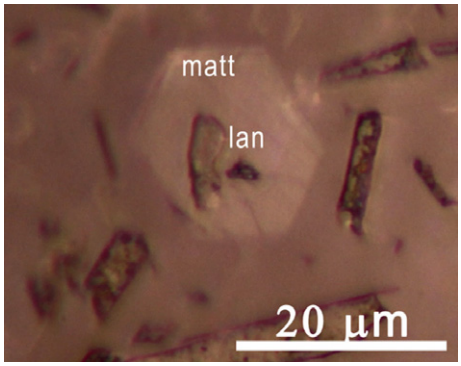

FIGURE 8 Optical microscopy image in reflected light of a lanarkite crystallite inside a crystal of mattheddleite

The supposed disadvantage initially considered based on the $PbO–PbSO_4$ phase diagram, of the high temperatures at which the decomposition of the lead sulfates and formation of a melt (~928°C) happen is not correct for the system $PbS–SiO_2$. Our data show that, in the system $PbS–SiO_2$ at a temperature as low as 775°C, a melt is formed and that, at 795°C, the lanarkite is already fully decomposed. Nevertheless, adequate oxidation conditions are necessary to help the oxidative process take place. Consequently, optimal firing conditions for the $PbS–SiO_2$ system are a temperature only slightly higher than those of the $PbO–SiO_2$ system provided adequate oxidative conditions are guaranteed.

5 | CONCLUSIONS

The transformations during the production of a lead glaze with galena $PbS–SiO_2$ were studied by means of a HT-SR-XRD. The phase transformations and thermal stability of the compounds formed were determined, and the results obtained were compared to the available data for the $PbO–SiO_2$ and $PbO–PbSO_4$ systems. The oxidation of galena gives rise to the formation of lanarkite, $PbO{\cdot}PbSO_4$, at 315°C and its decomposition at 795°C, a temperature lower than those found in the $PbO–PbSO_4$ system (916°C). Moreover, in agreement with the $PbO–PbSO_4$ system, once lanarkite decomposes, two basic lead sulfates, $2PbO{\cdot}PbSO_4$ and $4PbO{\cdot}PbSO_4$, form. Lead silicates do not form in the $PbS–SiO_2$ system contrary to what is observed in the $PbO–SiO_2$

system where they form at temperatures above 750°C. The presence of lead sulfates in the silicate melt prevents the formation of the lead silicates. The results obtained show that the optimal firing conditions for the PbS–SiO_2 system are a temperature rather similar to the PbO–SiO_2 system, but when galena is used, highly oxidative conditions need to be guaranteed in order to eliminate sulfur from the glaze.

A historical misfired lead glaze still retaining relics of galena was also studied, and the crystalline phases developed were identified. Different color areas—green, yellow, and honey—showing different crystalline compounds of the glaze were discussed. Galena, lanarkite, $PbO{\cdot}PbSO_4$, and mattheddleite, $(Ca,Pb)_{10}(SiO_4)_{3.5}(SO_4)_2Cl_2$, were identified. The crystallites are responsible for the opaque green (galena, lanarkite, and mattheddleite), opalescent yellow (lanarkite and mattheddleite), and transparent honey (mattheddleite) colors observed on the surface of the sample. The presence of galena and lanarkite indicates a maximum temperature of 795°C, although the reducing action of the flame could have delayed sulfur and sulfate oxidation even at higher temperatures. The crystallization of mattheddleite and its directional growth from the surface toward the glaze could be explained by the deposition of plant ashes on the glaze surface during the firing.

ACKNOWLEDGMENTS

Roberta Di Febo is grateful to the UVIC-UCC Scholarship Program, awarded by University of Vic, Central University of Catalonia. The authors are grateful to the project MAT2016-77753-R, 2017-2019 funded by the Ministerio de Ciencia e Innovación (Spain) and the ALBA Synchrotron Light Facility 2014060905 (BL04). Thanks are due to the project 2014SGR00581 (T.P.), 2014SGR1585 (J.M. and R.D.F.), and 2014SGR1661 (J.C.M.).

ORCID

Roberta Di Febo http://orcid.org/0000-0002-1102-8231
Judit Molera http://orcid.org/0000-0003-3116-0456
Trinitat Pradell http://orcid.org/0000-0002-8720-5492
Joan C. Melgarejo http://orcid.org/0000-0001-7544-1191
Oriol Vallcorba http://orcid.org/0000-0001-6499-7688

REFERENCES

1. Tite MS, Freestone I, Mason R, et al. Lead glazes in antiquity—methods of production and reasons for use. *Archaeometry*. 1998;40:241-260.
2. Wood N, Freestone I. A Preliminary Examination of a Warring States Pottery Jar with So-Called "Glass Paste" Decoration. In Guo J, ed. *Science and Technology of Ancient Ceramics: 3. Proceedings of the International Symposium on Ancient Ceramics*. Shanghai, Chine: Shanghai Res. Soc. Sci. Technol. Ancient Ceram.; 1995:12-17.
3. Wood N. *Chinese Glazes, the Origins, Chemistry and Re-Creation*. Philadelphia, PA: A&C Black London and University of Pennsylvania Press; 1999.
4. Walton M, Tite MS. Production technology of Roman lead glazed pottery and its continuance into late antiquity. *Archaeometry*. 2010;52:733-759.
5. Molera J, Pradell T, Salvadó N, et al. Lead Frits in Islamic and Hispano-Moresque Glazed Productions. In: Shortland AJ, Freestone IC, Rehren T, eds. *From Mine to Microscope: Advances in the Study of Ancient Technology*. Oxford: Oxbow Books; 2007:11-22.
6. Gómez A, Gil C, Di Febo R, et al. Casa Convalescència (Vic, Osona): Aproximació arqueológica i arqueomètrica a un conjunt de vasos ceràmics del segle XVIII. In: *Actes III Jornades d'Arqueologia de la Catalunya Central*. Publicacions d'Arqueologia i Paleontologia 9; 2015:70-81.
7. Lessler MA. Lead and lead poisoning from antiquity to modern times. *Ohio J Sci*. 1988;88:78-84.
8. Geller RF, Creamer AS, Bunting EN. The system PbO–SiO_2. *J Res Nut Bur Stand*. 1934;13:237-244.
9. Smart RM, Glasser FP. Compound formation and phase equilibria in the system PbO–SiO_2. *J Am Ceram Soc*. 1974;57:378-382.
10. Factsage. Phase diagram PbO–SiO_2. http://www.crct.polymtl.ca/fact/phase_diagram.php?file=Pb-Si-O_PbO-SiO2.jpg&dir=FToxid. Accessed June 8, 2017.
11. Eric RH, Timucin M. Phase equilibria and thermodynamics in the lead-lead sulphide system. *J S Afr Inst Min Metall*. 1969;88:353-361.
12. Kullerud G. The lead-sulfur system. *Am J Sci*. 1969;267:233-256.
13. Billhardt HW. New data on basic lead sulfates. *J Electrochem Soc*. 1970;117:690-692.
14. Abdel-Rehim AM. Thermal and XRD analysis of Egyptian Galena. *J Therm Anal Calorim*. 2006;86:393-401.
15. Hammersley P, Svensson SO, Hanfland M, et al. Two-dimensional detector software: from real detector to idealised image or two-theta scan. *High Press Res*. 1996;14:235-248.
16. Fauth F, Peral I, Popescu C, et al. The new material science powder diffraction beamline at ALBA synchrotron. *Powder Diffr*. 2013;28:360-370.
17. Richemond WE, Wolfe C. Crystallography of lanarkite. *Am Min*. 1938;23:799-804.
18. Livingstone A, Ryback G, Fejer EE, et al. Mattheddleite, a new mineral of the apatite group from Leadhills, Strathclyde Region. *Scott J Geol*. 1987;23:1-8.
19. Steele IM, Pluth JJ, Livingstone A. Crystal structure of mattheddleite: a Pb, S, Si phase with the apatite structure. *Min Mag*. 2000;64:915-921.
20. Pasero M, Kampf AR, Ferraris C, et al. Nomenclature of the apatite supergroup minerals. *Eur J Mineral*. 2010;22:163-179.
21. Essene EJ, Henderson CE, Livingstone A. The missing sulphur in mattheddleite, sulphur analysis of sulphates and paragenetic relations at Leadhills, Scotland. *Min Mag*. 2016;70:265-280.
22. Calvert PD, Shaw RR. Liquidus behavior in the silica-rich region of the system PbO–SiO_2. *J Am Ceram Soc*. 1970;53:350-352.
23. Jak E, Degterov S, Wu P, et al. Thermodynamic Optimization of the Systems PbO–SiO_2, PbO–ZnO, ZnO–SiO_2 and PbO–ZnO–SiO_2. *Metall Mater Trans B*. 1977;28:1011-1018.

24. Ponsot B, Salomon J, Walter P. RBS study of galena thermal oxidation in air with MeV O^{3+} ion beam. *Nucl Instr Meth Phys Res B*. 1998;136–138:1074-1079.
25. Perelló JMM. *Els minerals de Catalunya*. Barcelona: Institut d'Estudis Catalans; 1990.
26. Lynggaard F. *Tratado de cerámica*. Barcelona: Ediciones Omega; 1976.
27. Misra M, Raglund K, Baker A. Wood ash composition as a function of furnace temperature. *Biomass Bioenergy*. 1993;4:103-116.

How to cite this article: Di Febo R, Molera J, Pradell T, Melgarejo JC, Madrenas J, Vallcorba O. The production of a lead glaze with galena: Thermal transformations in the PbS–SiO_2 system. *J Am Ceram Soc*. 2017;00:1–11. https://doi.org/10.1111/jace.15346

5.2 *Technological implications of neo-formed hematite crystals in ceramic lead glazes*

STAR: Science & Technology of Archaeological Research, 3 (2), 366-375 (2018)
DOI: 10.1080/20548923.2017.1419675
Di Febo, R., Molera, J., Pradell,T., Vallcorba, O. Capelli, C.

5.2.1 Introduction

Hexagonal neo-formed and skeletal crystallites were observed in thin sections of different Medieval and Post-Medieval lead glazed ceramics. The medieval and post-medieval lead glazed ceramics share some common technical features: a moderately developed interface, red/orange Fe-rich bodies and transparent high lead glazes with a relatively low content of FeO. The hexagonal crystallites were clearly visible in thin section with transmitted light (PPL/TL). On the contrary, their plate shape and their tiny thickness made them barely visible on the polished sections by using scanning electron microscopy (SEM). In order to analyse them, Focus Ion Beam (FIB) was used to produce polished cross sections of the crystals, while EDS analysis were carried out on the cross sections to obtain chemical information. Furthermore, additional data from micro Raman spectroscopy and Synchrotron radiation micro-X ray diffraction were obtained. The hexagonal crystallites were identified together with skeletal crystals in the brown decorated areas. Then, their presence was discussed in terms of composition of the glaze, temperature, conditions of the firing process. In order to understand the thermal range at which the crystallites were formed replications were made in controlled laboratory conditions.

5.2.2 Results

Two types of crystallites were identified in thin section in the brown area of the glazes: elongated skeletal crystals of melanotekite ($Pb_2Fe_2Si_2O_9$) and hexagonal brown/orange crystals of hematites. The latter, weren't visible on the polished surface as hexagons in SEM-BSE images. For this reason, a polished thin section of the glaze was milled by FIB in the area of the crystallites. From that, it was possible to see that the crystallites have a thickness of about 200 nm. Reliable EDS analyses on the hexagonal crystallites were impossible to carry out due their very small thickness. A Raman investigation was also performed focusing on the crystals that lay under the polished glaze surface and getting the corresponding Raman spectra. However, the Raman instrumentation seemed not sensitive enough (that was possibly due to the tiny thickness of the crystals) and the presence of a specific phase was impossible to confirm. Finally, a micro X-ray diffraction using Synchrotron Light

was performed directly on the polished thin section. In this manner, the hexagonal crystallites that were under the polished surface were easily localized and unambiguously identified as hematite. Later, replications under laboratory controlled conditions were performed in order to understand the thermal behaviour of hematite and melanotekite. The results can be summarized as following:

- Hematite crystals growing at the ceramic body-glaze interface appeared in all replicas (850ºC, 900ºC, 925ºC, 950ºC, 980ºC and 1050ºC)
- Hematite in association with melanotekite was found in those replications fired at 850ºC.
- Above 920ºC melanotekite appeared completely absent.

STAR: SCIENCE & TECHNOLOGY OF ARCHAEOLOGICAL RESEARCH
2017, VOL. 3, NO. 2, 366–375
https://doi.org/10.1080/20548923.2017.1419675

Routledge
Taylor & Francis Group

OPEN ACCESS Check for updates

Technological implications of neo-formed hematite crystals in ceramic lead glazes

Roberta Di Febo [a], Judit Molera [a], Trinitat Pradell [b], Oriol Vallcorba [c] and Claudio Capelli [d]

[a]MECAMAT Research Group Engineering Department, Faculty of Sciences and Technology, University of Vic – Central University of Catalonia, Barcelona, Spain; [b]Physics Department, Barcelona Research Center in Multiscale Science and Engineering (BRCMSE), Universitat Politècnica de Catalunya, Barcelona, Spain; [c]Alba Synchrotron Light Source, Barcelona, Spain; [d]Universita degli Studi di Genova, Genova, Italy

ABSTRACT

Hexagonal neo-formed crystallites have been observed in thin section of different medieval and post-medieval lead-glazed ceramics. Although they are clearly visible in thin section using plane polarized light, their plate shape makes them barely seen on the polished cross sections. Basal sections have never been found on the polished sections and only few transversal very thin sections could be seen. In this case, the morphology resembles acicular and it is not possible to analyze them properly by SEM–EDX because the crystals are very thin and the glaze surrounding is analyzed as well. Micro-Raman microscopy was carried out directly on the polished thin sections. This technique allows specific areas as small as 1 µm in diameter to be analyzed and it is able to characterize inclusions that are not found on the glaze surface. However, the wavenumber features observed cannot be assigned to a specific compound. The thickness of the crystallites (a few hundred nanometers) seems to be responsible for the low sensitivity of the Raman instrumentation. 15×15 µm^2 micro-X-ray diffraction patterns using synchrotron radiation (SR-μXRD) in transmission geometry were obtained from the crystals using the same thin section preparation. SR-μXRD was able to localize the crystallites and avoid the overlapping signals corresponding to other mineral phases. In this way, the hexagonal crystallites present in the glaze have been unambiguously identified as hematite crystallites. Finally, some replications were made under laboratory-controlled conditions to determine the firing conditions in the formation of those crystallites. The presence of hematite coexisting with melanotekite indicates a firing temperature <925°C, while the presence of only hematite suggests a firing temperature >925°C

ARTICLE HISTORY
Received 9 May 2017
Accepted 14 December 2017

KEYWORDS
Hematite; ceramic lead glazes; OM; SEM–EDS; micro-Raman; SR-μXRD

1. Introduction

Studying lead-glazed potteries from different places and periods by thin section petrography, we found brown/deep orange hexagonal neo-formed crystallites precipitated at the body–glaze interface (Figure 1(a, b)). We documented these kinds of crystallites in green-glazed wares from North Africa (Figure 1(c)) and Italy (thirteenth century), Spanish-glazed coarse wares (eighteenth century), Ligurian Taches Noires wares (eighteenth century), Catalan and French imitations (Figure 1(d)) of the Ligurian Taches Noires wares (eighteenth–nineteenth century) and Catalan coarse-glazed wares (eighteenth century), (Capelli, Mannoni, and Cabella 2007; Capelli et al. 2013; Beltrán de Heredia Bercero et al. 2015; Gómez et al. 2015; Di Febo 2016; Capelli et al. 2017). The medieval and post-medieval lead-glazed ceramics taken into account for our study share some common technical features. All the ceramics exhibit a red/orange color of the bodies due to oxidizing firing conditions and an interface moderately developed. The ceramic bodies consist of Fe-rich clay while the glazes are of the transparent high lead type (Tite et al. 1998). They contain between 45 and 60% PbO, an alkali content normally lower than 2% ($Na_2O + K_2O$), an alumina content in the range 2–7% $A1_2O_3$ and an iron oxide content of about 4.5–6% (FeO wt%).

These crystallites are clearly visible in thin section with plane polarized light (PPL). This is due to the fact that petrographic inspection of the glaze thin sections gives a 3D perspective of the crystallites and is able to reveal their microstructural features and distribution in the glazes. On the contrary, the plate shape makes them barely seen on the polished cross sections using scanning electron microscopy (SEM). Consequently, if they are not recognized, it is very unlikely that they can be analyzed. The basal sections have never been found on the polished surfaces and only few transversal very thin sections could be seen. In this case, it is not possible to analyze them properly by SEM–EDX because the sections of the crystallites are thinner than the electron beam. In order to identify

CONTACT Roberta Di Febo roberta.di@uvic.cat

© 2018 The Author(s). Published by Informa UK Limited, trading as Taylor & Francis Group
This is an Open Access article distributed under the terms of the Creative Commons Attribution License (http://creativecommons.org/licenses/by/4.0/), which permits unrestricted use, distribution, and reproduction in any medium, provided the original work is properly cited.

the hexagonal crystallites, additional data from micro-Raman spectroscopy and synchrotron radiation micro-X-ray diffraction (SR-μXRD) were obtained using thin section preparation.

The use of Raman microscopy for identifying and studying archaeological materials has flourished in recent years in addition to the standard analytical techniques (De Faria, Silva, and de Oliveira 1997; Clark and Curri 1998; Smith and Clark 2001; De Faria and Lopes 2002; Colomban and Truong 2004; Casadio, Daher, and Bellot-Gurlet 2016; Howell, Edwards, and Vandenabeele 2016). Some advantages of the Raman microscopy include its molecular specificity, no destructiveness, high spatial and spectral resolution and *in situ* analysis. In the Raman microscopy, materials are identified by comparing their characteristic vibrational spectra with those in a database. In our case, we work directly on the polished thin sections of the samples, because we consider that it is extremely important to see and check the crystallites on which the analysis is performed. In addition, μXRD using synchrotron radiation patterns have been also acquired on the thin glaze sections. The advantage of using synchrotron light is the high brilliance and probe size spot of some tens of micrometers. Other benefits include the possibility to localize the crystallites even if they are not found on the glaze surface layer and to avoid the overlapping signals corresponding to other crystallites. In this way, the hexagonal crystallites present in the glaze have been identified. Once the nature of these crystallites was identified, replications were made in controlled laboratory conditions in order to determine the temperature and firing conditions for their formation.

2. Experimental

A French imitation of the Ligurian Taches Noires pottery from the workshop of Jouques (Provence, France) has been analyzed in order to identify the hexagonal crystallites. We choose this sample due to the abundance of large hexagonal crystallites, some of them larger than 50 µm. The sample 9703 (Figure 1(d)) selected for the combined analyses is dated from the first half of the nineteenth century and corresponds to a plate. According to written sources, the workshop of Joques was established by an Italian, possibly a Ligurian potter (Amouric and Vallauri 1993). The ware called Taches Noires was developed in Albisola (Liguria, NW Italy) during the eighteenth century (Cameirana 1970, 1977). This type of ware is characterized by a fine, hard, deep red fabric and transparent glazes decorated with wavy dark bands of manganese oxides (Blake 1981).

The crystallites were first studied by optical microscopy (OM) using a petrological microscope (LEICA DM 2700 P). All of the stages of the analysis were carried out on the same polished thin section.

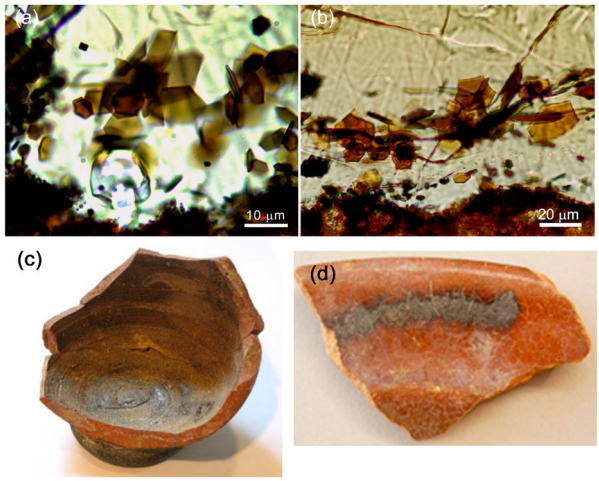

Figure 1 (a) and (b) OM images in PPL. Hexagonal crystallites in the glaze–body interface of a green-glazed ware and of a Ligurian Taches Noires pottery are visible. (c) Green-glazed ware from North Africa (thirteenth century). (d) French imitation of the Ligurian Taches Noires ware (eighteenth–nineteenth century).

In this manner, we were able to constantly observe and analyze the same inclusions. The ceramic sample was ground down to a standard thickness of 30 µm that permits the growth habits of the micro-crystallites to be identified by OM observation at magnifications ranging from about 10× to 100×. Details of thin section preparation methods can be found in Poole and Sims (2015). The crystallites as well as the glaze were analyzed by scanning electron microscopy with an energy-dispersive x-ray spectroscope attached (SEM–EDS) to ascertain their chemical composition. The bulk chemical composition of the glaze was determined by analyzing areas and avoiding the glaze–body interface, as well as other crystallites. A crossbeam workstation (Zeiss Neon 40) equipped with SEM (Shottky FE) column and EDS (INCAPentaFETx3 detector, 30 mm^2, ATW2 window) was employed. The microscope was operated at 20 kV, with 100 s measuring times, and backscattered electron (BSE) images were obtained. Quantitative analysis calibration was accomplished with mineral and glass standards.

Focus ion beam (FIB) was used to produce polished cross sections of the crystallites. A crossbeam workstation (Zeiss Neon 40) equipped with SEM (Shottky FE) and Ga + FIB columns was used to prepare cross sections of the crystals. First, the sample surface was coated with a thin protective Pt layer (1 µm) by ion-beam-assisted deposition; then the cross section was cut and polished and a thin layer of Pt deposited to enhance conductivity. Subsequently, secondary electron SEM images of the inclusions were obtained at 5 kV.

Micro-Raman analyses were carried out directly on the polished thin sections of the glazes at the Centres Científics i Tecnològics, University of Barcelona. Spectra were obtained with a HORIBA Jobin Yvon

LabRam HR 800 dispersive spectrometer, equipped with an Olympus BXFM optical microscope, using a 600 g/mm grating and a Synapse CCD detector cooled at −70°C. The Raman spectra reported in this study were recorded with the 532 nm excitation line of a solid state laser.

SR-μ-XRD was performed on the focused-beam station of the beamline BL04[12] at the ALBA Synchrotron. The areas of interest from the polished thin sections were selected using an on-axis visualization system and measured in transmission geometry with a focused beam of 15 × 15 μm^2 (full width at half-maximum). The energy used was 29.2 keV (λ = 0.4246 Å) and the diffraction patterns were recorded with a Rayonix SX165 CCD detector (active area of 165 mm diameter, frame size 2048 × 2048 pixels, 79 μm pixel size, dynamic range 16 bit). The calibration of the sample to detector distance and beam center (from a LaB_6 sample measured at the same conditions) and the radial integration of the images were performed with the Fit2D software.

Individual crystallites were measured at different rotation angles relative to a vertical axis centered on the crystal. The total oscillation ranges from −30° to 30° with each of the diffraction images comprising 10° oscillation. The radial integration of each image, although is not producing a powder pattern (missing reflections and intensities only from a single grain), contains enough peaks to identify the possible phases. Identification of the compounds has been performed based on the Powder Diffraction File (PDF) database from the International Centre for Diffraction Data (ICDD).

Reproductions of glazes, with the same composition than that of the sample 9703, were fired in oxidizing conditions at different temperatures; 850°C, 900°C, 920°C, 950°C, 980°C and 1020°C. The thermal paths were similar in all cases, 6 h of heating ramp, 10 min at maximum temperature and free cooling into the electric kiln. Samples were analyzed by OM and SEM.

3. Results

The sample 9703, selected for the combined analyses, corresponds to a nineteenth-century French imitation of Ligurian *Taches Noires* ware from Joques (Provence, France). This type of ware is characterized by transparent brown glazes decorated with wavy dark bands of manganese oxides (Blake 1981). The chemical composition of the sample 9703 shows high PbO (54.4 wt%) and SiO_2 (35.2 wt%) content, lower amounts of Fe_2O_3 (4.6 wt%), Al_2O_3 (2.5 wt%), MnO (0.8 wt%), CaO (0.7 wt%), MgO (0.3 wt%) and very low Na_2O and K_2O content (0.2 wt% and 0.9 wt%, respectively). The MnO content suggests that the manganese used for the dark decoration was partly dissolved into the glaze.

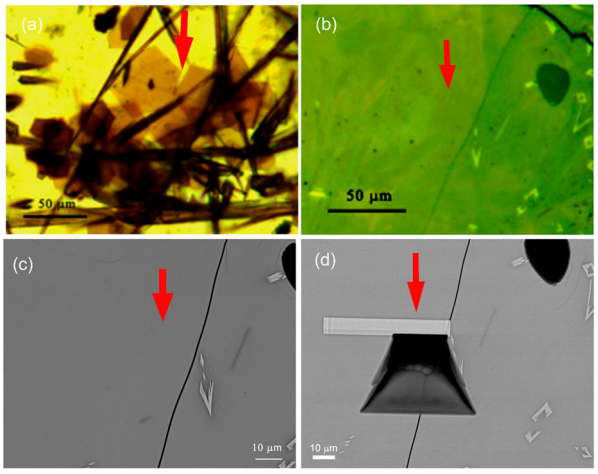

Figure 2. (a) OM image in plane polarized light of the thin section of the glaze 9703 (PPL). Hexagonal crystals (red arrow) in association with elongated honey skeletal crystals are clearly visible (b) The same area as in picture (a) in reflected light. Red arrow indicates the position of the hexagonal crystal marked on (a). It is not on the glaze surface and then it is not visible by reflection mode. (c) SEM backscattering image of the same area as in picture (a). The red arrow indicates the place of the same hexagonal crystal marked in (a). (d) SEM image of FIB polished cross section in the area of the hexagonal crystallite.

Two types of crystallites are found in the thin section of the glaze: elongated honey skeletal crystals and hexagonal brown/orange crystals (Figure 2(a)). The first ones were identified as melanotekite ($Pb_2Fe_2Si_2O_9$) formed during the firing process from the reaction among the constituents of the glaze mixture (Figure 3; Di Febo et al. 2017). Melanotekite crystals are easily seen in reflected light and in SEM backscattering mode as light crystals. On the contrary, the hexagonal crystallites are not found on the polished glaze surface and only a few very thin cross sections of these are visible (Figure 2(b,c)). They exhibit a light tinge in reflected light and grayish color in BSE images. In the area of the hexagonal crystallites of Figure 2(a) a

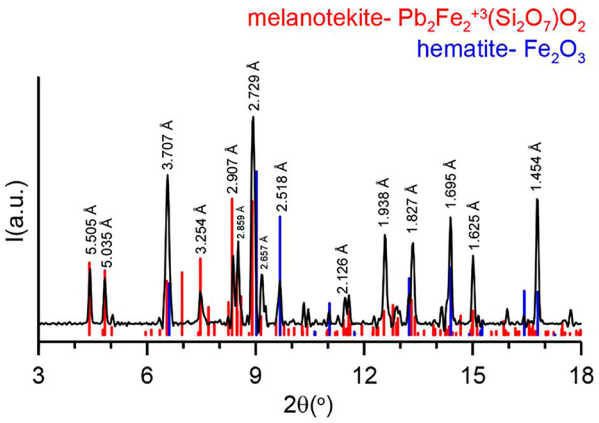

Figure 3. XRD pattern of melanotekite crystals. The references patterns marked correspond to the JCPDF database patterns 00-020-0585 for melanotekite and 01-079-1741 for hematite.

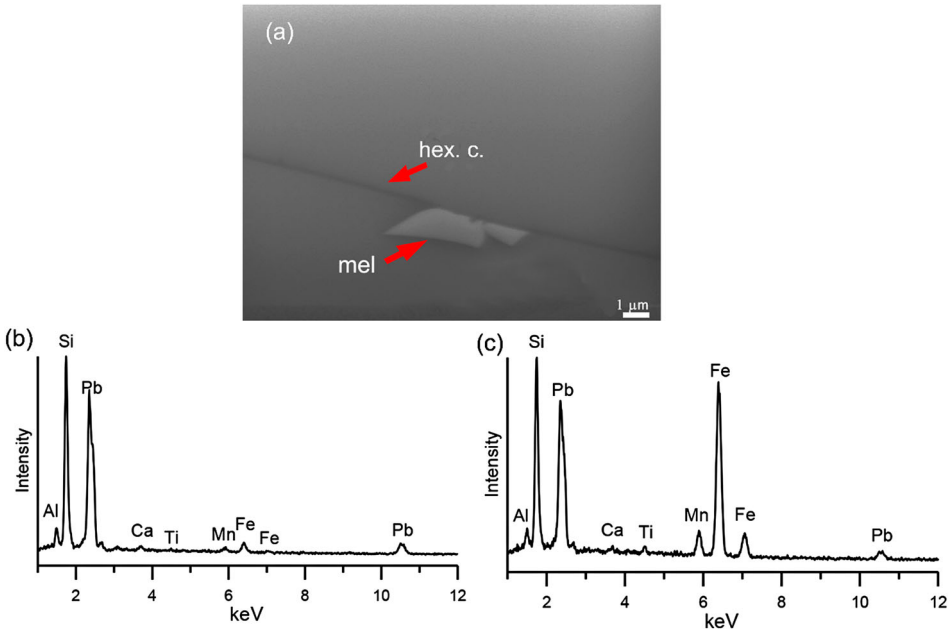

Figure 4. (a) SEM image of FIB polished cross-section cut through a hexagonal crystallite. A very thin laminar section of hexagonal crystallite (hex.c.) and a crossed crystal of melanotekite (mel, bright contrast) can be observed. (b) EDS analysis on the glaze surface. (c) EDS analysis on the laminar section of the hexagonal crystallite.

26×40 µm cross section was polished by FIB and observed using the secondary electrons (Figure 2(d)). Figure 4(a) shows the FIB polished cross-section cut through the hexagonal crystallites. From the FIB cross-section images, it is seen that the hexagonal crystallite was mostly found at a depth of about 20 µm in respect to the glaze preparation and that its thickness is about of 250 nm. The EDS analysis on the cross sections of the hexagonal crystallites is difficult because they are smaller than the electron beam probe volume. However, spectra from the cross sections of the hexagonal crystallites and from the glaze surface were obtained (Figures 4(b,c)). When we compare the spectra, we can see that the most remarkable difference is due to the iron content, which is very high in the spectrum of the cross sections of the crystallites. In addition, the crystallites were richer in Mn than the glaze. The Mn was found dissolved in the glaze and its presence is related to the dark decoration. As the crystallites are planar and oriented in the three dimensions, we did not manage to cut the crystallites to observe and analyze the basal sections.

In the next step, the hexagonal crystallites were subjected to Raman analysis. The optical microscope coupled with the Raman spectrometer permits hexagonal crystallites to be examined at high magnification and allows specific areas as small as 1 µm in diameter to be analyzed. In this instance, we took advantage of Raman microscopy that is able to provide analyzing inclusions that are not found on the glaze surface. We can defocus the image through the focus knob until the hexagonal crystallites are visible on the top of the glaze layer and analyze them. Figure 5(a,b) refers to the spectra acquired on the glaze surface and on the singular crystallite, respectively. When we compare the two spectra, we can see that the instrumentation is not sensitive enough. A wavenumber feature at about 689.5 cm^{-1}can be clearly observed and possibly another at about 1320 cm^{-1}. We have acquired different spectra on the hexagonal crystallites changing the laser power (0.5; 0.05; 1.5; 2 and 5.5 mW) and the laser wavelength (632 nm), but the presence of a specific phase cannot be confirmed based on the wavenumber features observed.

In addition, we also analyzed the thin cross sections rising on the glaze surface. Again, we were not able to

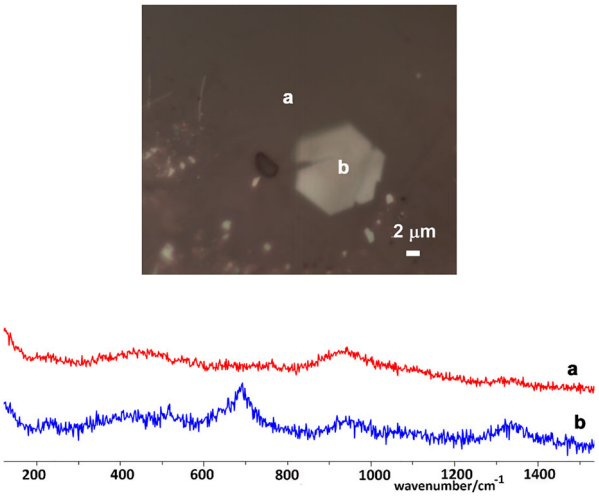

Figure 5. Above: Raman image of a hexagonal crystallite. Below: Raman spectra acquired on the glaze surface (a) and on the hexagonal crystallite (b). (Laser power: 2 mW; accumulation time: 5 s; number of accumulation: 10; objective magnification: 100×).

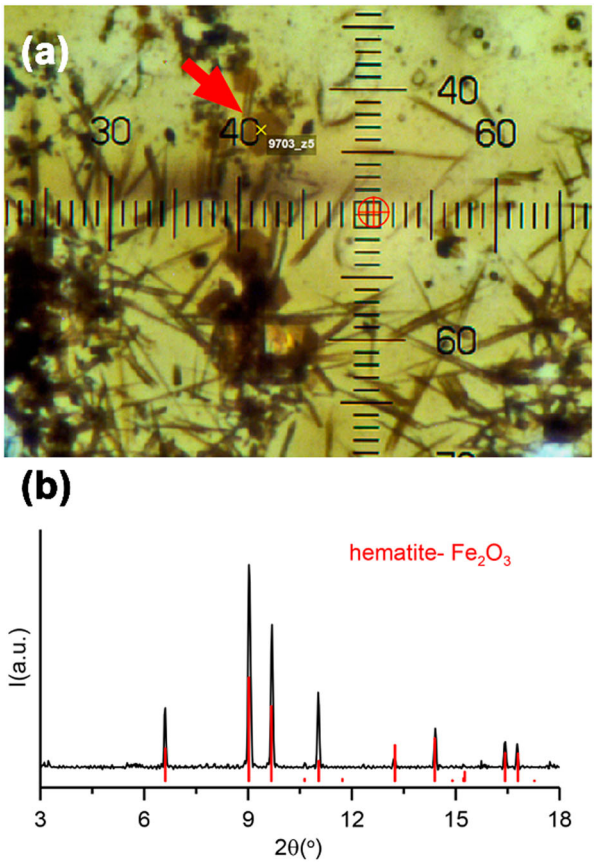

Figure 6. (a) Photomicrograph of the thin section of the sample 9703 from the Synchrotron camera. The hexagonal crystallites are clearly visible and the analysis spot (9703-z5) is shown in the picture. (b) XRD pattern of the crystal analyzed. The reference pattern marked corresponds to the JPDF database pattern 01-079-1741 for hematite.

determine any specific compound and a characteristic feature at about 625.2 cm^{-1} was observed.

Following this, a Micro-X-ray diffraction in transmission geometry using Synchrotron Light was performed directly on the polished thin section of the sample 9703 (Figure 6(a)). The advantage of using thin section is that the crystallites could be easily localized in the glaze, even if they were not found on the glaze surface layer. The 15 µm × 15 µm spot allowed to measure individual crystallites. The data obtained show unambiguously that the hexagonal phase corresponds to hematite (Figure 6(b)). We can also ascertain that the presence of Mn determined by SEM do not affect the lattice spacing and consequently the position of the hematite reflections. We can conclude that Mn is not substituting iron in the structure of hematite, but probably acted as a nucleation agent. We can highlight that the hematite crystallites often show a visible feature at the center.

4. Discussion

Hematite crystals are the principal mineral phase found in the Fe-rich glazes fired in oxidizing conditions (Dakhai, Orlova and Mikhailenko 1999). Nevertheless, the case study presented demonstrates the difficulty of identifying this type of crystallites in ceramic lead glazes using the most common routine analytical techniques. We observe two basic problems. The first one is the thickness (a few hundred nanometers) of the crystallites, which is probably responsible for the low sensitivity of the Raman instrumentation. In this way, the wavenumber features observed cannot be assigned to a specific mineral phase. The second one is the arrangement of these crystals in the glaze. Most of them were found at a depth of about 20 µm with respect to glaze preparation. The basal sections were never observed neither in the BSE nor in FIB cross-section images. Then, the work of thin section petrography is crucial to connect the hexagonal habit of these crystals to the thin cross sections observed in the SEM, to situate their distribution in the glaze matrix and analyze them by SR-µ-XRD.

The hematite micro-crystallites are formed in the glaze–body interface from the reaction between the components of the glaze mixture and the ceramic paste. During the cooling, the capacity of the melt to retain the Fe in solution is lessened and the excess is precipitated as thin plate crystals (Fraulini 1933). According to the literature, hexagonal crystals of hematite are found in the iron aventurine glazes (Bromberg 1915; Fraulini 1933; Dakhai, Orlova, and Mikhailenko 1999; Romero, Rincón, and Acosta 2004). This is the generic name for lead-free or low-lead glazes containing macroscopic laminar crystals, which cause a sparkling decorative effect. The effect, described as small glitters, probably originated in the seventeenth century in a furnace of Murano (Venice, Italy), when copper filings were accidentally spilled on molten glass, with such a surprising effect that it became part of factory production. The name “aventurine” comes from the Italian “a ventura”, which means “by chance”. In fact, Giovanni Darduin in a glassmakers’ book of recipes, known as the Darduin manuscript, says (149th recipe) that such a glass can be obtained more by chance than by the skill of the glassmakers (Zecchin 1986). The recipes used to obtain the aventurine effect have been very limited, confidential and restricted to the point of sometimes being forgotten over time. Darduin in the 149th recipe says to melt in a crucible 150 pounds of common glass and later to add 8 pounds of lead and tin oxides, 8 pounds of red copper oxide and, finally, 2.5 pounds of iron oxide. He recommends keeping the kiln at the same temperature for 8 or 10 h, then mix it again to homogenize the glass; close the door of the kiln, turn off the heat and let it cool naturally without touching it (Zecchin 2005). Fe_2O_3 is the most reported oxide in literature as an effective generator of aventurine glazes (Lazău et al. 2013). In these glazes, the sparkling effect is due to the difference in the index of refraction between the crystalline and glassy phases. The macroscopic optical effect depends

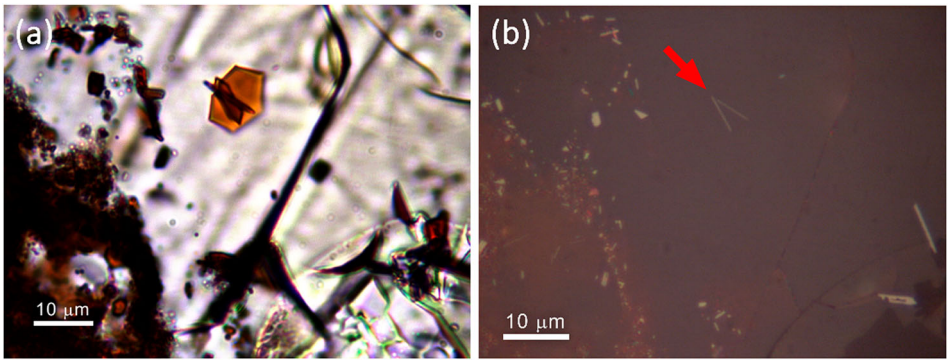

Figure 7. (a) OM image in PPL. Intergrowths of hexagonal crystals can be observed. (b) The same image as in picture (a) in reflected light. The growth habit of the hexagonal crystallites is missing and only two light laminar sections are visible.

on the size, volume fraction of crystallites, Fe_2O_3 content and viscosity of melt (Levitskii 2001). References about the aventurine glazes composition can be found today in the literature (Shchglova et al. 1996; Dakhai, Orlova, and Mikhailenko 1999; Levitskii 2001; Păcurariu et al. 2011; Lazău et al. 2013). In general, Fe_2O_3 contents range from 10% to 30% by weight, and there are two groups of glazes, lead and boric, since a molten phase with low viscosity is required for the laminar crystal growth (Bromberg 1915). The alumina content (0.5–11 wt%) must be low and the proportion of SiO_2 (30–60 wt%) is adjusted to obtain appropriate viscosity. The glazes can be obtained from glaze compositions consisting of natural raw materials or mixtures of frits and natural raw materials. The Fe_2O_3 may be part of the frit or not, although in most compositions it is directly mixed into the glaze, owing to the disadvantages of synthesizing colored frits and because crystallization occurs more easily than if a homogeneous glass is used (Levitskii 2001). The thermal cycle used to obtain these glazes usually consists of two stages: the first one for dissolving the metallic oxide in the melt, followed by slow controlled cooling that allows the laminar crystals to form or, otherwise, a certain dwell time at a lower temperature, where the crystalline growth rate is high. Cycle duration is very long, from 7–8 to 24 h (Dvornichenko and Matsenko 2000). In our case, the lead content is high while the iron content is low. In addition, the relatively small size of the hexagonal crystallites (few tens of micrometres) is due to a relatively fast cooling which also causes the formation of skeletal melanotekite crystals in the sample 9703 (Di Febo et al. 2017). For these reasons, the decorative effect in the coating is missing. However, some fragments of the Taches Noires wares, observed under stereomicroscope, show a golden shade which is more evident on the manganese brown decorated areas. In fact, these are the samples which are richer in hexagonal crystallites because the manganese can act as a nucleating agent for the growth of

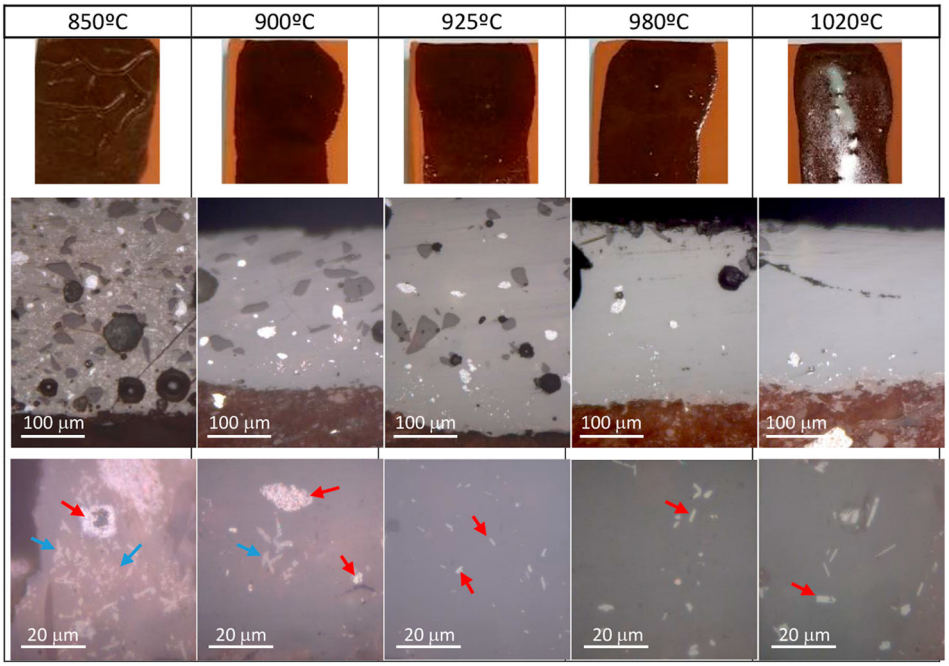

Figure 8. Above: reproductions of the glaze composition of the sample 9703 at different temperatures. Below: OM images of the glazes in reflection mode. Melanotekite crystals are marked in blue arrows and hematite in red arrows.

hexagonal planar hematite crystallites. Studies of aventurine glazes demonstrated that the introduction of about 3% MnO in an iron rich melt leads to an increase of 10–15% on the volume fraction of hematite crystals (Romero, Rincón, and Acosta 2004). Although an iron content of about 4–6 wt%, such as found in our ceramic glazes, may appear low as compared to the values expected in aventurine glazes, it is sufficient to generate a situation of iron oversaturation that leads to the precipitation of hematite. The rate of the crystals increases with increasing supersaturation. Then, we can observe individual crystals or intergrowths of hexagonal crystals (Figures 7(a,b)). The lamellar shape of the crystals is presumably determined by the growth conditions: increased melt viscosity and a high degree of melt oversaturation with iron oxide (Levitskii 2001). Taking into account the SEM–FIB observations above, the hematite crystallites were mostly found inside the glaze. This evidence is in good agreement with the literature data on aventurine glazes showing an increase in the amount of crystallites across the entire thickness of the coating up to a depth of about 100 μm (Levitskii 2001).

Finally, in order to determinate the thermal range at which hematite was formed, we replicated under laboratory-controlled conditions the same glaze composition than that of the sample 9703 (Figure 8) using chemical reagents (60.8 wt% of minium –Pb_3O_4–, 32.6 wt% of quartz, 4.3 wt% of kaolin, 5.53 wt% of Fe_2O_3, 1.34 wt% of wollastonite and 1 wt % of talc). The glazes were applied over a ceramic flat surface made with an illitic–kaolinitic clay containing 6% Fe_2O_3 and fired at different temperatures: 850°C, 900°C, 925°C, 950°C, 980°C and 1050°C. Hematite in association with melanotekite are found in those replications fired at 850°C, although the glaze appears not fully molten. Moreover, we observe clusters resembling the grains of hematite originally present in the glaze mixture and hematite and melanotekite recrystallized around them. At 900°C the glaze is completely molten and melanotekite and hematite are also present (Figure 9). Above 920°C melanotekite appears

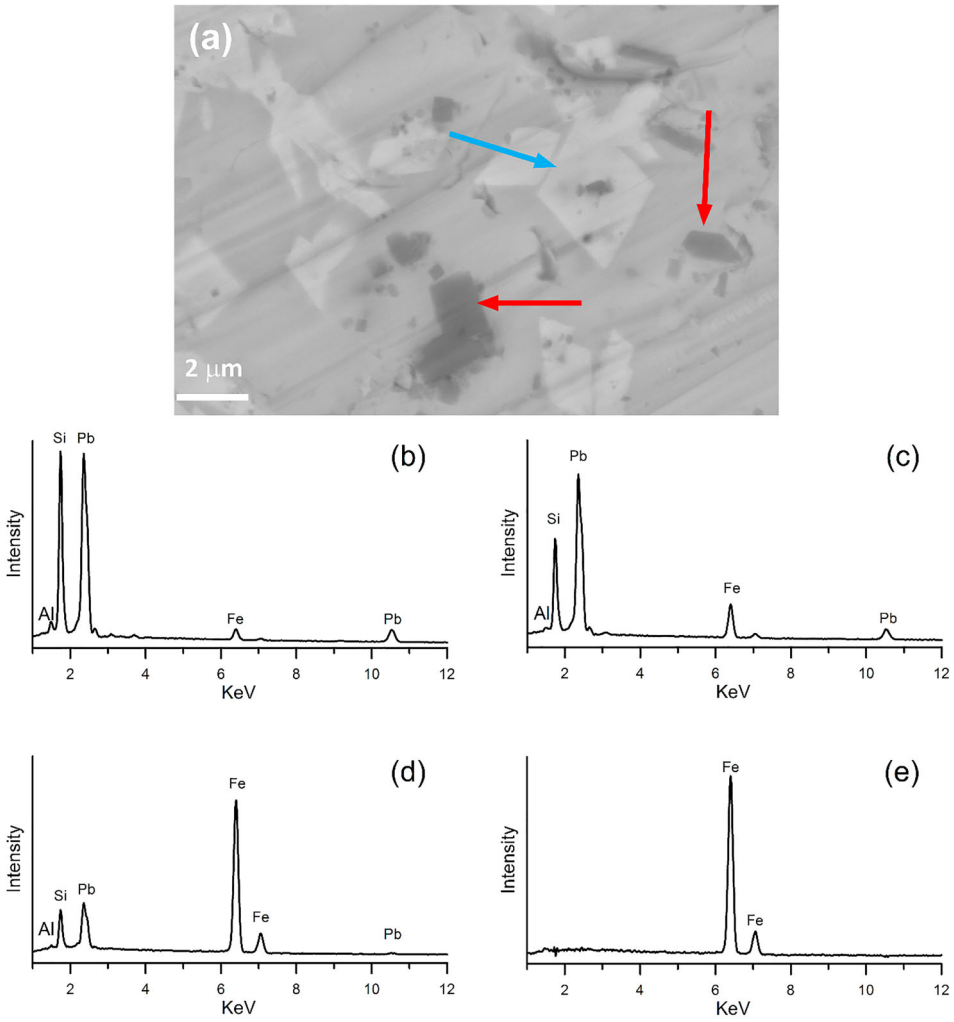

Figure 9. (a) SEM backscattering image of the glaze reproduction of the sample 9703 fired at 900°C. Light crystals correspond to melanotekite (blue arrow) and dark crystals correspond to hematite (red arrows) are visible. (b) EDS spectrum of the glaze. (c) EDS spectrum of melanotekite crystals (blue arrow). (d) EDS spectrum of hematite crystal (central red arrow). (e) EDS spectrum of hematite crystal (central red arrow) subtracting the glaze spectrum.

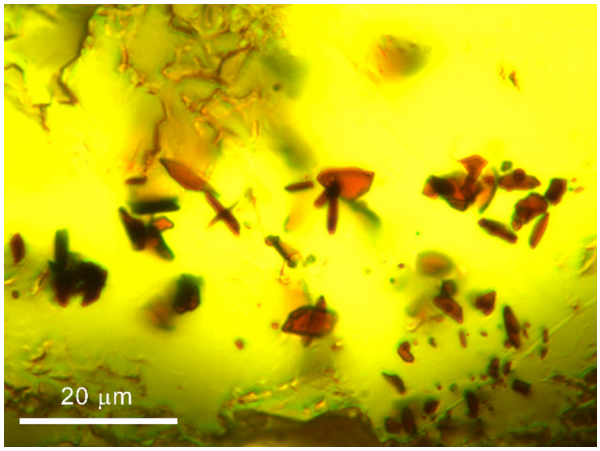

Figure 10. OM images in PPL. Glaze reproduction of the sample 9703 fired at 925°C. Only hematite crystallites can be observed.

completely absent. On the contrary, hematite crystals growing at the ceramic body–glaze interface appear in all replicas and these are larger and thicker for those replicas fired at higher temperature. These results demonstrate that melanotekite and hematite nucleate and grow during the heating. Melanotekite is formed by the reaction between lead oxide, quartz and iron oxide during the melting. At temperatures over 900° C, melanotekite is dissolved in the melt (Figure 10). Hematite hexagonal crystals are preferentially formed at the ceramic–glaze interface where nucleating sites exist. The original hematite grains appear more dissolved at higher temperatures. At 950–1020°C few recrystallized grains of the original hematite grains remain and bigger hexagonal hematite crystals are observed near the interface. The presence of hematite in association with melanotekite in the sample 9703 from Jouques, suggests that it was fired at about 900° C and below 925°C.

5. Conclusions

This case study shows how a multi-analytical approach is crucial to identify the hexagonal neo-formed crystallites of hematite in ceramic lead glazes. In particular, the optical observation in PPL was able to localize the micro-crystallites in the glaze and show their distribution and growth habits, while SR-μXRD carried out directly on the thin section was able to identify their nature. Taking into account that the hexagonal habits of crystallites were never found on the polished surfaces of the glazes, the optical observation in PPL is a very powerful tool to correlate the hexagonal morphologies of these crystallites to thin cross sections that can be observed in the SEM. Based on the experimental data, the presence of hematite in association with melanotekite in high lead glazes is indicative of low firing temperatures (<925°C), while the presence of only hematite seems to be a fingerprint of higher temperatures (>925°C).

As noted in this work, the hexagonal neo-formed hematite crystals found in our ceramic lead glazes are also a typical feature of the aventurine glazes. Although these crystals have been observed in archaeological ceramics of different provenance and chronology, their presence is more the chance result of the interaction between paste and glaze of a specific composition than a deliberated decorative effect. In fact, the presence of these crystals can be noted only by petrographic observations, while on the brown decorations using a stereomicroscope. However, also on the brown decorations, the sparkling effect is limited. The difficulty in obtaining the aventurine effect, together with the clear dependence on the glaze composition and the firing cycle led to an unreliability of duplicating the results. The method of the temperature treatment is important as well as the composition of the body to which the glaze is applied. The chief difficulty in producing aventurine is not in the nucleation but is in the enlargement and dispersion of the crystals. This process occurs during a very slow cooling period. The glass must be cooled slowly until it reaches ambient temperature. It is during this time that the crystals growth becomes almost visible to the naked eye.

Acknowledgement

Roberta Di Febo is grateful to the UVICUCC Scholarship Program, awarded by University of Vic, Central University of Catalonia. The authors are grateful to the project MAT2016-77753-R, 2017-2019 funded by the Ministerio de Ciencia e Innovación (Spain), the ALBA Synchrotron Light Facility 2014060905 (BL04) and the Generalitat de Catalunya project 2014 SGR 00581 (T.P.), 2014 SGR1585 (J.M. and R.D.F.).

Disclosure statement

No potential conflict of interest was reported by the authors.

Notes on contributors

Roberta Di Febo completed her Ph.D. in Archaeological Science at the University of Barcelona (Spain) in 2016. In 2018, she will conclude her second Ph.D. in Archaeometry at the University of Vic (Spain). The use of thin section petrography in combination with other analytical tools is the focus of her interest in ceramic glazes.

Judit Molera born in Barcelona July 1966. Ph.D. in Geology at the Universitat de Barcelona (UB) in 1996. Assistant professor in the Department of Crystallography and Mineralogy (UB) 1990–2004. Researcher RyC in the University of Girona (UdG) 2004–2007 and Professor of the University of Vic-Central University of Catalonia (UVIC-UCC) since 2007. Expert in Ceramic Materials mainly devoted to the study of crystals developed in glazes and decorations of ancient ceramics using micro-XRD, optical and electron microscopy. 59 papers published. H index 21, 1289 cites (Scopus).

Trinitat Pradell born in Barcelona march 1961. Ph.D. in Applied Physics at the Universitat de Barcelona in 1992. Full Professor in Applied Physics in the Department of Physics of the Universitat Politècnica de Catalunya (BarcelonaTech) since 2010. Research projects in Materials Science mainly devoted to the study of amorphous and nanocrystalline materials and Historical and Artistic materials, specially of ceramic, glaze technology with particular input to glass decorations, enamels and paintings. Over 125 papers published. H index from the WOS, 21. 1517 cites without self citations.

Oriol Vallcorba PhD in Chemistry from the Universitat Autònoma de Barcelona in 2010. Post-doc in the Materials Science and Powder Diffraction beamline at the ALBA synchrotron. Since 2014, his research is focused on the development of methodologies for crystal structure studies from diffraction techniques, specially polycrystalline x-ray diffraction and microdiffraction. 34 publications indexed in the WOS (H-index 8).

Claudio Capelli born in Savona (Italy) december 1963. Ph.D. in Earth Sciences in 1993, University of Genova. Researcher at the Department for the Earth, Environment and Life Sciences (DISTAV) of the University of Genova. External collaborator to the Centre Camille Jullian (Aix-Marseille Université/CNRS, UMR 7299) of Aix-en-Provence (France). Main research topic: archaeometry of Prehistoric to post-Medieval Mediterranean pottery by means of mineralogical and petrographic methods. Over 260 papers published.

ORCID

Roberta Di Febo http://orcid.org/000-0002-1102-8231
Judit Molera http://orcid.org/0000-0003-3116-0456
Trinitat Pradell http://orcid.org/0000-0002-8720-5492
Oriol Vallcorba http://orcid.org/0000-0001-6499-7688
Claudio Capelli http://orcid.org/0000-0003-1318-880X

References

Amouric, H., and L. Vallauri. 1993. La fabrique de Villemus. In *Un goût d'Italie, Céramiques et céramistes italiens en Provence du Moyen Âge au XXème siècle*, Catalogue Exposition, Narration, Aubagne, 118–120.

Beltrán de Heredia Bercero, J., C. Capelli, R. Di Febo, M. Madrid i Fernández, and J. Buxeda i Garrigós. 2015. Imitaciones de ceràmicas Taches Noires en Barcelona en el siglo XVIII. Datos arqueológicos y arqueométricos. In *Actas do X Congresso Internacional A Cerâmica Medieval no Mediterrâneo- Silves 2012-, Camera Municipal de Silves & Campo Arqueológico de Mértola*, 613–618.

Blake, H. 1981. "Pottery Exported from Northwest Italy Between 1450 and 1830: Savona, Albisola, Genoa, Pisa, and Montelupo." In *Archaeology and Italian Society. Prehistoric, Roman and Medieval Studies*, edited by G. Barker, and R. Hodges, 99–124. Oxford: BAR International Series 102.

Bromberg, N. 1915. "A Study of Compositions Suitable for Aventurine Glazes." (*Thesis (MS)*). University of Illinois. http://hdl.handle.net/2142/53956.

Cameirana, A. 1970. La terraglia nera ad Albisola all'inizio dell'800. In *Atti III Convegno Internazionale della Ceramica 1969*, Centro Ligure per la Storia della Ceramica, Firenze, 63–95.

Cameirana, A. 1977. La ceramica albisolese a Taches Noires. In *Atti del X Convegno Internazionale della Ceramica 1976*, Centro Ligure per la Storia della Ceramica, Firenze, 277–293.

Capelli, C., R. Di Febo, H. Amouric, R. Cabella, and L. Vallauri. 2017. Importazioni e imitazioni locali di ceramica a Taches noires in Provenza nel XVIII-XIX secolo. Dati archeologici e archeometrici. In *Atti IL Convegno Internazionale della Ceramica 2016*, Centro Ligure per la Storia della Ceramica, Firenze.

Capelli, C., T. Mannoni, and R. Cabella. 2007. Analisi archeometriche e Archeologiche integrate sulla ceramica invetriata da fuoco dal Palazzo Ducale di Genova (XII-XIII sec.). In *Atti XXXIX Convegno Internazionale della Ceramica 2006*, Centro Ligure per la Storia della Ceramica, Firenze, 7–16.

Capelli, C., F. Richez, L. Vallauri, R. Cabella, and R. Di Febo. 2013. L'epave du Grand Congloué 4: Caractérisation archéologique et archéométrique d'un lot de céramiques à Taches Noires de Albisola-Savona. In *Atti XLV Convegno Internazionale della Ceramica 2012*, Centro Ligure per la Storia della Ceramica, Firenze, 7–16.

Casadio, F., C. Daher, and L. Bellot-Gurlet. 2016. "Raman Spectroscopy of Cultural Heritage Materials: Overview of Applications and New Frontiers in Instrumentation, Sampling Modalities, and Data Processing." *Topics in Current Chemistry* 374: 1434. doi:10.1007/s41061-016-0061-z.

Clark, R. J. H., and M. L. Curri. 1998. "The Identification by Raman Microscopy and X-ray Diffraction of Iron-Oxide Pigments and of the Red Pigments Found on Italian Pottery Fragments." *Journal of Molecular Structure* 440: 105–111.

Colomban, P., and C. Truong. 2004. "Non-destructive Raman Study of the Glazing Technique in Lustre Potteries and Faience (9th–14th Centuries): Silver Ions, Nanoclusters, Microstructures, and Processing." *Journal of Raman Spectroscopy* 35: 195–207.

Dakhai, S., L. A. Orlova, and N. Y. Mikhailenko. 1999. "Types and Compositions of Crystalline Glazes." *Glass and Ceramics* 56 (5): 177–180.

De Faria, D. L. A., and F. N. Lopes. 2002. "Natural Hematite or Heated Goethite: Can Raman Microscopy Differentiate Them?" In *XVIIIth International Conference on Raman Spectroscopy*, edited by J. Mink, G. Jalsovszhy, and G. Keresztury, 825–826. New York: Wiley.

De Faria, D. L. A., V. Silva, and M. T. de Oliveira. 1997. "Raman Microspectroscopy of Some Iron Oxides and Oxyhydroxides." *Journal of Raman Spectroscopy* 28: 873–878.

Di Febo, R. 2016. "La ceràmica de Barcelona entre els segles XIII i XVIII a través de la seva caracterització arqueomètrica. El paper de l'anàlisi petrográfica." (*Doctoral diss.*). University of Barcelona, Barcelona. http://diposit.ub.edu/dspace/handle/2445/.

Di Febo, R., J. Molera, T. Pradell, O. Vallcorba, and C. Capelli. 2017. "Thin Section Petrography and SR-μXRD for the Identification of Micro-crystallites in the Brown Decorations of Ceramic Lead Glazes." *European Journal of Mineralogy*, doi:10.1127/ejm/2017/0029-2638.

Dvornichenko, I. N., and S. V. Matsenko. 2000. "Production of Iron-containing Crystalline Glazes." *Glass and Ceramics* 57 (1–2): 67–68.

Fraulini, F. 1933. "Aventurine Glazes." (*Bachelors Theses*). Missouri School of Mines and Metallurgy, Missoury. http://scholarsmine.mst.edu/bachelors_theses/309.

Gómez, A., C. Gil, R. Di Febo, and J. Molera. 2015. Casa Convalescència (Vic, Osona): Aproximació arqueológica i arqueomètrica a un conjunt de vasos ceràmics del segle XVIII. In *III Jornades d'Arqueologia de la Catalunya Central*, Roda de Ter, 70–81.

Howell, G., M. Edwards, and P. Vandenabeele. 2016. "Raman Spectroscopy in Art and Archaeology." *Philosophical Transaction of the Royal Society A* 374 (2082), doi:10.1098/rsta.2016.0052.

Lazău, I., S. Borcănescu, C. Păcurariu, and C. Vancea. 2013. "Kinetic Study of the Non-isothermal Crystallization Process of Hematite in Ceramic Glazes Obtained from CRT Wastes." *Journal of Thermal Analysis and Calorimetry* 112 (1): 345–351. doi:10.1007/s10973-012-2736-1.

Levitskii, I. A. 2001. "Mechanism of Phase Formation in Aventurine Glaze." *Glass and Ceramics*, 58 (5): 223–226. doi:10.1023/A:1012351301045.

Păcurariu, C., R. I Lazău, I. Lazău, D. Tița, and D. Dumitrel. 2011. "Nonisothermalcrystallization kinetics of some aventurine decorative glaze." *Journal of Thermal Analysis and Calorimetry* 105: 1130–0.

Poole, A. B., and I. Sims. 2015. *Concrete Petrography: A Handbook of Investigative Technique*. 2nd ed. CRC Press.

Romero, M., J. Rincón, and A. Acosta. 2004. "Development of Mica Glass-Ceramic Glazes." *Journal of the American Ceramic Society* 87: 819–823. doi:10.1111/j.1551-2916.2004.00819.x.

Shchglova, M. D., T. V. Babenko, S. G. Polozhai, and V. M. Svistun. 1996. "Mechanism of Aventurine Formation in Copper-containing Alkali-lead Silicate Glass." *Glass and Ceramics* 53 (1–2): 14–17.

Smith, G. D., and R. J. H. Clark. 2001. "Raman Microscopy in Art History and Conservation Science." *Reviews in Conservation* 2: 92–106.

Tite, M. S., I. Freestone, R. Mason, J. Molera, M. Vendrell-Saz, and N. Wood. 1998. "Lead Glazes in Antiquity – Methods of Production and Reasons for Use." *Archaeometry* 40 (2): 241–260.

Zecchin, L. 1986. *Il Ricettario Darduin, un codice vetrario del Seicento, trascritto e commentato*. Stazione Sperimentale del Vetro e Arsenale, Venezia.

Zecchin, L. 2005. "La Pasta Venturina, Vetro Speciale Muranese." *Journal of Glass Studies* 47: 93–106.

5.3 *Thin-section petrography and SR-μXRD for the identification of micro-crystallites in the brown decorations of ceramic lead glazes*

European Journal of Mineralogy, 29 (5), 861-870 (2017)
DOI: 10.1127/ejm/2017/0029-2638.
Di Febo, R., Molera, J., Pradell, T., Vallcorba, O., Melgarejo, J.C., Capelli C.

5.3.1 Introduction

In this work, we considered two case studies concerning the brown decorations: French imitations of the Ligurian *Taches Noires* wares (first half of the 19th century) and decorated Catalan tablewares (17th century). The first case study is directly related to the long and well appreciated ceramic tradition of Albisola (Liguria, NW Italy). At the beginning of the 18th century, a new high-quality, low-cost production called Taches Noires ware was developed. It became a global pottery in a few years, spreading all over the Mediterranean (Italy, France, Spain, Tunisia and Greece) and also in the New World (Canada, the Caribbean Islands and Mexico). The success of the Taches Noires ware was so massive that it was soon copied by different Spanish and French workshops. Two sherds of French imitations from the Provençal workshop of Jouques were analysed and compared to existing data of reference samples from Albisola.

Regarding the Catalan brown tablewares considered in this work, as we have explained before, they are cheaper versions of the traditional blue majolica pottery. They consist of brown decorations on white glazes and motives similar to those of the blue decorations of majolica.

The three samples of brown decorations taken into account are characterised by the presence of different types of micro-crystalline precipitates. The integrated approach here presented allowed to illustrate which kinds of raw materials (glazes and pigments) were used, the conditions of the firing process, the technological choices made as well as the technical knowledge transfers.

5.3.2 Results

Melanotekite ($Pb_2Fe_2Si_2O_9$), cristobalite, relict hematite grains and new formed hematite crystallites were the main crystalline phases identified in the glazes of the French imitations of the Ligurian *Taches Noires* wares from the Jouques workshop.

Relict hematite was found all over the glazes both in the decorated and undecorated areas. The decorated areas are also rich in skeletal melanotekite crystals which were observed to grow around relict grains of hematite. Cristobalite crystallites, new formed hematite or associations of both -cristobalite and hematite- were found all over the glazes and close to the glaze-body interface.

In respect to the Catalan brown tablewares, braunite (Mn_7SiO_{12}) and kentrolite ($Pb_2Mn_2Si_2O_9$) were the two mineralogical phases associated to the manganese decoration. Based on the optical observation, the Mn crystallites were located on top of the opaque glaze suggesting an overglaze application of the pigment. The glaze also contains large amounts of quartz and feldspars grains. The optical study in thin section showed different crystalline habits for the Mn compounds. In particular, braunite displays both euhedral bipyramidal and thin lath-like crystallites, while kentrolite crystallites show a dendritic texture.

Eur. J. Mineral.
2017, **29**, 861–870
Published online 5 April 2017

Thin-section petrography and SR-μXRD for the identification of micro-crystallites in the brown decorations of ceramic lead glazes

Roberta DI FEBO[1,*], Judit MOLERA[1], Trinitat PRADELL[2], Oriol VALLCORBA[3], Joan Carles MELGAREJO[4] and Claudio CAPELLI[5]

[1] UScience Tech, MECAMAT Group, University of Vic – Central University of Catalonia, C. de la Laura 13, 08500 Vic, Spain
*Corresponding author, e-mail: roberta.di@uvic.cat
[2] Departament de Física, Universitat Politècnica de Catalunya, Campus Baix Llobregat, c. Esteve Terrades 8, 08860 Castelldefels, Spain
[3] ALBA Synchrotron Light Source, Cerdanyola del Vallès, 08290 Barcelona, Spain
[4] Departament de Mineralogia, Petrologia i Geologia Aplicada, Universitat de Barcelona, C/ Martí i Franquès, s/n, 08028 Barcelona, Spain
[5] Dipartimento di Scienze della Terra, dell'Ambiente e della Vita (DISTAV), Università degli Studi di Genova, Corso Europa, 26, 16132 Genova, Italy

Abstract: The Mn- and Fe-rich micro-crystalline precipitates formed in the decorations of lead glazes during ceramic firing are responsible for colour, shine and opacity, among other visual characteristics, besides being the most important relics of the technology. Due to their small size and growth habits, the micro-crystalline precipitates may remain unidentified on polished cross sections of the glazes. Thin-section petrography, combined with synchrotron-radiation X-ray micro-diffraction, appears to be a very powerful tool to reveal the presence, growth habits, distribution and nature of the micro-crystallites. This is illustrated here by two case studies directly related to the brown decorations technology: the 19th century French imitations of the Ligurian *Taches Noires* pottery from the Joques workshop and the 17th century Catalan-decorated tablewares. Melanotekite, cristobalite and hematite micro-crystallites were found in the glazes of the French imitations. Hematite acted as nucleating agent effective in promoting both the crystallization of melanotekite and cristobalite. The presence of cristobalite is not related to alkali ions, which are normally responsible for its formation far from equilibrium conditions. Melanotekite and cristobalite can be considered as technological markers associated to the Joques production and then be used to identify imitations of this workshop. Braunite and kentrolite were identified in the brown decoration of the Catalan tablewares. The manganese pigment was probably mixed with a lead oxide compound and applied directly over the raw glaze. The presence of braunite and kentrolite indicates a firing temperature of about 950 °C. Thin-section petrography reveals that the crystallite growth has taken place under two different conditions. Euhedral braunite crystallites were produced during the heating. A drop in temperature during the firing process gave rise to the crystallization of dendritic braunite and kentrolite.

Key-words: cristobalite; melanotekite; kentrolite; braunite; thin-section petrography; SR-μXRD; lead glazes; brown decoration; ceramic technology; archaeometry.

1. Introduction

The aim of this study is to identify micro-crystallites present in the glaze decorations of ceramics, with emphasis on their description and characterization by means of thin-section petrography. Most of the literature published on ancient ceramics and involving thin-section petrography focuses on provenance studies, through the compositional characterization of the non-plastic inclusions in the ceramic bodies of the artefacts (*e.g.* Shepard, 1965; Freestone *et al.*, 1982; Middleton & Freestone, 1991; Reedy, 1994, 2008; Quinn, 2009, 2013). A few petrographic studies have addressed the methods of fabrication of slips, paint, enamel, decorative and surface treatments and glazing methods (*e.g.* Arnold, 1972; Kamilli & Lamberg-Karlovsky, 1979; Jiazhi, 1984; Harrison Hall, 1997; Reedy, 2008). In principle, finishing methods, glaze raw materials, colourants as well as the formation of the glaze are best investigated by scanning electron microscopy with energy-dispersive spectrometry (SEM-EDS), the main limitation of optical microscopy being the size of the crystallites (<1 μm). This very small size may explain the paucity of petrographic publications for the identification of crystallites in ceramic glazes, as compared to the widespread application of the method to ceramic bodies. On the other hand, the principal restriction

DOI: 10.1127/ejm/2017/0029-2638 0935-1221/17/0029-2638 $ 391.50
Downloaded from https://pubs.geoscienceworld.org/eurjmin/article-pdf/4098314/ejm_29_5_0861_0870_di_febo_2638_online.pdf
by UNIVERSITAT DE BARCELONA user
© 2017 E. Schweizerbart'sche Verlagsbuchhandlung, D-70176 Stuttgart

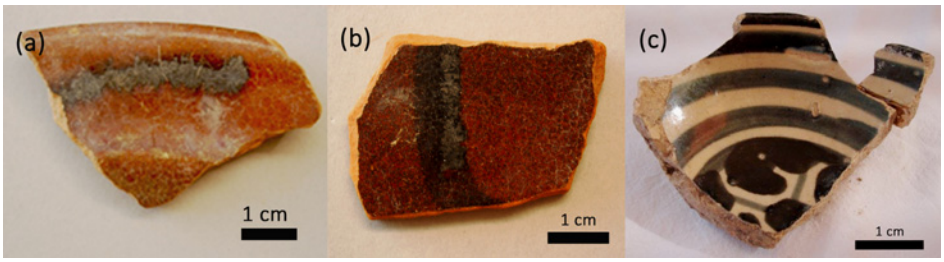

Fig. 1. (a), (b) Brown decorated fragments (samples 9703 and 9708). French imitations of the Ligurian *Taches Noires* pottery from Jouques (first half of 19th century). (c) Brown decorated Catalan tableware (sample SBG10) from the old Church of Sant Bartomeu del Grau (17th century). (Online version in colour.)

of the SEM is the lack of adequate contrast in back-scattered electron (BSE) images (glaze and crystallites of similar composition show similar grey tones) and poor discrimination of the crystallite shape. Indeed, if crystallites are needle or plate shaped, they can be barely recognized, and therefore analysed, on the polished cross-section surfaces.

To overcome these difficulties, the combination of various micro-analytical techniques is crucial. Petrographic inspection of polished thin sections of the glazes gives a 3D perspective of the micro-crystallites and is able to reveal their microstructural features and distribution in the glazes. The same polished thin sections are analysed by SEM, in order to determine the composition of the glazes and the micro-crystallites. Finally, synchrotron-radiation X-ray micro-diffraction (SR-μXRD) performed directly on the polished thin sections allows us to localize the crystallites even if they are not found on the glaze surface layer, and to determine their nature. In a former study concerning glaze technology, micro-crystallites found in ceramic glazes were identified combining SR-μXRD (50 μm footprint) and SEM-EDS analyses (Pradell *et al.*, 2010, 2013; Molera *et al.*, 2013). However, in these glaze cross sections (~100 μm thickness), many micro-crystallites can contribute to the diffraction pattern, increasing the peak overlap and limiting the detection and identification of other smaller or less abundant crystallites. In the present study, we used polished thin sections (−30 μm thick) to reduce the volume of diffracting material, resulting in a less 'diluted' and overlapped pattern for minor phases. A smaller diffraction volume can also be an advantage if absorption problems due to the sample composition are present. In contrast, as this is a through-the-substrate measurement (Rius *et al.*, 2011), the glass support of the polished thin section is increasing the background considerably (depending on its thickness) compared to the free-standing cross section. However, the contribution of the glass can be subtracted during the data-processing step. In this manner, we can properly identify the crystalline phases and illustrate them by BSE and optical images.

The three samples of brown decorations selected for this study are characterized by the presence of micro-crystallites that are difficult to determine by more conventional methods. Therefore, they are excellent examples of the value added by the use of our methodology for the study of decorations.

These case studies are: (i) French imitations of the Ligurian *Taches Noires* wares and (ii) decorated Catalan tablewares. The different types of micro-crystalline precipitates, their distribution and growth habits are determined and discussed in terms of the materials (glazes and pigments) and thermal paths.

2. Materials and methods

Three samples of tablewares showing brown decorations applied on lead glazes (Fig. 1) were selected for the analyses. They contain different types of micro-crystalline precipitates which illustrate the raw materials selection, technical knowledge transfer and specific technical choices. They consist of:

– Two sherds (9703 and 9708) of French imitations of the Ligurian *Taches Noires* pottery from the workshop of Jouques (Provence, France). These samples are macroscopically comparable in terms of glaze and decoration and show the same association of crystalline phases. Nevertheless, we present two samples of this French production due to the state of conservation of the glazes. They commonly exhibit cracked areas that make it difficult to recognize the crystallites and to obtain clearly defined optical images. Both samples correspond to dishes and are dated from the first half of the 19th century. According to written sources, the workshop was established by an Italian, possibly a Ligurian potter (Amouric & Vallauri, 1993). The ware called *Taches Noires* was developed in Albisola (Liguria, NW Italy) during the 18th century (Cameirana, 1970, 1977). The success of the *Taches Noires* ware was so massive that it was soon copied by Spanish and French workshops (Beltrán de Heredia Bercero & Miró i Alaix, 2010; Capelli *et al.*, 2013). This type of ceramic is characterized by a fine, hard, deep-red fabric and brown transparent glazes decorated with wavy dark bands (Blake, 1981). According to original glaze recipe (Assereto, 1994), galena, the lead compound used in the glazing mixture was purchased in Genoa (Liguria, Italy) or imported from Almeria (Spain) and mixed with sand from Antibes (France) or ground quartz from Noli (Liguria, Italy). The addition of one-twelfth of iron oxide gave an orange-brown colour to the glazes, while the manganese decorations were applied under the glaze before the second firing.

Downloaded from https://pubs.geoscienceworld.org/eurjmin/article-pdf/4098314/ejm_29_5_0861_0870_di_febo_2638_online.pdf
by UNIVERSITAT DE BARCELONA user

Table 1. Chemical compositions of the decorated areas of the glazes (wt%) measured by SEM-EDX.

	Chemical composition (wt%)									
Sample	Na_2O	K_2O	Al_2O_3	SiO_2	CaO	MgO	MnO	FeO	TiO_2	PbO
9703	0.2	0.9	2.5	35.2	0.7	0.3	0.8	4.6	–	54.4
9708	0.3	0.1	3.0	35.5	1.1	0.6	1.4	5.1	0.6	51.8
SBG10	0.3	3.4	2.6	46.8	1.2	0.2	3.5	0.6	0.3	40.5

– A sherd (SBG10) of a Catalan decorated production dated from the 17th century. It was found in the old Church of Sant Bartomeu del Grau (Catalonia, Spain). The ware represents a cheap version of the traditionally blue-decorated ceramics with the substitution of the cobalt pigment by a manganese pigment (Coll Conesa, 2009).

We have prepared two types of thin sections, which were employed during all the analytical stages. In this way, we were able to constantly observe and analyse the same inclusions. The first type included ceramic paste and glaze for the study of body–glaze interface and the distribution of the micro-crystallites in the glaze. The second type included only the glaze for the specific characterization of the micro-crystallites. The ceramic samples were ground down to a standard thickness of 30 μm. Subsequently, the surfaces were polished, allowing them to be used for the reflected-light microscopy, SEM-EDS and SR-μXRD analyses.

Details of thin-section preparation methods can be found in Poole & Sims (2015). The standard thickness of 30 μm permits the growth habits of the micro-crystallites to be identified by optical microscopy at magnifications ranging from about 10× to 100×.

The crystallites and the glazes were analysed by SEM-EDS to ascertain their chemical composition. The bulk chemical composition of the glazes was determined by analysing areas and avoiding the glaze–body interface as well as mineral inclusions. A crossbeam workstation (Zeiss Neon 40) equipped with SEM (Shottky FE) column and EDS (INCAPentaFETx3 detector, 30 mm^2, ATW2 window) was employed. The microscope was operated at 20 kV, with 100-s measuring time, and BSE images were obtained. Quantitative analysis calibration was accomplished with mineral and synthetic standards.

SR-μ-XRD was performed on the focused-beam station of the beamline BL04 (Fauth *et al.*, 2013) at the ALBA Synchrotron (Cerdanyola del Vallès, Spain). The areas of interest from the polished thin sections were selected using an on-axis visualization system and measured in transmission geometry with a focused beam of 15 × 15 μm^2 (full width at half maximum). The energy used was 29.2 keV (λ = 0.4246 Å) and the diffraction patterns were recorded with a Rayonix SX165 CCD detector (active area of 165 mm diameter, frame size 2048 × 2048 pixels, 79 μm pixel size, dynamic range 16 bit). The calibration of the sample-to-detector distance and beam centre (from a LaB_6 sample measured at the same conditions) and the radial integration of the images were performed with the Fit2D software (Hammersley *et al.*, 1996).

Identification of the compounds was performed using the Powder Diffraction File database from the International Centre for Diffraction Data.

3. Results

3.1. French imitations of the Ligurian *Taches Noires* pottery

Samples 9703 and 9708 correspond to dishes which exhibit a transparent glaze and a brown decoration consisting of wavy dark bands (Fig. 1a, b). The chemical composition of the glaze is typical of a lead glaze (Table 1). However, the iron content is relatively high, ~5 wt%. Relict iron oxide particles are still visible at thin-section scale, confirming the addition of iron oxide in the glaze recipe (Assereto, 1994).

Figure 2a shows iron oxide grains identified as hematite by SR-μXRD (Fig. 2b). The hematite grains are present all over the glaze both in the decorated and undecorated areas. The decorated areas are also rich in acicular crystallites (Fig. 3a). SEM-EDS analysis shows that these crystallites contain ~23.5 wt% FeO, ~59 wt% PbO and ~15 wt% SiO_2. They are identified by SR-μXRD as melanotekite, $Pb_2Fe_2Si_2O_9$ (Fig. 3b). The petrographic images show how the acicular crystals of melanotekite have grown towards the ceramic body (Fig. 4a, b). Melanotekite displays a honey colour in plane-polarized light (PPL). Under cross-polarized light (XPL), it exhibits yellow/dark orange colours and straight extinction (Fig. 4b). In some cases, it is possible to observe how the crystals of melanotekite have grown around opaque grains of hematite (Fig. 4c). The acicular crystals are easily visible in transmission mode. In reflected light, as well as by SEM, it is difficult to imagine the 3D morphology of these crystals. Only a few elongated and basal sections are visible (Fig. 4d–f).

Petrographic observation reveals the presence of small crystallite aggregates spread all over the glaze and particularly in the undecorated areas (Fig. 5a). They consist of the association of cristobalite and hematite (Fig. 5b; Fig. 6e in SEM backscatter mode). In thin section, cristobalite appears as small euhedral/subhedral tabular crystals, colourless in PPL. These crystallites, formed close to the glaze–body interface, appear to have grown around opaque grains or micro-crystallites of hematite (Fig. 6a, b). The opaque grains of hematite correspond to relict iron oxides added directly to the glaze mixture, while the hematite micro-crystallites formed in

Downloaded from https://pubs.geoscienceworld.org/eurjmin/article-pdf/4098314/ejm_29_5_0861_0870_di_febo_2638_online.pdf
by UNIVERSITAT DE BARCELONA user

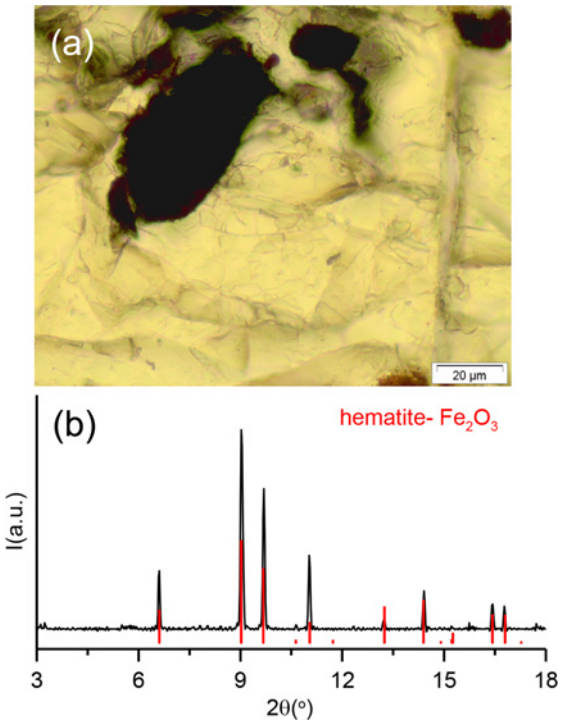

Fig. 2. (a) Photomicrograph of the undecorated area (sample 9703, plane-polarized light = PPL). Iron oxide grains are visible. (b) XRD pattern of analysed crystals. The reference pattern marked corresponds to the JCPDF database pattern 01-079-1741 for hematite. (Online version in colour.)

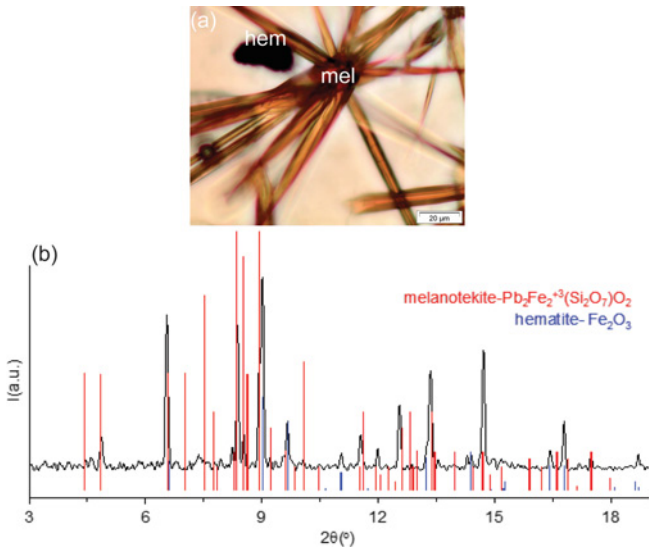

Fig. 3. (a) Photomicrograph of the glaze thin section (sample 9703, PPL). Melanotekite (mel) crystals and a hematite (hem) grain are visible. (b) XRD pattern of analysed crystals. The reference patterns correspond to JCPDF patterns 00-020-0585 for melanotekite and 01-079-1741 for hematite. (Online version in colour.)

the glaze–body interface are recrystallizations of hematite from the ceramic paste (Fig. 6c, d). In addition, some of the cristobalite crystals exhibit embayments and rounded edges that are evidence for resorption (Fig. 6a, b).

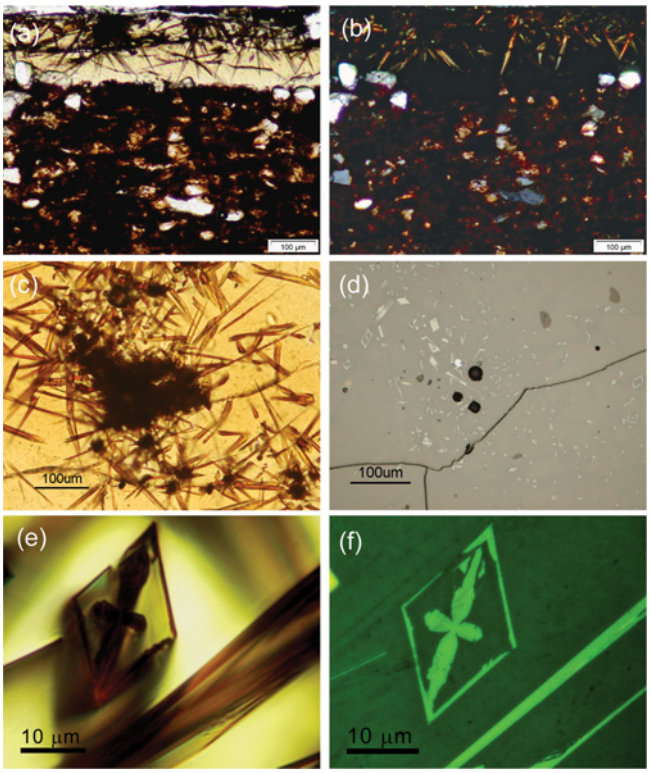

Fig. 4. (a) Photomicrograph of the glaze thin section (sample 9703, PPL), showing acicular crystals of melanotekite grown from the glaze surface towards the ceramic interface. (b) Same as in (a) under cross-polarized light (XPL). (c) Photomicrograph of the acicular crystals of melanotekite grown around opaque hematite grains, PPL. (d) Same as in (c) in reflected light. The melanotekite crystals (light crystallites) are partially visible. (e) Photomicrograph showing the basal section of an acicular crystal of melanotekite with a skeletal texture (PPL). (f) Same image as in (e) in reflected light. (Online version in colour.)

3.2. Brown decorations in a 17th-century Catalan production

Sample SBG10 corresponds to a Catalan majolica which exhibits a brown decoration (Fig. 1c). This was painted on top of the white glaze, according to the distribution of the crystallites (Fig. 7a). In addition, the white glaze contains large amounts of quartz and feldspars grains (Fig. 7b). From a chemical point of view, the glaze is rich in lead and silica and relatively poor in alkali. The manganese content related to the brown decoration is also high (Table 1).

Initially, the crystallites were identified as braunite (Mn_7SiO_{12}) by SR-µXRD (Molera *et al.*, 2013). The thin-section study also revealed the presence of kentrolite, $Pb_2Mn_2Si_2O_9$. Petrographic images of braunite and kentrolite crystallites and the corresponding XRD patterns are shown in Fig. 8a–d, respectively.

Braunite crystallites show two different morphologies, dark-brown bipyramidal crystallites (br1) and brown thin lath-like crystallites (br2) (Fig. 9a). Under XPL, the strong absorption colour masks their interference colours. In reflected light, they appear greyish white with a brownish tinge and a low reflectance (Fig. 9b). The second type of

Downloaded from https://pubs.geoscienceworld.org/eurjmin/article-pdf/4098314/ejm_29_5_0861_0870_di_febo_2638_online.pdf
by UNIVERSITAT DE BARCELONA user

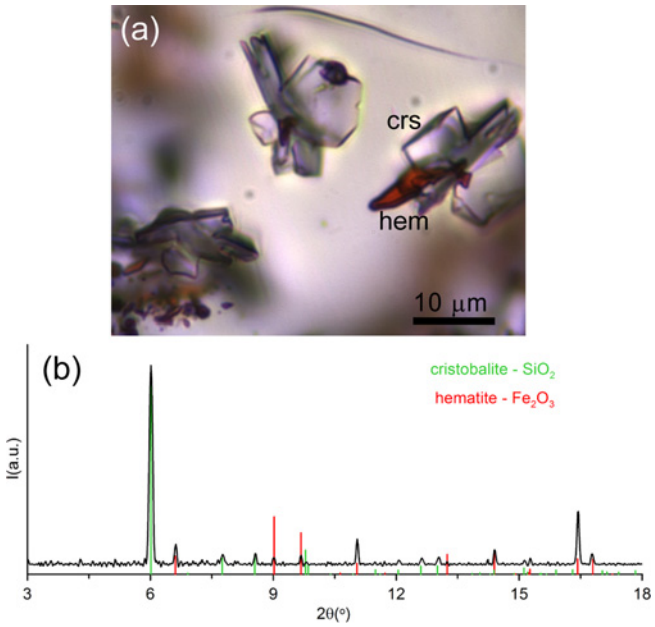

Fig. 5. (a) Photomicrograph of the glaze thin section (sample 9708, PPL) showing colourless crystallites of cristobalite (crs) and reddish crystallites of hematite (hem). (b) XRD pattern of the analysed crystals. The reference patterns correspond to JPDF patterns 01-075-0923 for cristobalite and 01-079-1741 for hematite. (Online version in colour.)

brown braunite crystallites (br2) is barely visible in reflected light, due to the thin lath-like shape (Fig. 9b). In some cases, it is possible to see how they have grown from the dark-brown bipyramidal crystals (br1) and formed dendritic aggregates (Fig. 9c).

The thin crystals of kentrolite (ken) are lath-like and honey colour (Fig. 9c). They exhibit a dendritic texture and are mainly found on the surface of the glaze (Fig. 9d). In reflected light, they have a greyish colour with many orange and brown internal reflections and a low reflectance (Fig. 9e). The two types of braunite crystals (br1–br2) show a dark tone in SEM-BSE images, whereas the kentrolite crystals (Pb-rich) are brighter (Fig. 9f).

4. Discussion

Melanotekite, cristobalite and hematite are the three crystalline phases identified in the glazes of the French imitations from the Joques workshop.

Melanotekite ($Pb_2Fe_2Si_2O_9$), which occurs only in the brown decorated areas, is a rare mineral of the sorosilicate group (Ito & Frondel, 1966) forming a complete solid solution with kentrolite ($Pb_2Mn_2Si_2O_9$), the manganese analogue. Glasser (1967) synthesized pure melanotekite by heating a mixture of composition $2PbO{\cdot}Fe_2O_3{\cdot}2SiO_2$ at 700 °C. Crystals of melanotekite and kentrolite were also obtained from the crystallization of a PbO-enriched melt at 850 °C by Dörsam *et al.* (2008). In historical objects, melanotekite has been found by μXRD in the *grisailles*, an opaque paint made of hematite and lead glass, from Spanish stained glasses dating from the early 16th to the 20th century (Pradell *et al.*, 2015).

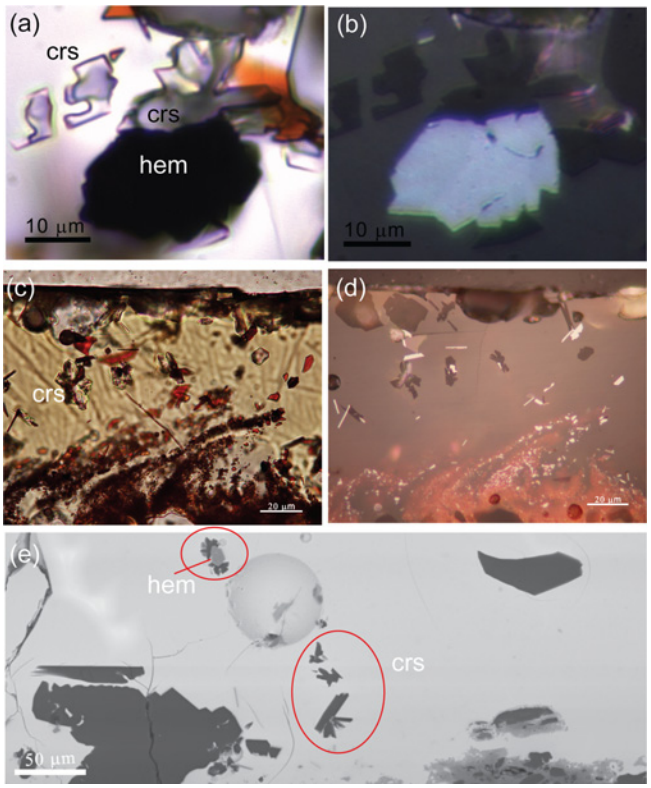

Fig. 6. (a) Photomicrograph of the glaze thin section (sample 9708, PPL) showing crystallites of cristobalite (crs) growing around an opaque grain of hematite (hem). (b) Same image as in (a) in reflected light. The colourless crystals of cristobalite appear very dark, while the opaque grain of hematite displays a light tone. (c) Photomicrograph (PPL) showing hematite micro-crystallites in the glaze–body interface, as well as colourless micro-crystallites of cristobalite (crs). (d) Same as in (c) in reflected light. (e) SEM-BSE image. Cristobalite crystals (crs) appear dark while hematite (hem) shows a light tinge. (Online version in colour.)

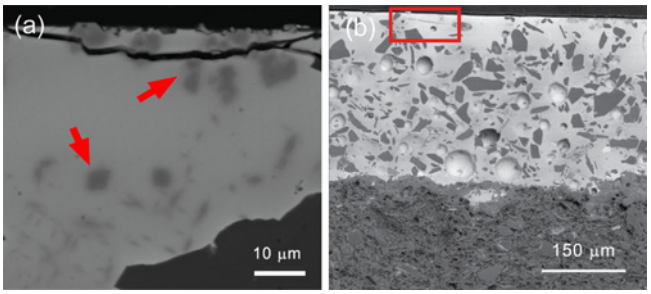

Fig. 7. (a) SEM image in BSE mode of the decoration area of the Catalan tableware. On top of the glaze, grey Mn-rich crystallites are clearly visible. (b) SEM image in BSE mode of the ceramic body and glaze. Many quartz and feldspar grains are present in the glaze. The red rectangle indicates the decoration area with the Mn-rich crystallites.

In our case study, the melanotekite crystals were formed during the glaze firing from the reaction of the decoration components with the constituents of the glaze mixture. The low Mn (0.8 wt% MnO) content of the glaze compared to Fe (4.6 wt% FeO) suggests that the manganese was mainly dissolved, although it cannot be excluded that the melanotekite crystals incorporate some

Downloaded from https://pubs.geoscienceworld.org/eurjmin/article-pdf/4098314/ejm_29_5_0861_0870_di_febo_2638_online.pdf
by UNIVERSITAT DE BARCELONA user

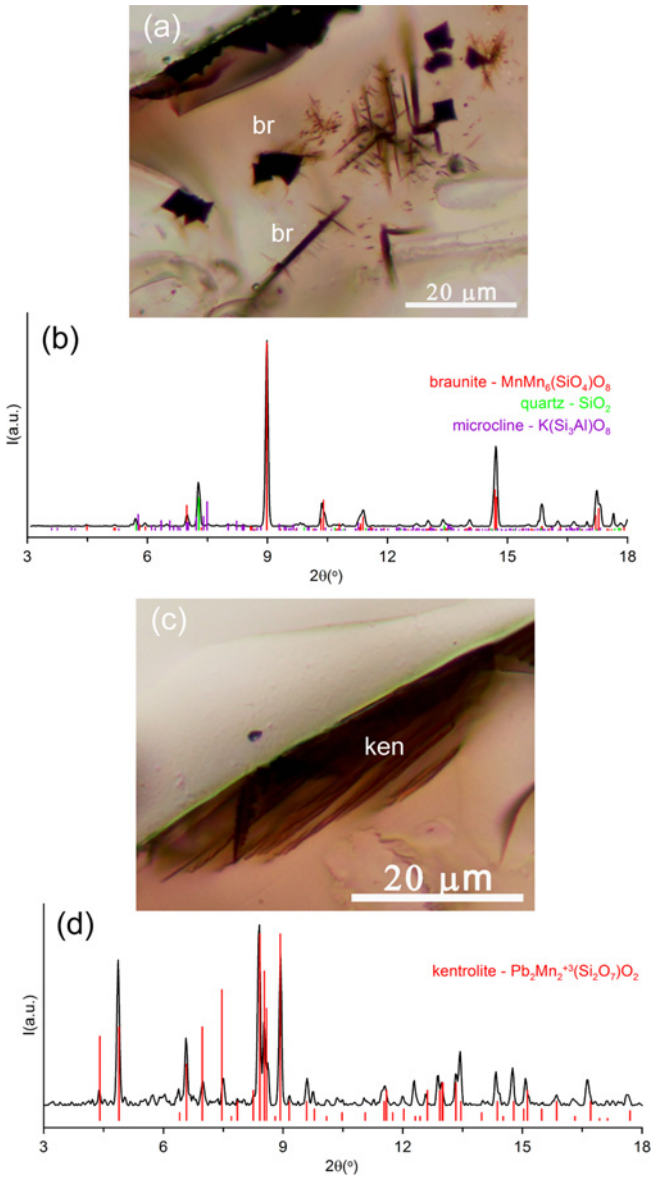

Fig. 8. (a) Photomicrograph of glaze thin section (sample SGB10, PPL) showing brown crystallites of braunite (br). (b) XRD pattern of the analysed crystals. The reference pattern corresponds to JCPDF pattern 01-071-1791 for braunite. (c) Photomicrograph of glaze thin section (sample SGB10, PPL) showing honey-colour crystals of kentrolite (ken). (d) XRD patterns of the analysed crystals. The reference pattern corresponds to JCPDF 01-075-2088 for kentrolite. (Online version in colour.)

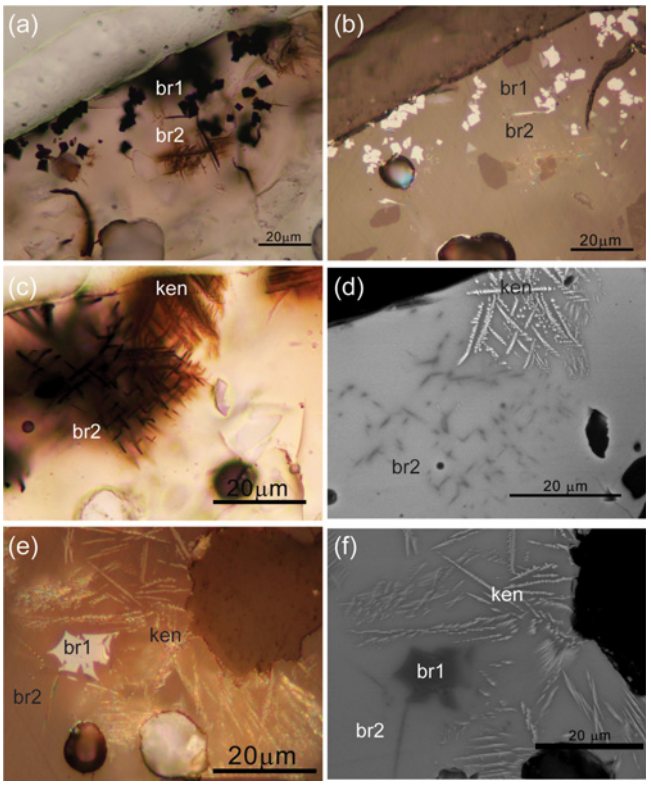

Fig. 9. (a) Photomicrograph of glaze thin section (sample SGB10, PPL), showing dark-brown bipyramidal crystallites of braunite (br1). In addition, brown thin lath-like crystals of braunite (br2) are also visible. (b) Same as in (a) in reflected light. (c) The brown, thin crystals of braunite (br2) form aggregates which look like a dendritic texture. Honey-colour, thin lath-like crystals of kentrolite (ken) are also visible. (d) Same as in (c) in SEM, BSE mode. (e) Photomicrograph, in reflected light, showing the low reflectance of the three types of crystallite (br1, br2 and ken). (f) Same as in (e) in SEM, BSE mode at 20 keV. (Online version in colour.)

manganese, as melanotekite and kentrolite show complete solid solution. Even though the glaze recipe of this type of ceramic indicates the use of a manganese pigment for the decorations, no Mn-rich crystallites have been found in these decorations. The relatively high Fe and low Mn contents of the glaze enhance the formation of melanotekite. Moreover, thin-section petrography appears very useful to understand the conditions for melanotekite crystallization. Melanotekite crystals, nucleated around hematite grains, exhibit skeletal morphologies (Fig. 4e, f) which are normally related to phases formed in quick cooling conditions (*e.g.* Lofgren, 1980). By contrast, cristobalite is found all over the glaze and is particularly abundant in the undecorated areas. Tridymite and cristobalite are high-temperature polymorphs of silica. According to Fenner (1913), tridymite is stable between 870 °C and 1470 °C and transforms to cristobalite at higher temperatures. However, the solid-state transformation of the silica polymorphs does not necessary happen in the same way in a melt. In fact, isothermal firings conducted at 710°, 820° and 910 °C showed that in the PbO–SiO_2 system, both tridymite and cristobalite crystallize at each of these temperatures (Negas & Sorrell, 1968). Artioli *et al.* (2008) noted that in an alkaline environment cristobalite starts to form as cristobalite/tridymite intergrowth, evolving towards cristobalite or tridymite depending on the temperature and alkali concentration (especially Na and K). In our case, the glazes contain Pb and very low amounts of alkali ($Na_2O + K_2O < 0.50$ wt%). During the firing, an iron-saturated liquid was formed at the glaze–ceramic interface and ascended to the glaze surface. In this liquid, the precipitated micro-crystallites of hematite acted as nucleation centres effective in promoting the crystallization of cristobalite. The presence of hematite–

Downloaded from https://pubs.geoscienceworld.org/eurjmin/article-pdf/4098314/ejm_29_5_0861_0870_di_febo_2638_online.pdf
by UNIVERSITAT DE BARCELONA user

cristobalite intergrowths is particularly abundant in the undecorated areas. The relative absence of these intergrowths in the brown decorations suggests a limited dissolution of iron oxide from the ceramic paste. In fact, if the glaze recipe is correct (Assereto, 1994), a manganese pigment was applied directly on the ceramic paste to produce the brown decorations, and then during the firing, the manganese pigment was dissolved in the glaze. This evidence would limit the dissolution of the iron-rich ceramic paste in the decorated areas and consequently reduce the presence of the hematite–cristobalite intergrowths. The manganese–iron rich melt would ascent to the surface finding in the hematite grains of the glaze nucleation centres for the melanotekite crystallites. The high iron and the relatively low manganese content would favour the growth of the iron-rich end-member melanotekite, which appears only in the decorated areas. The brown colour observed is a combination of the manganese and iron dissolved in the glaze and the melanotekite crystallites.

With regard to the production technology of these glazes (9703 and 9708), the presence of relict hematite grains confirms a glaze recipe similar to the one used in Albisola, clearly indicating a perpetuation and transmission of the techniques employed at Ligurian workshops. A technical transmission may have occurred through the move of Albisola potters to France, as it is attested in other Spanish sites (Álvaro Zamora, 1987, 1997, 1999; López Torres & Rueda Galán, 1999; Pleguezuelo, 2002; Carta, 2003). On the contrary, no hematite grains were found in the glazes of other French (Roquefeuille, Provence) and Spanish (Barcelona and Manises) imitations, which reveal a completely different technology production without any technical relationship to the Albisola type (Beltrán de Heredia Bercero *et al.*, 2015; Capelli *et al.*, 2013). However, the original Albisola ceramics do not contain melanotekite crystals in the brown decorations, and the manganese and iron dissolved in the decorated areas of the glazes are responsible for the black-brownish colour shown by these decorations. The lack of melanotekite precipitates in the Albisola production can be explained by a higher firing temperature (above 950 °C) compared to those of Jouques workshop. The presence of melanotekite crystals and the hematite–cristobalite micro-crystallites in the glazes of these imitations can be considered as a technological marker associated to the brown decorations of the Jouques workshop. They were found neither in other French (Roquefeuille) and Spanish (Barcelona and Manises) imitations, nor in the original Albisola wares (Beltrán de Heredia Bercero *et al.*, 2015; Capelli *et al.*, 2013). Moreover, the imitations from Roquefeuille (Provence, France) and from Manises (Valencia, Spain) show the presence of kentrolite, $Pb_2(Mn,Fe)_2Si_2O_9$, crystallites associated to brown decorations, while the hematite grains are not present. The growth of kentrolite crystallites indicates a manganese-rich pigment but firing temperatures similar to those of Jouques. Finally, the presence of iron-oxide grains in the glaze and the large dissolution of ceramic paste, in combination with relatively low firing temperature and fast cooling, is responsible for the characteristic crystallization of melanotekite and hematite–cristobalite in the Jouques glazes.

Braunite and kentrolite are found in the glaze of a sample of the Catalan majolica (SBG10) and associated to the brown decoration. Braunite (Mn_7SiO_{12}) is one of the most common manganese ore minerals and is usually found in association with bixbyite, hausmannite and pyrolusite (De Villiers, 1975). Kentrolite ($Pb_2Mn_2Si_2O_9$) is a rare mineral of the sorosilicate group, which occurs in Mn- and Pb-rich skarn ore deposits (Dörsam *et al.*, 2008). During melting of the glazes, manganese was used as a strong oxidizing agent. Above 600 °C, Mn^{4+} is first reduced to Mn^{3+}, which is responsible for the purple colour of the glazes and then to Mn^{2+} (Janssens, 2013). In the analysed sample, Mn^{4+} was presumably reduced to Mn^{3+} and Mn^{2+} as indicated by formation of kentrolite ($Pb_2Mn^{3+}{}_2Si_2O_9$) and braunite ($Mn^{2+}Mn^{3+}{}_6SiO_{12}$). According to the $MnO–SiO_2$ phase diagram, braunite forms at a temperature of about 500 °C and is stable up to 1150 °C (Factsage, 2010). On the other hand, the crystallization of kentrolite occurs at a temperature between 700 and 850 °C. Although braunite is stable up to very high temperatures, kentrolite tend to dissolve at high temperatures (~950 °C; Ito & Frondel, 1966; Glasser, 1967; Dörsam *et al.*, 2008). Braunite and kentrolite have already been documented in brown decorated glazes and tiles by micro-XRD and micro-Raman (Coentro *et al.*, 2012; Molera *et al.*, 2013; Pradell *et al.*, 2013; Vieira Ferreira *et al.*, 2014).

Our case studies offer the opportunity to examine the additional information provided by thin-section analysis. Careful inspection of these inclusions shows that the crystalline growth must have taken place under two different conditions. The first type of braunite (br1) exhibiting euhedral crystals indicates that it had time and space to grow. By contrast, the second type of braunite (br2), as well as kentrolite, shows dendritic textures, characteristic of a rapid crystallization (*e.g.* Lofgren, 1980). Therefore, the euhedral braunite crystals formed early during the heating. Then, some disequilibrium (*e.g.* temperature drop) must have occurred during the firing process. Braunite continued to grow under these new conditions, but with a different crystalline habit. Thin-section petrography is able to document the incipient formation of the dendritic braunite from the euhedral braunite (Fig. 10a–d). The drop of temperature must have occurred when lead and manganese were still available in the glaze. This can explain the formation of dendritic kentrolite crystals jointly to the second type of braunite (br2).

With respect to the production technology of sample SBG10, cheaper versions of the traditional blue majolica pottery are not unusually found in the small production centres of the Iberian Peninsula. They commonly consist of brown or green decorations on white glazes and motives similar to those of the blue decorations of majolica (Coll Conesa, 2009). In this case, the manganese pigment was

Downloaded from https://pubs.geoscienceworld.org/eurjmin/article-pdf/4098314/ejm_29_5_0861_0870_di_febo_2638_online.pdf
by UNIVERSITAT DE BARCELONA user

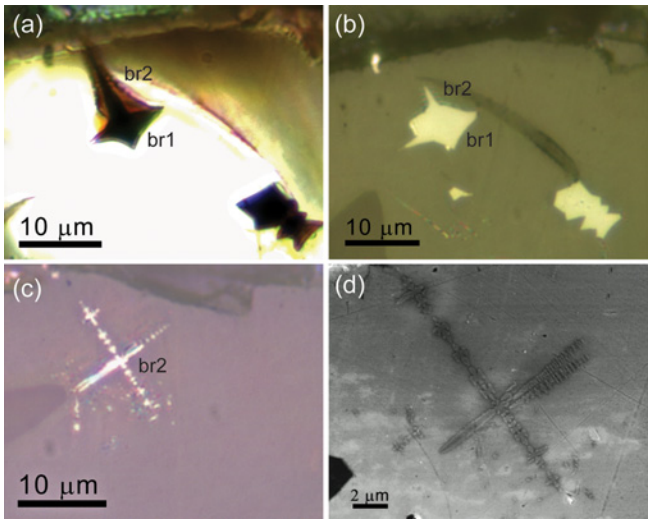

Fig. 10. (a) Photomicrograph of glaze thin section (sample SGB10, PPL). Two types of braunite morphologies can be observed, with incipient crystallization of the thin laths of braunite (br2) from a bipyramidal crystal (br1). (b) Same as in (a) in reflected light. (c) The second type of braunite crystals (br2) in reflected light. (d) Secondary-electron image of (c) at 5 keV. (Online version in colour.)

not pure, probably mixed with a lead oxide compound and applied directly over the raw glaze. This can explain the presence of kentrolite crystallites which were found on top of the white glaze. The raw glaze and the brown decoration were fired together in a second firing. Besides, the procedure to obtain the white opaque glaze is relatively inexpensive. Different particles have been used and several ways of producing glazes have been designed throughout history to obtain white opaque glazes (Mason, 1994; Caiger Smith, 1973). In our case study, to reduce the costs of production, SnO_2 was substituted by a thick glaze full of large quartz and feldspar grains. These inclusions and the bubbles that result from the firing process absorb, scatter, and/or reflect incident light, giving the transparent glaze a whitish translucent appearance which reduced the ability of the ceramic paste colour to show through (Molera *et al.*, 1999; Tite *et al.*, 2008).

5. Concluding remarks

Thin-section petrography in combination with SR-µXRD and SEM-EDS provides a unique look at the microstructures of decorated glazes, detecting and identifying the micro-crystallites formed during firing. The determination of their distribution and growth habits allows a better understanding of the technological process involved in the manufacturing of these ceramics.

In the French imitations of the *Taches Noires* pottery (Jouques workshop), the presence of hematite grains in the glaze confirms a glaze recipe similar to the one used in Albisola, clearly indicating a perpetuation and transmission of the techniques employed in the Ligurian workshops. The hematite acts as a nucleating agent effective in promoting the crystallization of melanotekite and cristobalite. Melanotekite and cristobalite can be considered as a technological marker associated with the production of the Joques workshop and might be therefore used to identify possible productions from this workshop. Remarkably, no melanotekite and cristobalite crystals were found in the glazes of other French and Spanish imitations and in the Albisola reference materials. The lack of melanotekite growth in the production of the Albisola wares can be explained by the use of a higher firing temperature compared to those of Joques workshop. Finally, cristobalite appears to grow around precipitated micro-crystallites of hematite, and it is not related to the presence of alkali ions, which are normally considered responsible for the formation of cristobalite crystallites far from equilibrium conditions.

In the Catalan brown tablewares, a manganese pigment mixed with lead oxide was applied on top of the raw glaze. The presence of braunite and kentrolite in the decoration area indicates a firing temperature ~950 °C. Thin-section analysis was able to document a process of crystallization in two stages. Euhedral braunite crystallites were produced during heating. A temperature drop during the firing process gave rise to the crystallization of dendritic braunite and kentrolite. Finally, the use of large quartz and feldspar grains to enhance the opacity of the glaze, instead of cassiterite, as well as the use of manganese instead of cobalt for the decorations are both indicative of a low-cost production.

Acknowledgements: Roberta Di Febo acknowledges receipt of a studentship from the UVIC-UCC Scholarship Program, awarded by University of Vic, Central University of Catalonia. The authors thank Lucy Vallauri for the archaeological samples from Jouques and acknowledge support from project MAT2013-41127-R funded by the Ministerio de Ciencia e Innovación (Spain) and the ALBA Synchrotron Light Facility 2014060905 (BL04), and from projects 2014 SGR 00581 (T.P.), 2014 SGR1585 (J.M. and R.D.F.) and 2014 SGR 1661 (J.C.M.).

References

Álvaro Zamora, M.I. (1987): Sobre los modos de irradiación de la cerámica ligur y la presencia de ceramistas de esta procedencia en la Zaragoza del siglo XVII. *Artigrama*, **4**, 137–156.

— (1997): La penetración de la moda cerámica ligur en los alfares peninsulares de los siglos XVII-XVIII: el caso de Aragón. *in* "Transferències i comerç de ceràmica a l'Europa mediterrània (segles XIV-XVII)". Instituto De Estudios Baleáricos (IEB), Palma de Mallorca, 185–212.

— (1999): La emigración de ceramistas ligures a Aragón (España) en el siglo XVII y la influencia de sus repertorios decorativos en la producción de los alfares locales. *in* "Atti XXXI Convegno Internazionale della Ceramica 1998". Centro Ligure per la Storia della Ceramica, Firenze, 151–169.

Amouric, H. & Vallauri, L. (1993): La fabrique de Villemus. *in* "Un goÛt d'Italie. Céramiques et céramistes italiens en Provence du Moyen Âge au XXème siècle". Catalogue Exposition, Narration, Aubagne, 118–120.

Downloaded from https://pubs.geoscienceworld.org/eurjmin/article-pdf/4098314/ejm_29_5_0861_0870_di_febo_2638_online.pdf
by UNIVERSITAT DE BARCELONA user

Arnold, D.E. (1972): Mineralogical analyses of ceramic materials from Quinua, department of Ayacucho, Peru. *Archaeometry*, **14**, 93–102.

Artioli, G., Angelini, I., Polla, A. (2008): Crystals and phase transitions in protohistoric glass materials. *Phase Transitions*, **81**, 233–252.

Assereto, G. (1994): G. Chabrol De Volvic, Statistica delle provincie di Savona, di Oneglia, di Acqui e di parte della provincia di Mondovì, che formavano il dipartimento di Montenotte. Comune di Savona, Savona.

Beltrán de Heredia Bercero, J. & Miró i Alaix, N. (2010): El comerç de cerámica a Barcelona als segles XVI-XVII: Itàlia, França, Portugal, els tallers del Rin i Xina. *in* "Quarhis – Quaderns d'Arqueologia i Història de la Ciutat de Barcelona". Ajuntament de Barcelona, Barcelona, 15–91.

Beltrán de Heredia Bercero, J., Capelli, C., Di Febo, R., Madrid i Fernández, M., Buxeda i Garrigós, J. (2015): Imitaciones de ceràmicas Taches Noires en Barcelona en el siglo XVIII. Datos arqueológicos y arqueométricos. *in* "Actas do X Congresso Internacional A Cerâmica Medieval no Mediterrâneo". Silves 2012, Camera Municipal de Silves & Campo Arqueológico de Mértola, 613–618.

Blake, H. (1981): Pottery exported from Northwest Italy between 1450 and 1830: Savona, Albisola, Genoa, Pisa, and Montelupo. *in* "Archaeology and Italian Society. Prehistoric, Roman and Medieval Studies", G. Barker & R. Hodges, eds., BAR, International Series 102, Oxford, 99–124.

Caiger Smith, A. (1973): Tin-glaze pottery in Europe and the Islamic World. The tradition of 1000 years. *in* "Maiolica, Faience & Delfwarer. Technique, Tradition and Innovation in Islam and the Western World". Faber & Faber, London, UK.

Cameirana, A. (1970): La terraglia nera ad Albisola all'inizio dell'800. *in* "Atti III Convegno Internazionale della Ceramica 1969". Centro Ligure per la Storia della Ceramica, Firenze, 63–95.

— (1977): La ceramica albisolese a Taches Noires. *in* "Atti del X Convegno Internazionale della Ceramica 1976". Centro Ligure per la Storia della Ceramica, Firenze, 277–293.

Capelli, C., Richez, F., Vallauri, L., Cabella, R., Di Febo, R. (2013): L'epave du Grand Congloue 4: Caracterisation archeologique et archeometrique d'un lot de ceramiques a Taches Noires de Albisola-Savona. *in* "Atti XLV Convegno Internazionale della Ceramica 2012". Centro Ligure per la Storia della Ceramica, Firenze, 7–16.

Carta, R. (2003): Un gruppo di maioliche liguri a smalto berettino rinvenute nell'Alhambra di Granada. *in* "Atti XXXV Convegno Internazionale della Ceramica 2002". Centro Ligure per la Storia della Ceramica, Firenze, 129–139.

Coentro, S., Mimoso, J.M., Lima, A.M., Silva, S., Pais, A.N., Muralha, V.S.F. (2012): Multi-analytical identification of pigments and pigment mixtures used in 17th century Portuguese azulejos. *J. Eur. Ceram. Soc.,* **32**, 37–48.

Coll Conesa, J. (2009): La Cerámica Valenciana (Apuentes para una síntesis). Asociación Valenciana de Cerámica, Gremio/RM Ediciones, Valencia.

De Villiers, J.P.R. (1975): The crystal structure of braunite with reference to its solid-solution behaviour. *Am. Mineral.*, **60**, 1098–1104.

Dörsam, G., Liebscher, A., Wunder, B., Franz, G. (2008): Crystal structures of synthetic melanotekite ($Pb_2Fe_2Si_2O_9$), kentrolite ($Pb_2Mn_2Si_2O_9$), and the aluminum analogue ($Pb_2Al_2Si_2O_9$). *Am. Mineral.,* **93**, 573–583.

Factsage (2010): Phase diagram $MnO–SiO_2–O_2$ $p(O_2) = 0.21$ atm. Phase diagram $MnO–SiO_2–O_2$ $p(O_2) = 0.01$ atm. Date from FT Oxide – FACT Oxide Database.

Fauth, F., Peral, I., Popescu, C., Knapp, M. (2013): The new material science powder diffraction beamline at ALBA Synchrotron. *Powder Diffr.*, **28**, 360–370.

Fenner, C.N. (1913): The stability relations of the silica minerals. *Am. J. Sci.*, **36**, 331–338 (Series 4)

Freestone, I., Johns, C., Potter, T. (eds.) (1982): Current research in ceramics: thin section studies. British Museum Occasional Paper 32. British Museum, London.

Glasser, F.P. (1967): New data on kentrolite and melanotekite: ternary phase relations in the system $PbO–Fe_2O_3–SiO_2$. *Am. Mineral.*, **52**, 1085–1093.

Hammersley, A.P., Svensson, S.O., Hanfland, M., Fitch, A.N., Häusermann, D. (1996): Two-dimensional detector software: from real detector to idealised image or two-theta scan. *High Pressure Res.*, **14**, 235–248.

Harrison Hall, J. (1997): Chinese porcelain from Jingdezhen, Pottery in the making: ceramic traditions. I.C. Freestone & D. Gaimster, eds. Smithsonian Institution Press, Washington, 182–187.

Ito, J. & Frondel, C. (1966): Syntheses of the kentrolite-melanotekite series. *Ark. Mineral. Geol.*, **4**, 387–390.

Janssens, K.H.A. (ed.) (2013): Modern methods for analysing archaeological and historical glass. Wiley and Sons, West Sussex.

Jiazhi, L. (1984): The evolution of Chinese pottery and porcelain technology. *in* "Ancient technology to Modern science", W.D. Kingery, ed. American Ceramic Society, Columbus, 135–162.

Kamilli, D.C. & Lamberg-Karlovsky, C.C. (1979): Petrographic and electron microprobe analysis of ceramic from Tepe Yahya, Iran. *Archaeometry*, **21**, 47–59.

Lofgren, G. (1980): Experimental studies on the dynamic crystallization of silicate melts. *in* "Physics of magmatic processes", R.B. Hargraves, ed. Princeton University Press, Princeton, 487–551.

López Torres, P. & Rueda Galán, M.M. (1999): La imitación de la "berettina" en las producciones sevillanas. *in* "Atti XXXI Convegno Internazionale della Ceramica 1998". Centro Ligure per la Storia della Ceramica, Firenze, 171–177.

Mason, R.B. (1994): Islamic Glazed Pottery: 700–1250. Ph.D. Thesis, Oxford University, Oxford, UK.

Middleton, A. & Freestone, I. (eds.) (1991): Recent developments in ceramic petrology. *in* "British Museum Occasional Paper 81". London.

Molera, J., Pradell, T., Salvado, N., Vendrell-Saz, M. (1999): Evidence of tin oxide recrystallization in opacified lead glazes. *J. Am. Ceram. Soc.*, **82**, 2871–2875.

Molera, J., Coll, J., Labrador, A., Pradell, T. (2013): Manganese brown decorations in 10th to 18th century Spanish tin glazed ceramics. *Appl. Clay Sci.*, **82**, 86–90.

Negas, T. & Sorrell, C.A. (1968): Silica Transformation in the system $PbO–SiO_2$. *J. Am. Ceram. Soc.*, **51**, 622–625.

Pleguezuelo, A. (2002): Lozas y azulejos de Sevilla en el Siglo de Oro. Lozas y azulejos de la colección Carranza, 1, Toledo, 203–226.

Poole, A.B. & Sims, I. (2015): Concrete petrography: a handbook of investigative technique, 2nd edition. CRC Press.

Downloaded from https://pubs.geoscienceworld.org/eurjmin/article-pdf/4098314/ejm_29_5_0861_0870_di_febo_2638_online.pdf
by UNIVERSITAT DE BARCELONA user

Pradell, T., Molera, J., Salvadó, N., Labrador, A. (2010): Synchrotron radiation micro-XRD in the study of glaze technology. *App. Phys. A*, **99**, 407–417.

Pradell, T., Molina, G., Molera, J., Pla, J., Labrador, A. (2013): The use of micro-XRD for the study of glaze color decorations. *App. Phys. A*, **111**, 121–127.

Pradell, T., Molina, G., Murcia, S., Ibáñez, R., Liu, C., Molera, J., Shortland, A.J. (2015): Materials, techniques and conservation of historic stained glass grisailles. *IJAGS*, 1–18.

Quinn, P.S. (2009): Interpreting silent artefact: petrographic approaches to archaeological ceramics. Archaeopress Oxford, England.

— (2013): Ceramic petrography: the interpretation of archaeological pottery & related artefacts in thin section. Archaeopress, Oxford, 39–150, 181–188.

Reedy, C.L. (1994): Thin section petrography in studies of cultural materials. *JAIC*, **33**, 115–129.

— (2008): Thin section petrography of stone and ceramic cultural materials. *Archetype, London*, 124–172, 194–206.

Rius, J., Labrador, A., Crespi, A., Frontera, C., Vallcorba, O., Melgarejo, J.C. (2011): Capabilities of through-the-substrate micro-diffraction: application of Patterson-function direct methods to synchrotron data from polished thin sections. *J. Synchrotron Radiat.*, **18**, 891–898.

Shepard, A.O. (1965): Rio Grande glaze-paint pottery: a test of petrographic analysis. *in* "Ceramics and man", F.R. Matson, ed. Chicago, 62–87.

Tite, M., Pradell, T., Shortland, A. (2008): Discovery, production and use of tin-based opacifiers in glasses, enamels and glazes from the late Iron Age onwards: a reassessment. *Archaeometry*, **50**, 67–84.

Vieira Ferreira, L.F., Conceição, D.S., Ferreira, D.P., Santos, L.F., Casimiro, T.M., Ferreira Machado, I. (2014): Portuguese 16th century tiles from Santo António da Charneca's kiln: a spectroscopic characterization of pigments, glazes and pastes. *J. Raman Spectrosc.*, **45**, 838–847.

Received 1 December 2016
Modified version received 22 February 2017
Accepted 27 February 2017

Downloaded from https://pubs.geoscienceworld.org/eurjmin/article-pdf/4098314/ejm_29_5_0861_0870_di_febo_2638_online.pdf
by UNIVERSITAT DE BARCELONA user

6 Discussion

The first article here presented and entitled *The production of a lead glaze with galena: Thermal transformations in the PbS–SiO_2 system*, provides the possibility to bring to the readers' attention a series of relevant issues from a technological point of view.

First of all, the choice of the sample, that it to say a glaze which retains relict galena grains is itself extremely interesting from its archaeological and technical implications. The archaeometric studies on archaeological lead glazes normally deal with final products, that it to say glazes in which the original raw materials of the glaze recipe have been completely decomposed during the firing process. For this reason, the chance to find evidence of the starting glaze recipe is extremely low. Second, the use of galena in a glaze recipe would have the advantage of eliminating the stage of roasting to obtain lead oxide. In spite of this benefit, there is no archaeological evidence or literature demonstrating the use of galena or roasted galena (PbO) in the production of lead glazes in Roman times. Another relevant aspect that we have to consider is that galena is found in association with lanarkite and mattheddleite, two types of crystallites that had never been documented before in archaeological lead glazes. Along this line, the archaeometric study of these phases could provide guidelines in the future investigations on lead glazes made by using galena.

The present contribution has showed as galena, lanarkite and mattheddleite are responsible for the appearances of the glaze. Such evidence could be employed as a valuable criterion from the archaeologists during the macroscopic inspections on others archaeological samples that exhibit comparable features. In fact, galena is responsible for the opacity of the glaze, lanarkite for the opalescence observed in the yellow area and mattheddleite is responsible for the transparent adamantine luster. The three different colours of the glaze can be explained in terms of its chemical composition and the firing conditions. The green colour is related to the presence of Fe^{2+} ions dissolved in the glaze and the glazed surface might had been exposed directly to the flame. In fact, the delayed decomposition of galena and the reduction in the iron ions could be explained because of the reducing atmosphere during the firing. On the opposite, the yellow and honey tinges are due to the presence of Fe^{3+} ions in the glaze. In this case, both areas would not have been exposed to the flame directly.

From a microscopic point of view, the SEM-OM (RL-TL mode) integrated approach revelled effective in producing guidelines for the possible identification of lanarkite and mattheddleite in other archaeological samples. As it has been showed, some properties observed in RL mode - polishing relief and reflectance - can be very useful to identify glaze phases of similar compositions often indistinguishable from one another using SEM. Lanarkite (a very soft mineral) shows a pronounced negative relief and a lower reflectivity compared to mattheddleite.

Finally, the presence of mattheddleite, a rare mineral of the apatite supergroup (ellestadite) that contains chlorine has been explained in terms of possible sources and raw materials used. More probably, its occurrence is linked to the use of halophyte plants during the firing. The production of ashes generated burning these plants and its deposition on the glaze surface might explain both the presence of mattheddleite in the glaze and the preferential direction of growth of these crystals.

Regarding the high temperature resolved X-ray Diffraction experiments, the data showed that the oxidation of galena gives rise to the formation of lanarkite ($PbO{\cdot}PbSO_4$) at 315ºC and its decomposition at a temperature lower (916ºC) than those found in the $PbO\text{-}PbSO_4$ system. The sudden disappearance of lanarkite can be related to the presence of SiO_2 which gives rise to a melt at ~775°C. The lack of lead silicates in the $PbS\text{-}SiO_2$ system studied is probably due to remaining sulphates in the glaze mixture that handicapped the crystallization of the $PbO/\ SiO_2$ compounds as observed in the $PbO\text{-}PbSO_4$ phase diagram. Therefore, when galena is used, highly oxidative conditions need to be guaranteed in order to eliminate sulphur from the glaze. In agreement with these results, the green and yellow areas of the archaeological glaze also show a silica melt and lanarkite, but $PbO/\ SiO_2$ compounds are not found. As reported by the $PbO\text{-}PbSO_4$ system, two lead oxysulfates ($2PbO{\cdot}PbSO_4$ and $4PbO{\cdot}PbSO_4$) also formed in our experiment after the lanarkite decomposition. However, lead oxysulfates are not found in the misfired glaze. The presence of galena and lanarkite suggests a low firing temperature (below 795°C) and a short time of firing. In addition, the direct hit of the flame on the glaze surface which produces a reducing atmosphere probably affected the oxidation of galena and decomposition of lanarkite. Finally, although anglesite has been found in our experiment, its absence in the misfired glaze could be an indicative that it was not present in the galena used by the potters.

The second article here presented and entitled "*Technological implications of neo-formed hematite crystals in ceramic lead glazes"* is suggestive for both its methodological implications and its technological significances.

Concerning the first aspect, this case study demonstrates the difficulty of identifying this type of thin crystallites of hematite in ceramic glazes using the most common routine analytical techniques. As we have seen through the different examples here presented, the possibility that crystallites are located under the polished surface of the sample is a very common situation in ceramic glazes. The methodological approach employed presents benefits and limitations in using one or another technique and provides effective solutions that could be applied to other crystals and in other samples of ceramic glazes that show similar difficulties.

The presence of hematite in ceramic glazes moves the discussion on some technological considerations. The hematite micro-crystallites found in our archaeological glazes are formed in the glaze–body interface from the reaction between the components of the glaze mixture and the ceramic paste. Hematite is the principal mineral phase in hematite crystalline glazes under oxidizing conditions and also the typical feature of the so called "iron aventurine glazes". In the specific case of the aventurine glazes, the optical sparkling effect observed is due to the sizes of the hematite crystallites, the high content of iron and to the viscosity of the melt. As we have seen in our case study, the relatively low quantity of iron and the fast cooling are probably responsible for the loss of the decorative effect in the coating. In addition, the difficulty in obtaining the aventurine effect makes that the presence of these hematite hexagons in our archaeological glazes is more the accidental result of the interaction between paste and glaze of a specific composition than a deliberated decorative effect. However, it is intriguing to observe how the widespread presence of these hematite crystallites in our archaeological samples can provide key data to understand what happened during the cooling process. At that moment, the capacity of the melt to retain the Fe in solution was lessened and the excess was precipitated as thin plate crystals. Despite of the relatively low content of Fe detected by SEM-EDS, the glaze microstructure observed by OM provides us an invaluable information: an oversaturation took place and the hematite crystallites represent the evidence of this process.

On the other hand, the experimental data are very useful to estimate firing conditions and ranges stability of hematite and melanotekite crystals (or kentrolite, the manganese analogue) providing guidelines to use them as technological markers of temperature. In fact, the presence of hematite in association with melanotekite is indicative of low firing temperatures (<925ºC), while the occurrence of only hematite seems to be a fingerprint of higher temperatures (>925ºC). Melanotekite ($Pb_2Fe_2Si_2O_9$) in association with hematite has been identified in iron-coloured high-lead glazes (Roisine et al., 2017). The results obtained by Roisine et al. on the thermal range of stability of melatotekite and hematite are substantially in agreement with our experimental data. Such data have been recently used by Di Febo et al. (2018) in the study of some Catalan imitations of the Ligurian Taches Noires ware found in the city of Barcelona (Spain). In this case, hematite has been found in association with kentrolite ($Pb_2Mn_2Si_2O_9$), suggesting a firing temperature below 925° C for these imitations.

The third article entitled "*Thin-section petrography and SR-μXRD for the identification of micro-crystallites in the brown decorations of ceramic lead glazes*" proposes two examples of lead glazes decorated with iron and manganese pigments. Both articles show how the optical information on the

glaze microstructures can be used to infer about the technological processes and manufacturing choices.

Along this line, the glazes of the French imitations from the Jouques workshop provide significant data about the transfer of technological knowledge. In fact, the relict hematite grains found in the glazes allow to confirm both the intentional addition of iron oxides and a glaze recipe similar to the one used in Albisola. On the other hand, the melanotekite crystallites are formed during the glaze firing from the reaction of the decoration components with the constituents of the glaze mixture. Even though the glaze recipe of this type of ceramic indicates the use of a manganese pigment for the decorations, no Mn-rich crystallites have been found in the decorations of the French samples studied. The high iron and the relatively low manganese content promoted the growth of the iron-rich end-member melanotekite. The skeletal morphologies observed during the thin section work suggest a fast cooling conditions for these crystallites. Melanotekite along with manganese and iron dissolved in the glaze are responsible for the brown colour of these decorations. However, we have to note that the original Albisola ceramics do not contain melanotekite/kentrolite crystals in the brown decorations. The lack of these precipitates in the Albisola productions can be explained by a higher firing temperature (above 950ºC) compared to those of Jouques workshop.

Cristobalite, the other mineralogical phase identified in the French imitations, is found all over the glazes and it is particularly abundant in the undecorated areas. The presence of cristobalite is not related to alkali ions, which are normally responsible for its formation far from equilibrium conditions. In fact, cristobalite is found to grown around relict hematite grains or precipitated micro-crystallites of hematite formed at the glaze–ceramic interface. In this case, hematite acted as nucleation centre effective in promoting the crystallization of cristobalite.

Melanotekite and cristobalite crystallites have been found neither in other French and Spanish imitations, nor in the original Albisola wares. Then, they might be considered as technological markers associated to the brown decorations of the Jouques workshop and they might be therefore used to identify possible productions from this workshop in the Mediterranean consumption sites.

The manganese decorations of the Catalan majolica tablewares contain both braunite (Mn_7SiO_{12}) and kentrolite ($Pb_2Mn_2Si_2O_9$) crystallites. As this study showed, the manganese pigment was not pure and probably mixed with a lead oxide compound and applied directly over the raw glaze. This could be explain the presence of kentrolite crystallites, which have been found on the top of the white glaze. Braunite and kentrolite can be considered as technological markers of temperature since their presence in the decoration area suggests a firing temperature of about 950ºC. The study of the crystalline habits of both braunite and kentrolite provided valuable information on the process of crystallization and indirectly on the firing stage. In fact, as showed by the optical study, braunite exhibits two different morphologies - euhedral bipyramidal and thin lath-like crystallites-, while

kentrolite displays a dendritic texture. That is to say, that the first type of braunite, that with euhedral crystals, formed early during the heating. Then, some disequilibrium must have occurred during the firing process. Braunite continued to grow under these new conditions, but with a different crystalline habit. The formation of dendritic kentrolite crystals along with the second type of braunite reflects the new conditions of the crystalline environment. Possibly, this change must have occurred when lead and manganese were still available in the glaze.

7 Conclusions

We have studied three kinds of glazes: misfired lead glazes, lead glazes with iron decorations and lead glazes with manganese decorations. In all the three case studies, the glaze microstructure investigated is the result of the combination of different factors such as the raw materials used, the temperature reached, time of the firing process, kiln conditions and cooling state. The methodology has been based on specific and complementary analytical techniques depending on each type of sample. OM has been the first step in the experimental investigation sequence. In the next step, OM has been combined with SEM-EDS, FIB, EPMA and SR-μ-XRD depending on the cases. Replications of the manufacturing process have been carried out to understand methods of production and technological choices.

In the light of this thesis, much work still remains to be done. In the case of lead glazes made with galena, the next step planned will be the study of one series of modern glazed ceramics for which we are aware of the use of galena in the glaze mixture. One of the short-term objectives will be the possible identification of PbO/SiO_2 compounds that haven been found neither in our archaeological sample nor in the experimental replications. Moving towards long-term goals and depending on the compounds identified, other replications will be necessary in order to understand ranges of stability, methods of production and cycles of firing.

With regard to the Taches Noires wares which have been object of study in two articles of this thesis, there are some tricky questions that remain to investigate. One of this is surely the presence of cristobalite and tridymite in such glazes (work in progress). An important result has been achieved in this work and concerns both the identification of hematite as nucleation agent of cristobalite and the actual irrelevance of the alkali environment for the formation of this silica polymorph. However, the sequence of nucleation of cristobalite and tridymite in ceramic glazes is not clear and neither their stability ranges. While cristobalite is a mineralogical phase common in ceramic glazes, evidence of tridymite seems to be difficult to find. In reality, preliminary results (work in progress) seem suggest that tridymite is not so unusual in ceramic glazes and the difficulty to locate it is probably related to the way in which tridymite forms into the glaze matrix. On the other hand, a milestone will be the integration of all the information obtained on the technological production of the original Taches Noires wares and its foreign imitations (mainly French and Spanish copies) in order to complete the picture on the technological transfer of knowledge from Italy to the outside productions sites.

8 References

Acosta-Maeda, T. E., Scott, E. R. D., Sharma, S. K., Misra, A. K., "The pressures and temperatures of meteorite impact: Evidence from micro-Raman mapping of mineral phases in the strongly shocked Taiban ordinary chondrite", *Am Min*, **98** [5-6], 859-869 (2013).

Amigues, F. and Mesquida, M., Les Ateliers et la Céramique de Paterna, XIIIe-XIVe Siècles, Musée Saint-Jacques, Béziers, France (1993).

Amouric, H. and Vallauri, L., "La fabrique de Villemus", in *Un goût d'Italie, Céramiques et céramistes italiens en Provence du Moyen Âge au XXème siècle*, Catalogue Exposition, Narration, Aubagne, 118-120 (1993).

Ashok, R. (Ed.), Artists' Pigment: A Handbook of their History and Characteristics, National Gallery of Art, Washinghton, DC (1997).

Assereto, G., Chabrol De Volvic, Statistica delle provincie di Savona, di Oneglia, di Acqui e di parte della provincia di Mondovì, che formavano il dipartimento di Montenotte, Comune di Savona, 2 (1994).

Bajnóczi, B., Nagy, G., Tóth, M., Ringer, I., Ridovics, A., "Archaeometric characterization of 17th century tin-glazed Anabaptist (Hutterite) faience artefacts from North-East-Hungary", *Journal of Archaeological Science*, **45**, 1–14 (2014).

Barton, K.J., "Terres cuites provenant de la forteresse de Luisbourg", *Historie et Archéologie*, **55**, Direction des lieux et des parcs historiques nationaux (s.a.s.), Ottawa, 4-78 (1970).

Berti, G. and Mannoni, T., "Rivestimenti vetrosi e argillosi su ceramiche medievali e risultati emersi da ricerche archeologiche e analisi chimiche e mineralogiche", in T. Mannoni and A. Molinari (Eds.), *Scienze e Archeologia*, All'Insegna del Giglio, Firenze, 89-124 (1990).

Birks, L., Electron Probe Microanalysis, Interscience, New York, (1963).

Blake, H., Pottery exported from Northwest Italy between 1450 and 1830: Savona, Albisola, Genoa,

Pisa, and Montelupo. In G. Barker and R., Hodges (Eds.), Archaeology and Italian Society. Prehistoric, Roman and Medieval Studies, BAR, International Series 102, Oxford, 1981, pp. 99-124.

Borgia, I., Brunetti, B., Mariani, I., Sgamellotti, A., Cariati, F., Fermo, P., Padeletti, G., "Heterogeneous distribution of metal nanocrystals in glazes of historical pottery", *Applied Surface Science*, **185** [3], 206–216 (2002).

Caggiani, M.C., Colomban, P., Valotteau, C., Mangone, A., Cambon, P., "Mobile Raman spectroscopy analysis of ancient enamelled glass masterpieces", *Anal. Meth,* **5**, 4345–4354 (2013).

Caggiani, M. and Colomban, P., "Raman microspectroscopy for Cultural Heritage studies", *Physical Sciences Reviews*, 1-18 (2018).

Caggiani, M., Valotteau, C., Colomban, P., "Inside the glassmaker technology: search of Raman criteria to discriminate between Emile Gallé and Philippe-Joseph Brocard enamels and pigment signatures", *Journal of Raman Spectroscopy*, **45**, 456–464 (2014).

Caiger-Smith, A., Luster Pottery: Technique, Tradition and Innovation in Islam and the Western World, Faber and Faber, London, U.K. (1985).

Cameirana, A.,"La terraglia nera ad Albisola all'inizio dell'800", in *Atti III Convegno Internazionale della Ceramica 1969*, Centro Ligure per la Storia della Ceramica, All' Insegna del Giglio, Firenze, 63- 95 (1970).

Cameirana, A., "La ceramica albisolese a Taches Noires", in *Atti del X Convegno Internazionale della Ceramica 1976*, Centro Ligure per la Storia della Ceramica, All' Insegna del Giglio, Firenze, 277-293 (1977).

Capelli, C. and Cabella, R., "Il contributo delle analisi archeometriche alla conoscenza della maiolica ligure: risultati recenti e problemi aperti", in *Atti XLV Convegno Internazionale della Ceramica* 2012, Centro Ligure per la Storia della Ceramica, All'insegna del Giglio, 373-382 (2012).

Capelli, C. and Cabella, R. "Le radici di una produzione a diffusione internazionale. La storia della ceramica di Savona e Albisola dal punto di vista dell'archeometria", *Ceramica contemporanea all'aperto, Studi sulla conservazione e il restauro*, Aracne, Roma, 45-62 (2013).

Capelli, C. and Marescotti, P., "Caratterizzazione mineralogico-petrografica degli ingobbi delle ceramiche basso-medievali savonesi", in M. Martini (Ed.), *Atti del Primo Congresso Nazionale dell'Associazione Italiana di Archeometria*, Patron, Bologna, 389-400 (2000).

Capelli, C., Richez, F., Vallauri, L., Cabella, R., Di Febo, R., "L'epave du Grand Congloue 4: Caracterisation archéologique et archéometrique d'un lot de ceramiques a Taches Noires de Albisola-Savona", in *Atti XLV Convegno Internazionale della Ceramica 2012*, Centro Ligure per la Storia della Ceramica, All' Insegna del Giglio, Firenze, 7-16 (2013).

Carratoni, L. and Di Santo, V. A., "Micro-Raman Investigation of Coloured Glazes on Majolica Sherds from the Monk's Palace Waste Shaft in Capena (Rome)", *Journal of Applied and Laser Spectroscopy* **2**, 20–28 (2015).

Casadio, F., Daher, C., Bellot-Gurlet, L., "Raman Spectroscopy of cultural heritage Materials: Overview of Applications and New Frontiers in Instrumentation, Sampling Modalities, and Data Processing", *Top Curr Chem. (Z),* 362-374 (2016).

Cavaletto, M., "La ceramica a Taches Noires", in. R. Comba (Ed.), *Cuneo dal XIII al XVI secolo, Impianto ed evoluzione del tessuto urbano*, L'Arciere, Cuneo, 183-189 (1989).

Chen, X.Q., Huang, R.F., Sun, J., Chen, S.P., Ruan, M.L., "Morphology of multipleliquid phase separation in iron oxide red glaze and chemical composition of various phases", *J. Chin. Ceram. Soc.*, **12,** 236–242 (1984).

Coentro, S., Da Silva, R., Relvas, C., Ferreira, T., Mirão, J., Pleguezuelo, A., Muralha, V., "Mineralogical Characterization of Hispano-Moresque Glazes: A µ-Raman and Scanning Electron Microscopy with X-Ray Energy Dispersive Spectrometry (SEM-EDS) Study", *Microsc Microanal*, **24** [3], 300-309 (2018).

Coentro, S., Lima, A.M., Silva, A.S., Pais, A.N., Mimoso, J.M., Muralha, V.S.F., "Pigments and pigment mixtures in Portuguese 17th century Azulejos", *J. Eur. Ceram. Soc.*, **32** [1], 37-48 (2012).

Coutinho, M.L., Veiga, J.P., Alves, L.C., Mirão, J., Dias, L., Lima, A.M., Muralha, V.S., Macedo, M.F, " Characterization of the glaze and in-glaze pigments of the nineteenth-century relief tiles from the Pena National Palace, Sintra, Portugal", *Applied Physics A*, 122-696 (2016).

Coll Conesa, J., Pérez, J., Pradell, T., Molera, J., Capelli, C., Blanes, S., Caroscio, M., Di Febo, R., "La loza negra de Manises hallada en El barri dels Obradors", in *Actas del XIX Congreso de la Asociación de Ceramología* 2016, Museo de la terrissa de Quart, Girona, 171-196 (2017).

Colomban, P., "Polymerization degree and Raman identification of ancient glasses used for jewelry, ceramic enamels and mosaics", *Journal of Non-Crystalline Solids*, **323** [1], 180–187 (2003).

Colomban, P., "The Destructive/Non-Destructive Identification of Enamelled Pottery, Glass Artifacts and Associated Pigments—A Brief Overview", in Arts, Vol. 2, No. 3, 77-110 (2013).

Colomban, P., Liem, N. Q., Sagon, G., Tinh, H. X., Hoành, T. B., "Microstructure, composition and processing of 15th century Vietnamese porcelains and celadons", *JCH* , **4** [3], 187–197 (2003).

Colomban, P., Milande, V., Le Bihan, L., "On-site Raman analysis of Iznik pottery glazes and pigments", *Journal of Raman Spectroscopy*, **35** [7], 527–535 (2004).

Colomban, P. and Prinsloo, L.C., "Optical spectroscopy of silicates and glasses", in J. Yarwood, R. Douthwaite and S. Duckett (Eds.), *Spectroscopic properties of inorganic and organometallic chemistry*, Vol. 40, Cambridge: RSC Publishing, 128–50 (2009).

Colomban, P., Sagon, G., Faurel, X., "Differentiation of antique ceramics from the Raman spectra of their coloured glazes and paintings", *J. Raman Spectrosc*., **32**, 351-360 (2001).

Colomban, P. and Slodzyck A., "Raman intensity: an important tool to study the structure and phase transitions of amorphous/crystalline materials", *Opt Mater*., **31**, 1759–1763 (2009).

Colomban, P. and Treppoz, F, "Identification and differentiation of ancient and modern European porcelains by Raman macro and micro-spectroscopy", *J Raman Spectrosc*., **32**, 93–102 (2001).

Colomban, P. and Truong, C.," Non-Destructive Raman Study of the Glazing Technique in Lustre Potteries and Faience (9^{th}–14^{th} centuries): Silver Ions, Nanoclusters, Microstructures, and Processing", *Journal Raman Spectrosc*., **35**, 195–207 (2004).

Dadea, M., "La cerámica a Taches Noires a Cagliari", in *Atti XXVII Convegno Internazionale della Ceramica* 1993, Centro Ligure per la Storia della Ceramica, All'insegna del Giglio, 295-299 (1994).

De Lucas, M., Moncada, F., Rosen, J., "Micro-Raman study of red decorations in French faiences of the 18th and 19th centuries", *Journal of Raman Spectroscopy*, **37**, 1154–1159 (2006).

Dent Glasser, L.S. and Smith, I.B., "Oriented transformations in the system MnOeH2O", *Mineral. Mag.*, **36**, 976-987 (1968).

Di Febo, R., La ceràmica de Barcelona entre els segles XIII i XVIII a través de la seva caracterització arqueomètrica. El paper de l'anàlisi petrogràfica, PhD Thesis, University of Barcelona, Barcelona, Spain (2016), https://tesisenred.net/handle/10803/400557.

Di Febo, R., Casas, L., Capelli, C., Cabella, R., Vallcorba, O., "Catalan Imitations of the Ligurian Taches Noires Ware in Barcelona (18th–19th Century): An Example of Technical Knowledge Transfer", *Minerals*, **8** [5] (2018).

Dik, J., Hermens, E., Peschar, R., Schenk, H., "Early production recipes for lead antimonate yellow in Italian art", *Archaeometry*, **47** [3], 593–607 (2005).

Fiocco, C. and Gherardi, G., "Mastro Giorgio, il Lustro di Gubbio e L'Istoriato del Ducato d'Urbino", in G.C. Bojani (Ed.), Mastro Giorgio da Gubbio: Una Carriera Sfolgorante, (1998).

Foy, D., Richez, F., Vallauri, L., "La céramique en usage dans l'atelier de Verrier de Roquefeuille (Pourrières, Var): exemple d'un dépotoir domestique de la première moitié du XVIIIe siècle", *Archeologie du Midi Medieval*, **IV**, 135- 149 (1986).

Freestone, I. C., "Application and potential of electron probe micr-analysis in technological and provenance investigations of ancient ceramics, Archaeometry, **24** [2], 99–116 (1982).

Freestone, I. and Middleton, A, "Mineralogical applications of the analytical SEM in archaeology", *Mineral Mag*, **51**, 21-31 (1987).

Fries, M. and Steele, A., Raman Spectroscopy and Confocal Raman Imaging in Mineralogy and Petrography, in T. Dieing, O. Hollricher and J. Toporski J. (Eds), *Confocal Raman Microscopy*, Springer Series in Optical Sciences, Springer, Berlin, Heidelberg, vol. 158 (2010).

Fukang, Z., "Techical studies of Changsha ceramics", *Archeomaterials*, **2**, 83-92 (1987).

Ghiribelli, B., Frezzotti, M.L., Palmeri, R., "Coesite in eclogites of the Lanterman Range (Antarctica): Evidence from textural and Raman studies", *EJM* , **14** [2], 355–360 (2002).

Goldstein, J. I., Newbury, D. E., Joy, D. C., Lyman, C. E., Echlin, P., Lifshin, E., Sawyer, L. C., Michael, J. R., Scanning Electron Microscopy and X-ray Microanalysis, 3rd edn, Kluwer Academic/Plenum, New York, (2003)

Gómez, A., Gil, C., Di Febo, R., Molera, J., "Casa Convalescència (Vic, Osona): Aproximació arqueològica i arqueomètrica a un conjunt de vasos ceràmics del segle XVIII", in *III Jornades d'Arqueologia de la Catalunya Central*, Roda de Ter, 70-81 (2015).

Greene, K., "Late Hellenistic and early Roman invention and innovation: the case of lead-glazed pottery", *American Journal of Archaeology*, **111**, 653–671 (2007).

Gutiérrez Neira, C., Pradell, T., Molera, J., Smith, A., Climent-Font, A., Tite, M., "Color and Golden Shine of Silver Islamic Luster", *JACS*, **93**, 2320–2328 (2010).

Hatcher, H., Kaczmarczyk, A., Scherer, A., Symonds, R.P., "Chemical Classification and Provenance of Some Roman Glazed Ceramics." American Journal of Archaeology, **98** [3], 431 (1994).

Henshaw, C. M., "Early Islamic Ceramics and Glazes of Akhsiket, Uzbekistan", PhD Thesis, University College of London (2010).

Herbst, W. and Hunger, K., "Industrial organic pigments: production, properties, applications", 3rd completely revised ed. Federal Republic of Germany: Wiley VCH, (2004).

Iñañez, J., Madrid Fernández, M., Molera, J., Speakman, R., Pradell, T., "Potters and pigments: Preliminary technological assessment of pigment recipes of American majolica by synchrotron radiation micro-X-ray diffraction (Sr-μXRD)", *Journal of Archaeological Science*, **40**, 1408–1415, 2013.

Jiazhi, L., "The evolution of Chinese pottery and porcelain technology", in Kingery, W.D. (Ed.), *Ancient technology to Modern science*, American Ceramic Society, Columbus, 135-162 (1984).

Kaindl, R., Tropper, P., Deibl, I., "A semi-quantitative technique for determination of CO2 in cordierite by Raman spectroscopy in thin sections, *EJM* , **18** [3], 331–335 (2006).

Kingery, W. D. and Aronson, M., "On the technology of Renaissance maiolica glazes", *Faenza*, **5**, 226 –35 (1990).

Kingery, W.D. and Vandiver, P.B., "An Islamic Lusterware from Kashan", in *Ceramic Masterpieces: Art, Structure and Technology*, Free Press, NewYork, 111–121(1986).

Kock, L. D. and De Waal, D., "Raman analysis of ancient pigments on a tile from the Citadel of Algiers", *Spectrochimica Acta Part A: Molecular and Biomolecular Spectroscopy*, **71**[4], 1348–1354 (2008).

Leon, Y., Lofrumento, C., Zoppi, A., Carles, R., Castellucci, E. M., Sciau, P., "Micro-Raman investigation of terra sigillata slips: a comparative study of central Italian and southern Gaul productions", *J. Raman Spectrosc.*, **41**, 1550-1555 (2010).

Lightbown, R., Caiger-Smith, A., Cipriano Piccolpasso's The Three Books of the Potter's Art. Editions la revue de la céramique et du verre, Vendin-le-Vieil (2007).

Llusar, M., Forés, A., Badenes, J.A., Calbo, J., Tena, M.A., Monrós, G., "Colour analysis of some cobalt-based blue pigments", *J. Eur. Ceram. Soc.*, **21**, 1121–1130 (2001).

Long, L. and Richez, F., "L'épave Grand-Conglué 4", in V. Abel and H. Amouric, (Coords.), *Un goût d'Italie, Céramiques et céramistes italiens en Provence du Moyen Âge au XXème siècle*, Catalogue de l'exposition, Narration, Aubagne, 93-95 (1993).

Mason, R. and Tite, M.S., "The beginnings of tin opacification of pottery glazes", *Archaeometry*, **39**, 41-58 (1997).

Mattei, P. and Cecchetti, T., Mastro Giorgio, L'Uomo, L'Artista, L'Imprenditore, Camera di Commercio, Industria, Artigianato e Agricoltura di Perugia, Todi, Italy, (1995).

Milanese, A., Biagini, M., Ventura, D., "La ceramica a Taches noires: un indicatore dell'archeologia

postmedievale mediterranea, in *Atti del XXVII Convegno Internazionale della Ceramica 1993*, Centro Ligure per la Storia della Ceramica, All'insegna del Giglio, 337-354 (1994).

Molera, J., "Evolució mineralògica i interacció de les pastes càlciques amb els vidrats de plom: implicacions arqueomètriques", Unpublished Ph.D thesis, Universitat de Barcelona (Spain) (1996).

Molera, J., Bayes, C., Roura, P., Crespo, D., Pradell, T., "Key parameters in the production of medieval luster colors and shines", *J Am Ceram Soc*., **90**, 2245-2254 (2007).

Molera, J., Coll, J., Labrador, A., Pradell, T., "Manganese brown decorations in 10th to 18th century Spanish tin glazed ceramics", *App. Clay Sci*, , **82** 86-90 (2013).

Molera, J., Mesquida, M., Pérez-Arantegui, J., Pradell, T., Vendrell, M., "Lustre Recipes from a Medieval workshop in Paterna", *Archaeometry*, **43**[4], 455–460 (2001).

Molera, J., Pradell, T., Martínez-Manent, S., Vendrell-Saz, M., "The growth of sanidine crystals in the lead glazes of hispano-moresque pottery", *Appl. Clay Sci*., **7**, 483–491 (1993).

Molera, J., Pradell, T., Salvado, N., Vendrell-Saz, M., "Interactions between clay bodies and lead glazes", *J Am Ceram Soc.*, **84** [5], 1120-1128 (2001).

Molera, J., Pradell, T., Salvadó, N., Vendrell-Saz, M, "Evidence of Tin Oxide Recrystallization in Opacified Lead Glazes", *J Am Ceram Soc*., **82,** 2871–2875 (1999).

Molina, G., Odin, G. P., Pradell, T., Shortland, A. J., Tite, M. S., "Production technology and replication of lead antimonate yellow glass from New Kingdom Egypt and the Roman Empire", *Journal of Archaeological Science*, **41**, 171–184 (2014).

Moussette, M., "La poterie d'Albisola en Amérique du Nord", in V. Abel and H. Amouric. (Coords.), *Un goût d'Italie, Céramiques et céramistes italiens en Provence du Moyen Âge au XXème siècle*, Catalogue de l'exposition, Narration, Aubagne, 98-99 (1993).

Muan, A., "Phase equilibria in the system manganese oxide-SiO2 in air", *Am. J. Sci*., **257**, 297-315 (1959).

Muan, A. and Somiya, S., "The system iron oxide-manganese oxide in air", *Am. J. Sci*., **260**, 230-240 (1962).

Navarro Palazón, J., "Murcia como Centro Productor de Loza Dorada", in *La Ceramica Medievale nel Mediterraneo Occidentale*, Edizioni all'Insegna del Giglio, Firenze, Italy, 129-143 (1986).

Nigra, B. T., Faull, K. F., Barnard, H., "Analytical Chemistry in Archaeological Research", *Analytical Chemistry*, **87** [1], 3–18 (2015).

Olsen, S.L., Scanning electron microscopy in archaeology, Oxford: British Archaeological Reports (1998).

Orlova, L. A., "Types and compositions of crystalline glazes (A review)", *Glass and Ceramics* (English Translation of Steklo I Keramika), **56**, 177–180 (1999).

Padeletti, G. and Fermo, P., "Italian Renaissance and Hispano-Moresque lustre-decorated majolicas: imitation cases of Hispano-Moresque style in central Italy", *Applied Physics A*, **77**, 125–133 (2003).

Padeletti, G., Fermo, P., Bouquillon, A., Aucouturier, M., Barbe, F., "A new light on a first example of lustred majolica in Italy", *Applied Physics A*, **100**, 747–761 (2010).

Padeletti, G., Ingo, G.M., Bouquillon, A., Pages-Camagna, S., Aucouturier, M., Roehrs, S., et al. "First-time observation of Mastro Giorgio masterpieces by means of non-destructive techniques", *Applied Physics A*, **83**, 475–83 (2006).

Pérez-Arantegui, J., Molera, J., Larrea, A., Pradell, T., Vendrell-Saz, M., "Some Aspects of the Characterization of Decorations on Ceramic Glazes", *Applied Physics A*, **79** [2], 235–239, (2001).

Pérez-Arantegui, J., Montull, B., Resano, M., Ortega, J.M., "Materials and technological evolution of ancient cobalt-blue-decorated ceramics: Pigments and work patterns in tin-glazed objects from Aragon (Spain) from the 15th to the 18th century AD.", *J. Eur. Ceram. Soc*., **29**, 2499-2509 (2009).

Petrucci, J., "Céramiques provençales et albisolaises du 18éme au Canadà", in *Atti X Convegno Internazionale della Ceramica* 1976, Centro Ligure per la Storia della Ceramica, All'insegna del Giglio, 269-276 (1977).

Pishch, I. V. and Rotman, T. I, "Processes in forming silicate pigments", *Glass and Ceramics*, **46** [5], 207-209 (1989).

Pradell, T., Climent-Font, A., Molera, J., Zucchiatti, A., Ynsa, M., Roura, P., Crespo, D., "Metallic and nonmetallic shine in luster: An elastic ion backscattering study", *Journal of Applied Physics*, **101** [10], 103518-103518 (2007).

Pradell, T., Molera, J., Bayés, C., Roura, P., "Luster decoration of ceramics: Mechanisms of metallic luster formation", *Applied Physics A*, **83**, 203–208 (2006).

Pradell, T., Molera, J., Salvadó, N., Labrador, A., "Synchrotron radiation micro-XRD in the study of glaze technology", *App. Phys. A*, **99** [2] 407-417 (2010).

Pradell, T., Molera, J., Smith, A., Climent-Font, A., Tite, M., "Technology of Islamic Lustre", *Journal of Cultural Heritage*, **9**, (2008).

Pradell, T., Molera, J., Vendrell, M., Pérez-Arantegui, J., Pantos, E., Roberts, M., DiMichiel, M., "Role of Cinnabar in Luster Production", *J Am Ceram Soc*, **87**, 1018-1023 (2004).

Pradell, T., Molina, G., Molera, J., Pla, J., Labrador, A., "The use of micro-XRD for the study of glaze color decorations", *App. Phys. A*, **111** [1] 121-127 (2013).

Pradell, T., Molina, G., Murcia, S., Ibáñez, R., Liu, C., Molera, J., Shortland, A. J., "Materials, Techniques, and Conservation of Historic Stained Glass Grisailles", *International Journal of Applied Glass Science*, **7** [1], 41–58 (2015).

Quinn, P.S., Interpreting Silent Artefact: Petrographic Approaches to Archaeological Ceramics. Archaeopress Oxford, (2009).

Quinn, P.S., Ceramic Petrography: The Interpretation of Archaeological Pottery & Related Artefacts in Thin Section, Archaeopress, Oxford (2013).

Raskovska, A., Minceva-Sukarova, B., Grupce, O., Colomban, P., "Characterization of pottery from Republic of Macedonia II. Raman and infrared analyses of glazed pottery finds from Skopsko Kale", *J Raman Spectrosc.*, **41**, 431–439 (2010).

Reedy, C.L., “Image Analysis-Aided Light Microscopy of Glazed Ceramics: Identifying Technological Innovation and Style”, *Studies in Conservation*, **57**, S227–233 (2013).

Reedy, C. L., “Petrographic and Image Analysis of Thin Sections of Classic Wares of Song Dynasty” in S. Ningchang and M. Jianmin (Eds.), *Proceedings of International Symposium on Science and Technology of Five Great Wares of the Song Dynasty*, 390-381(2016).

Ricciardi P, Colomban P, Tournié, A, Milande, V., “Nondestructive on-site identification of ancient glasses: genuine artefacts, embellished pieces or forgeries?”. *J Raman Spectrosc*., **40**, 604–617 (2009).

Roisine, G., Capobianco, N., Caurant, D., Wallez, G., Bouquillon, A., Majérus, O., Gerbier, A., “The art of Bernard Palissy (1510–1590): influence of firing conditions on the microstructure of iron-coloured high-lead glazes, *Applied Physics A*, **123**, (2017).

Roqué, J., Molera, J., Sciau, P., Pantos, E., Vendrell-Saz, M., “Copper and silver nanocrystals in lustre lead glazes: Development and optical properties”, *Journal of the European Ceramic Society*, **26** [16], 3813–3824 (2006).

Roy, S., “Mineralogy of the different genetic types of manganese deposits”, Econ. Geol., **63**, 760-786 (1968).

Sakellariou, K., Miliani, C., Morresi, A., Ombelli, M., “Spectroscopic Investigation of Yellow Majolica Glass”, *Journal of Raman Spectroscopy*, **35**, 61–67 (2004).

Sandalinas, C., Ruiz-Moreno, S., López-Gil, A., Miralles, J., “Experimental confirmation by Raman spectroscopy of a Pb–Sn–Sb triple oxide yellow pigment in sixteenth-century Italian pottery”, *Journal of Raman Spectroscopy*, **37**, 1146–1153 (2006).

Sendova, M., Zhelyaskov, V., Scalera, M., Gulliford, C., “Micro-Raman spectroscopy characterization of Della Robbia Glazes”, *Archaeometry*, **49** [4], 655–64 (2007).

Smith, G.D. and Clark, R.J.H., Raman microscopy in art history and conservation science. Reviews in Conservation, **2**, 92–106 (2001).

Spitzer-Aronson, M., “Laser, X-ray Microfluorescence and Microscopic Studies of Metallic Luster on Ancient Overglazed Ceramics”, in J. S. Olin and M. J. Blackman (Eds.), *Proceedings of the 24th International Archaeometry Symposium* (Washington, DC, 1984), Smithsonian Institute Press, Washington, DC, 419-429 (1986).

Tite, M. S., “The Impact of Electron Microscopy on Ceramic Studies”, *Proceedings of the British Academy*, **22**, 111–131 (1992).

Tite, M.S.,“The production technology of Italian maiolica: a reassessment”, *Journal of Archaeological Science* , **36**, 2065–2080 (2009).

Tite, M.S., Freestone, I., Mason, R., Molera, J., Vendrell-Saz, M., Wood, N., “Lead glazes in antiquity- Methods of production and reasons for use”, *Archaeometry* **40** [2], 241-260 (1998).

Tite, M.S. and Shortland, A.J., “Production Technology of Faience and Related Early Vitreous Materials”, Monograph 72, Oxford University School of Archaeology, Oxford (2008).

Vandiver. P.B. and Kingery, W.D., “Song Dynasty celadon glazes from Dayo near Longquan”, in S. Chao (Ed.), *Scientific and Technological Insights on Ancient Chinese Pottery and Porcelain: Proceeding of the International Conference on Ancient Chinese Pottery and Porcelain*, Beijing: Shanghai Institute of Ceramics, 187-191 (1986).

Vieira Ferreira, L. F., Casimiro, T. M., Colomban, P., “Portuguese tin-glazed earthenware from the 17th century. Part 1: Pigments and glazes characterization”, *Spectrochimica Acta Part A: Molecular and Biomolecular Spectroscopy*, **104**, 437-444 (2013a).

Vieira Ferreira, L. F., Ferreira Machado, I., Ferraria, A. M., Casimiro, T. M., Colomban, P., “Portuguese tin-glazed earthenware from the 16th century: A spectroscopic characterization of pigments, glazes and pastes”, *Applied Surface Science*, **285**, 144-152 (2013b).

Viti, C., Borgia, I., Brunetti, B., Sgamellotti, A., Mellini, M., “Microtexture and microchemistry of glaze and pigments in Italian Renaissance pottery from Gubbio and Deruta, *JCH.*, **4**, 199-210 (2003).

Vogel, W., Chemistry of glass, in N. Kreidel (Ed.), American Ceramic Society, Westerville, OH, (1985).

Waal, D., “Micro-Raman and portable Raman spectroscopic investigation of blue pigments in selected Delft plates (17^{th} –20^{th} century)”, *Journal of Raman Spectroscopy*, **40**, 2162–2170 (2009).

Wainwright, I. N. M. R., Taylor, J. M., Harley R. D., Lead antimonate yellow, in R. L. Feller (Ed.), Artists’ pigments: a handbook of their history and characteristics, Cambridge University Press, Cambridge, UK/National Gallery of Art, Washington, DC, Vol. 1, (1986).

Weyl, W.A., Coloured Glasses, Society of Glass Technology, Sheffield (1976).

Wopenka, B., Popelka, R., Pasteris, J. D., Rotroff, S., “Understanding the Mineralogical Composition of Ancient Greek Pottery through Raman Microprobe Spectroscopy”, *Applied Spectroscopy*, **56** [10], 1320–1328 (2002).

Ylla Català, M., “Els pots de farmàcia de l’hospital de la Santa Creu de Vic”, *Ausa XX*, **150**, 725-738 (2002).

Zucchiatti, A., Bouquillon, A., Katona, I., D’Alessandro, A., “The Della Robbia blue: a case study for the use of cobalt pigments in ceramics during the Italian renaissance”, Archaeometry, **48**, 131–152 (2006).

Zuo, J., Changsui, W., Cunyi, X., “Non-Destructive In-Situ Study of White and Black Coating on Painted Pottery Sherds From Bancun Site (Henan, China) by Raman Microscopy”, *Spectroscopy Letters*, **31** [7], 1431-1440 (1998).

Annex 1

Glossary of terms

Aventurine glaze. It is the generic name used for lead free or low-lead glazes containing macroscopic laminar crystals, which cause a sparkling decorative effect.

Biscuit. It refers to a pottery that has been fired but not yet glazed. This can be a final product such an unglazed earthenware, often called terracotta, or, most commonly, an intermediary stage in a glazed final product.

Ceramic Interface. Reaction layer that can develops during the firing between a ceramic body and a covering layer (glaze, slip, enamel).

Devitrification. Process by which glassy substances change their structure into that of crystalline solids due to weathering processes.

EPMA. Electron Probe Micro-Analyser.

Glaze. Special slip applied to pottery that produces, on firing, an impermeable, glossy surface. It is made from finely ground mixtures of mineral and man-made powders and other compounds which provide colour, opacity and character desired visually. The glaze mixture is suspended in water and applied to ware by painting, dipping, or spraying. Ancient glazes must contain silica (SiO_2) plus a flux agent in order to lower the melting temperature of the silica. A number of compounds can be used as flux agents including lead, tin, sodium and potassium. Lead oxide is the strongest flux in pottery, it gives an attractive shine by increasing the refractive index of glazes. Glaze may also contain metal oxides as colorants, and various alumina (Al_2O_3) compounds, which help stabilize the glaze and bind it to the surface of the ceramic.

Ceramic. It is constituted by a body of mineral origin, which may be wet shaped, and which is afterwards fired resulting in a stone like synthetic material.

Majolica. Majolica is a type of pottery in which an earthenware clay body is covered with an opaque white glaze (traditionally a glaze including tin), then painted with stains or glazes and fired.

Opacifier. A substance that, when added to a glaze, transforms a transparent glaze into an opaque one. A very common opacifier is the tin oxide (SnO_2) which can be used alone or in association with other particles, such as quartz and/or feldspars to obtain an opaque surface.

µ-Raman. Micro-Raman.

OM. Optical Microscopy.

Overglaze. In this procedure, a pigment is applied over the glaze surface before firing.

Oxidation Atmosphere. An atmosphere in a kiln where there is sufficient supplies of oxygen to interact with the glaze and clay body surfaces. Oxidation glazes are typically more brightly coloured than reduction ones, especially at lower temperatures.

Petrographic Thin Section. A laboratory preparation of a rock, mineral, soil, pottery, metal sample for use with a polarizing petrographic microscope, electron microscope and electron microprobe. A thin chips cut from the sample with a diamond saw is ground and mounted on a glass slide and then ground smooth using progressively finer abrasive grit until the sample is only 30 µm thick.

Pigment. The term "pigment" comes from the Latin *pigmentum* and it meaning "drug". A pigment is a finely divided, insoluble material that is suspended in a medium and acts as a colouring agent. The adequate dispersion of the pigment throughout the medium is important for achieving an intense and uniform colour. Natural resins, glues, animal tallow, blood, casein, eggs, urine, oils, wax, and human saliva have all been used as a medium for pigments. Pigments can be either organic or inorganic, naturally occurring or artificial. In pigments, colour is based on the wavelengths absorbed as well as the size, shape, and texture of the grains. The degree of hydration in the pigment can also influence colour as well as the preparation of the pigment (e.g. an overgrinding may produce a less intense colour). Pigments used in ceramics are micro and nano-precipitates of compounds that either do not dissolve or recrystallize in the glassy matrix. Depending on the use, pigments may be used straight and just mixed with water, but they are more commonly added as colorants in clay bodies and glazes.

PPL. Plane polarized light (refers to the optical microscope).

Reduction Atmosphere. A reduction atmosphere is produced in a fuel fired kiln by reducing the draft and depriving the kiln of oxygen. This diminished level of oxygen causes incomplete combustion of the fuel and raises the level of carbon inside the kiln. The loss of oxygen results in a change in the colour of the glazes because it allows the metals in the glaze to be seen in an unoxidized form. A reduction atmosphere can also affect the colour of the clay body, mostly if iron is present in the clay body.

RL. Reflected light (refers to the optical microscope).

Saggar. A refractory box or container that protects ware from flames and ashes or creates a local atmosphere for the ware during firing.

SEM. Scanning electron microscopy.

TL. Transmitted light (refers to the optical microscope).

Underglaze. In this procedure, a pigment is applied to the surface of pottery before glazing.

SR-μXRD. Synchrotron-radiation X-ray micro-diffraction.

XPL. Crossed polarized light (refers to the optical microscope).

Annex 2

Petrography features of crystalline phases identified in this Thesis

<u>Mattheddleite,</u> $Pb_{10}(SiO_4)_{3.5}(SO_4)_2Cl_2$

Member of: Ellestadite Group > Apatite Supergroup
Crystal System: Hexagonal
Space Group: $P6_3/m$
Type: Uniaxial (-)
Surface Relief: Very High
RI values: n_ω= 2.017 n_ε= 1.999
Max Birefringence: δ = 0.018
Cleavage: Poor/Indistinct
on {0001}, or a parting

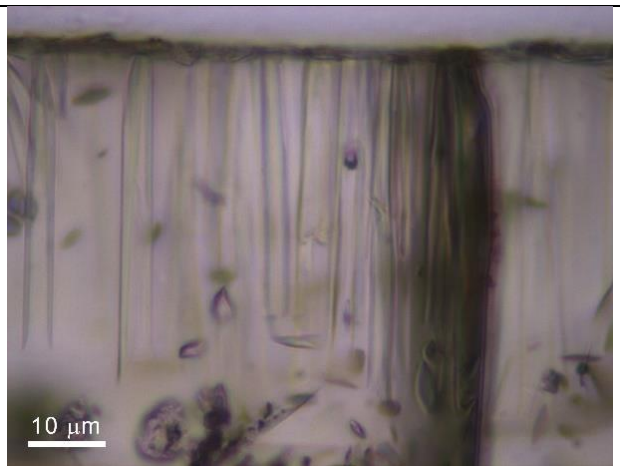

Figure 1. PPL (plane polarized light) mode: elongated, vertical tabular crystals of mattheddleite, colourless in transmitted light. Mattheddleite crystals exhibit medium relief because are embedded inside lead glazes

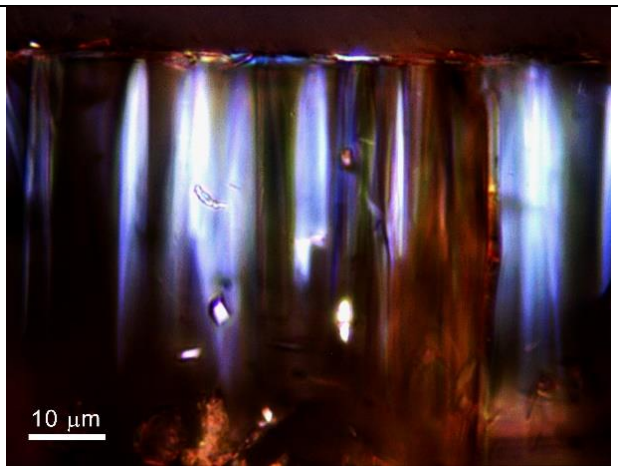

Figure 2. The same area as Figure 1 in XPL (crossed polarized light) mode: mattheddleite crystals show 1st order interference colors and straight extinction. In this picture the polarizers are at 45º instead of normal poalirising position in order to show the maximum interference colours in vertical crystals

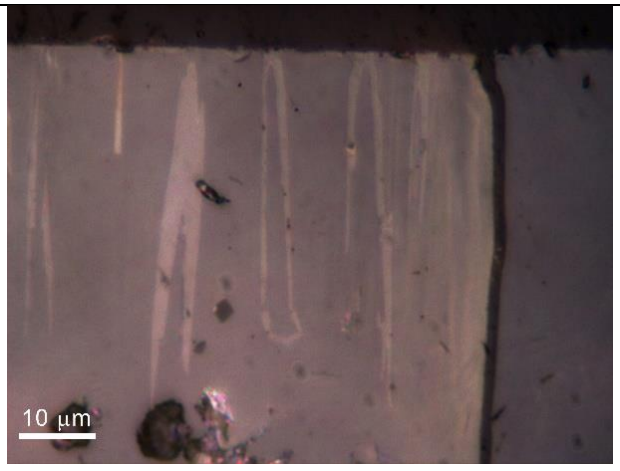

Figura 3. The same area as Figure 1 in RL (reflected light) mode. Matheddleite shows white reflectivity inside lead glazes

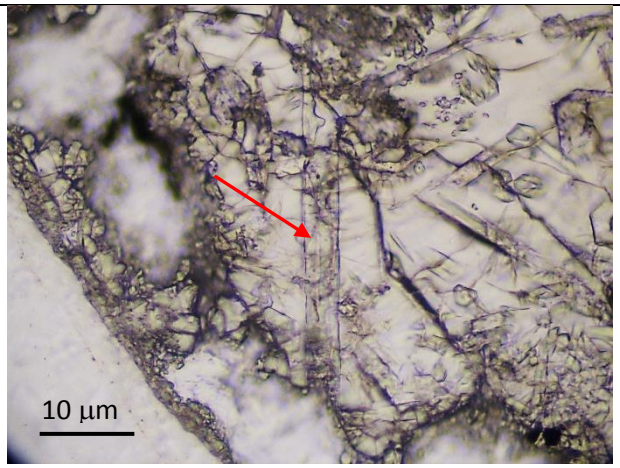

Figure 4. Vertical mattheddleite crystal in PPL (plane polarized light) mode marked with an arrow

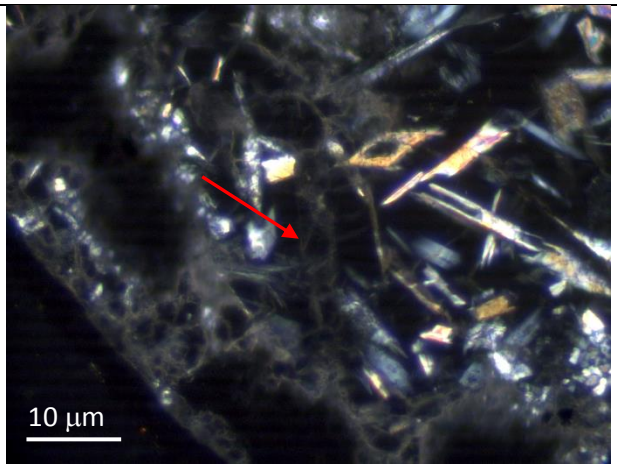

Figure 5. The same area as Figure 4 in XPL (crossed polarized light) mode. In this picture the polarizers are in normal position and vertical mattheddleite crystal marked with an arrow is completely extincted. Crystals with high birefingence correspond to lanarkite

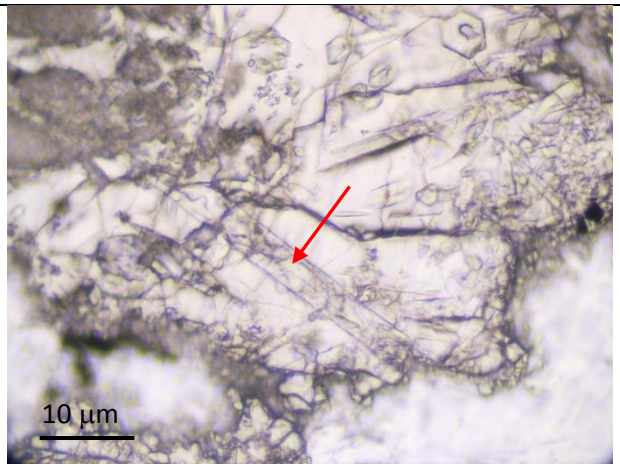

Figure 6. Mattheddleite crystal in PPL (plane polarized light) mode marked with an arrow

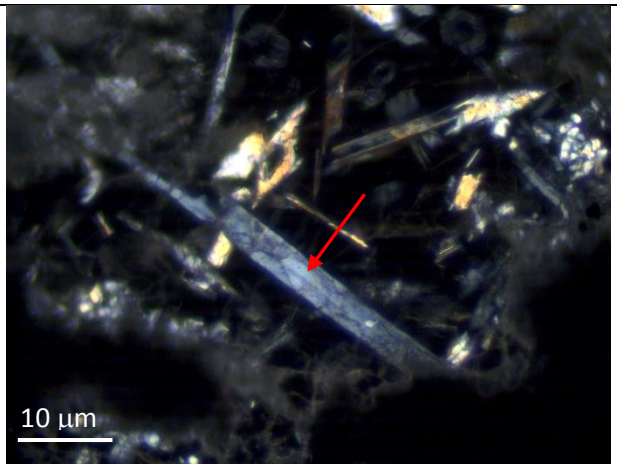

Figure 7. The same area as Figure 6 in XPL (crossed polarized light) mode. Mattheddleite crystal exhibits grey interference colours

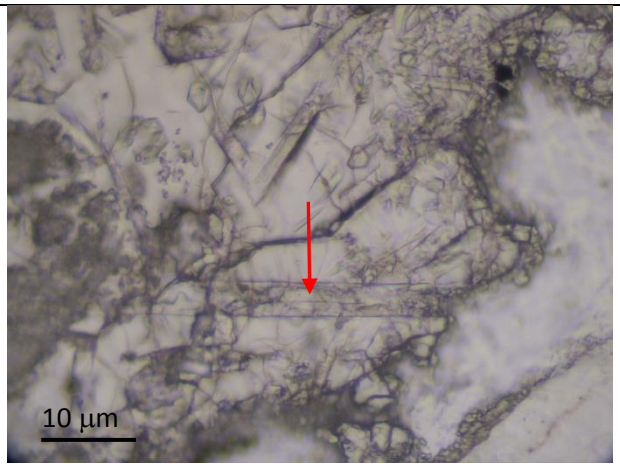

Figure 8. Horizontal mattheddleite crystal in PPL (plane polarized light) mode

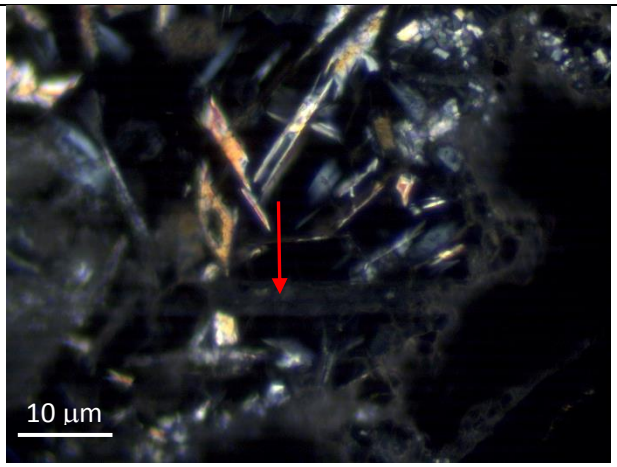

Figure 9. The same area as Figure 8 in XPL (crossed polarized light) mode. The horizontal mattheddleite crystal exhibits straight extinction

Lanarkite, $PbO \cdot PbSO_4$

Crystal System: Monoclinic
Space Group: *B*2/*m*
Type: Biaxial (-)
Surface Relief: Very High
RI values: n_α= 1.928n_β= 2.007n_γ= 2.036
Max Birefringence: δ = 0.108 (fourth order rand above)
Cleavage: Perfect
Perfect on {-201}, imperfect on {-402} and {201}; also on {010}
Twinning: Polysynthetic in zone [010], but rare

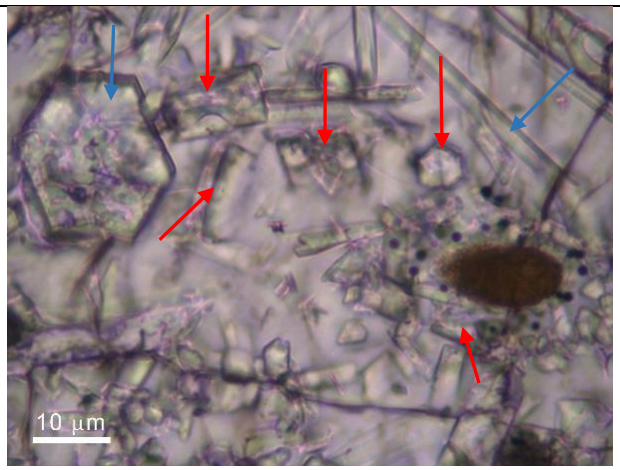

Figure 10. PPL (plane polarized light) mode: tabular colourless lanarkite crystals in transmitted light (marked with red arrows). Elongated matthedleite crystals and hexagonal basal sections are marked with blue arrows. An opaque sphalerite grain is also visible in the picture surrounded by lanarkite crystals

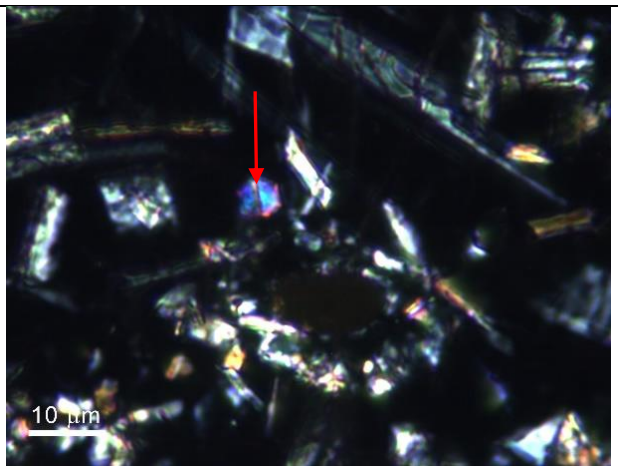

Figure 11. Similar area as Figure 10 in XPL (crossed polarized light) mode: lanarkite crystals exhibit 2nd/3rd order interference colors and inclined extinction. The red arrow shows a twinned crystal of lanarkite

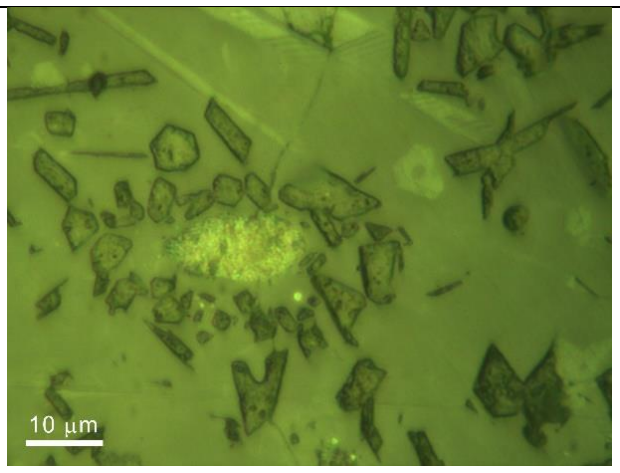

Figure 12. Similar area as Figure 11 in RL (reflected light) mode: lanarkite crystals around sphalerite grain. Lanarkite crystals exhibit low reflectivity while matthedleite shows white reflectivity.

Figure 13. Lanarkite crystals in RL (reflected light) mode

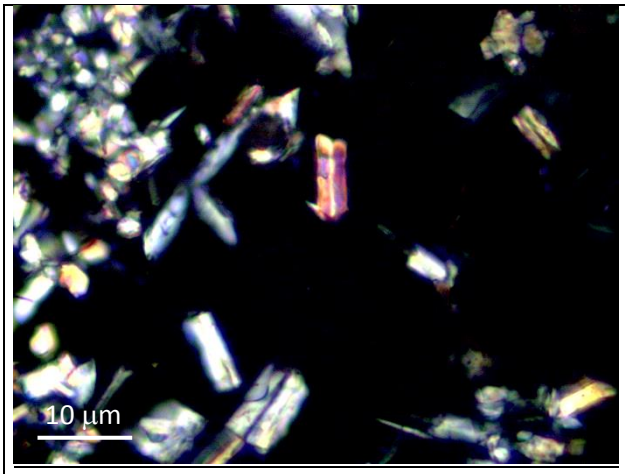

Figure 14. The same area as Figure 13 in XPL (crossed polarized light) mode. Lanarkite crystals exhibit twinning and high birefringence

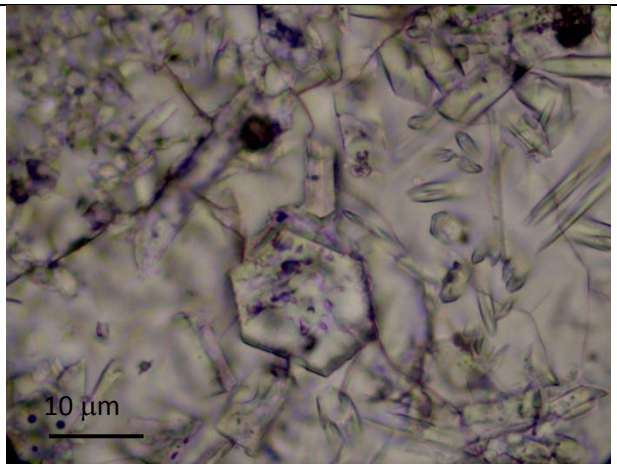

Figure 15. The same area as Figure 14 in PPL (plane polarized light) mode. The hexagonal crystal corresponds to a basal section of matthedleite

Figure 16. RL (reflected light) mode: grey crystals correspond to lanarkite, white crystals to matthedleite, yellowish grain to sphalerite and the very high reflectance grain at the bottom of the picture corresponds to galena

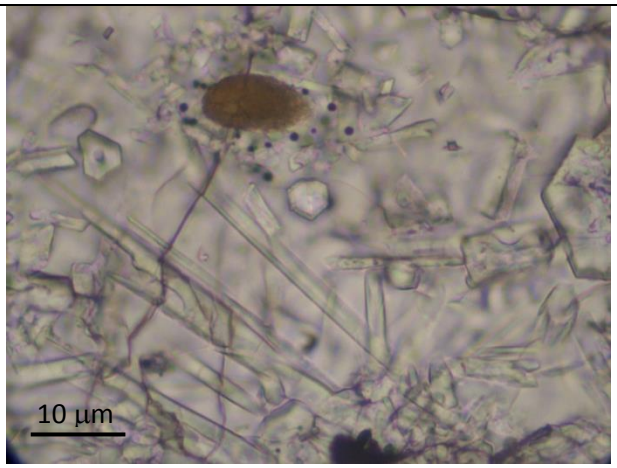

Figure 17. The same area as Figure 16 in PPL (plane polarized light) mode

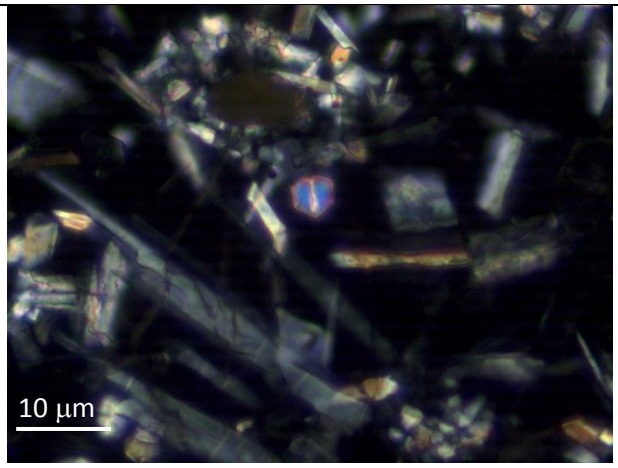

Figure 18. The same area as Figure 16 in XPL (crossed polarized light) mode

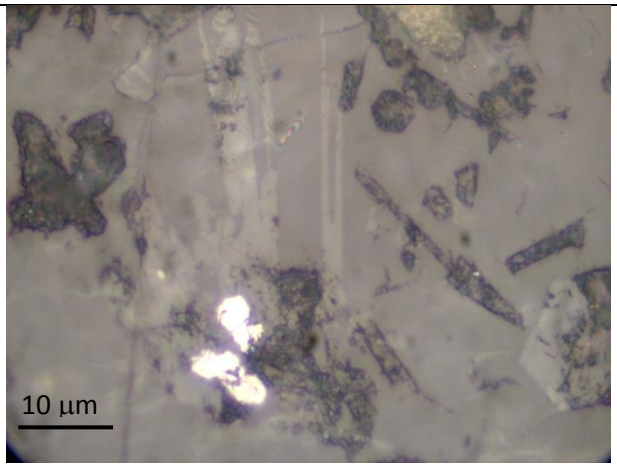

Figure 19. RL (reflected light) mode: grey crystals correspond to lanarkite, white crystals to matthedleite and the very high reflectance crystals correspond do galena grains

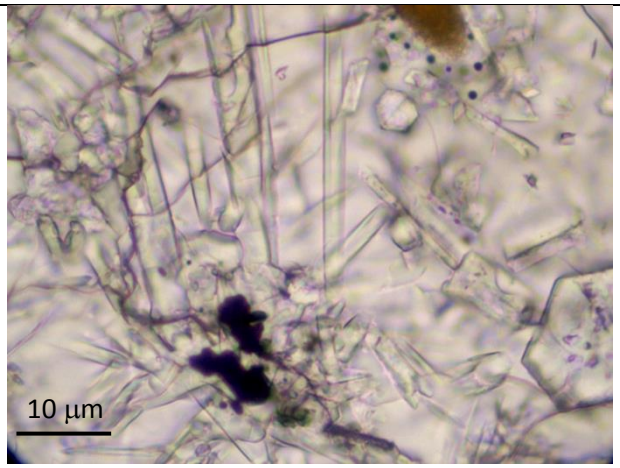

Figure 20. The same area as Figure 19 in PPL (plane polarized light) mode

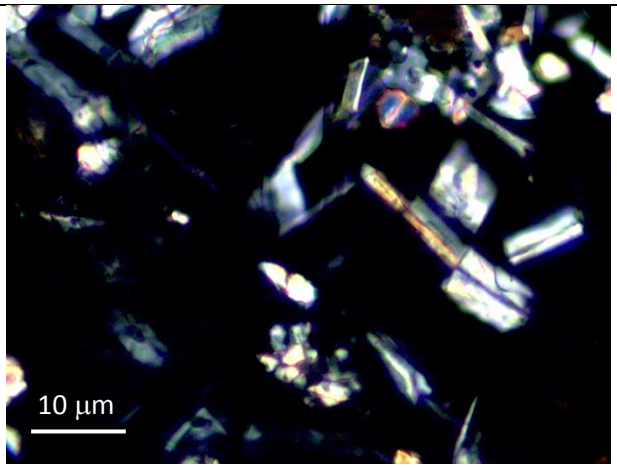

Figure 21. The same area as Figure 19 in XPL (crossed polarized light) mode

Cristobalite, SiO_2

Crystal System: Tetragonal
Space Group: $P4_1\,2_1\,2$
Type: Uniaxial (-)
Surface Relief: Moderate
RI values: n_ω= 1.487n_ε= 1.484
Max Birefringence: δ = 0.003 very low
Twinning: on {111} (paramorphs of cubic β-Cristobalite twins)

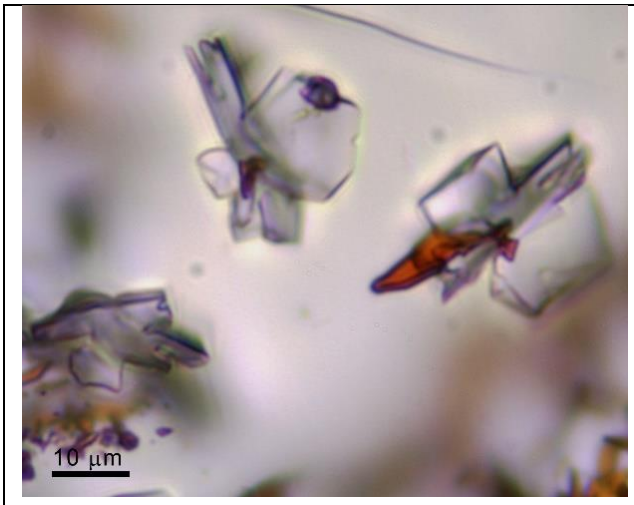

Figure 22. PPL (plane polarized light) mode: euhedral, subhedral crystals of cristobalite, most commonly dendritic to skeletal, colourless in transmitted light. Red crystals are hematite

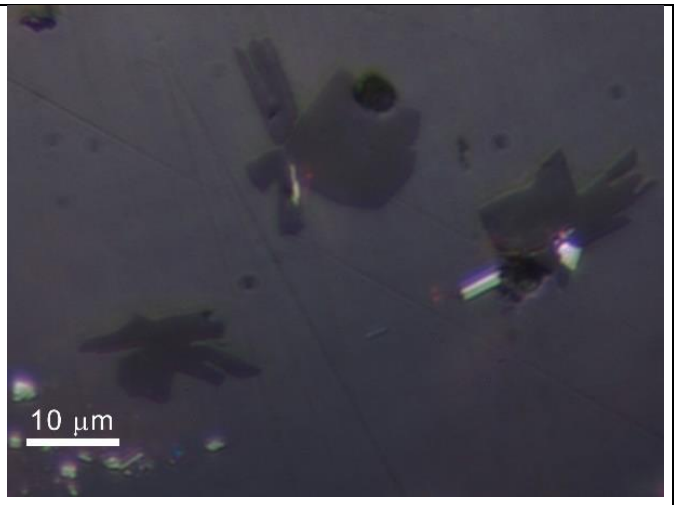

Figure 23. The same area as Figure 22 in RL (reflected light) mode: cristobalite crystals show a grey colour and low relief

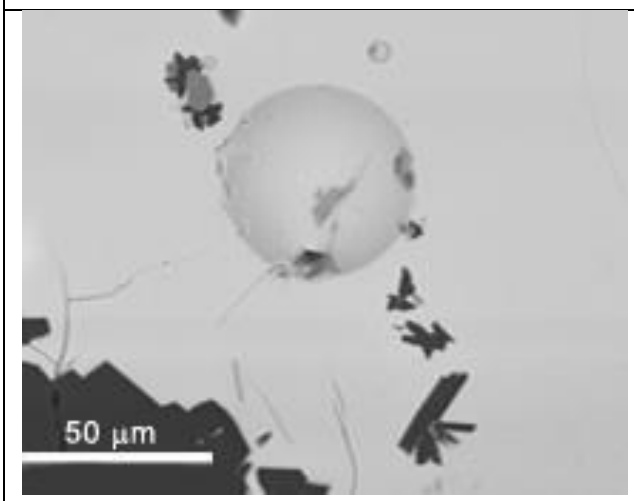

Figure 24. SEM-BSE image. Cristobalite crystals grown around hematite (light tinge) exhibit a dark colour in backscattering image

Hematite, Fe_2O_3

Crystal System: Trigonal
Space Group: *R*3*c*
Type: Uniaxial (-)
Surface Relief: Very High
RI values: n_ω= 3.150 - 3.220 n_ε = 2.870 - 2.940
Max Birefringence: δ = 0.280
Cleavage: None Observed
Twinning: Penetration twins on {0001}, or with {1010} as a composition plane. Frequently exhibits a lamellar twinning on {1011} in polished section
Internal Reflections: Red

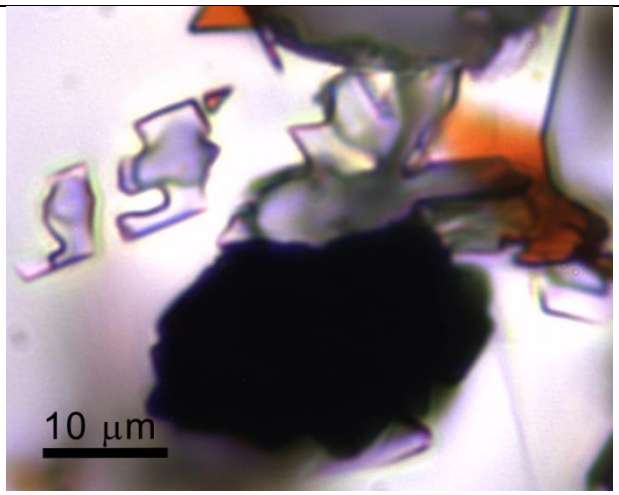

Figure 25. PPL (plane polarized light) mode: opaque, red/orange euhedral, anhedral, tabular, prismatic crystals of hematite (the colourless crystals correspond to cristobalite)

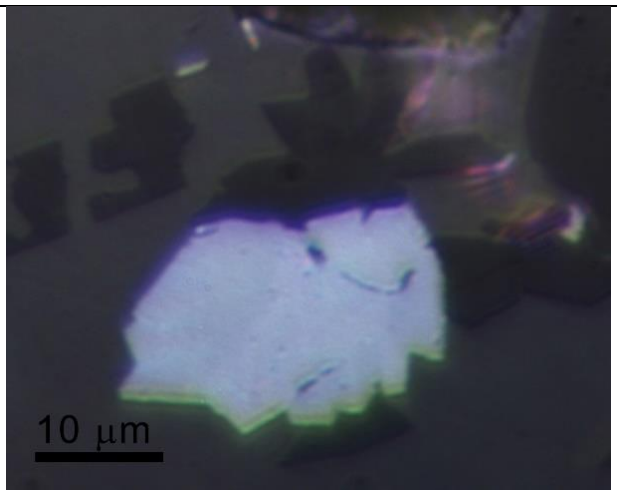

Figure 26. The same area as Figure 25 in RL (reflected light) mode: white to grey-white hematite crystals, with red internal reflections

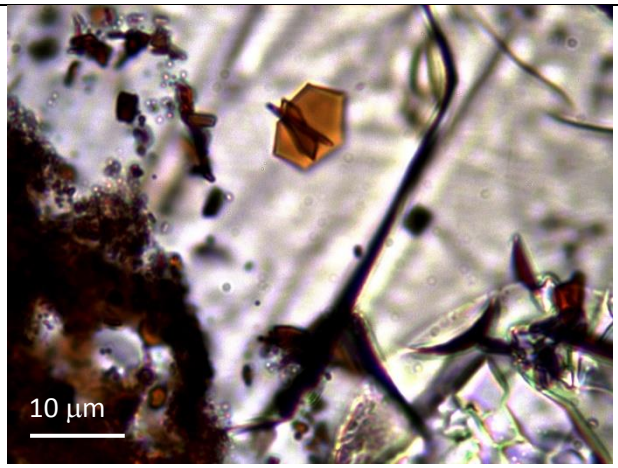

Figure 27. Hematite crystals in PPL (plane polarized light) mode

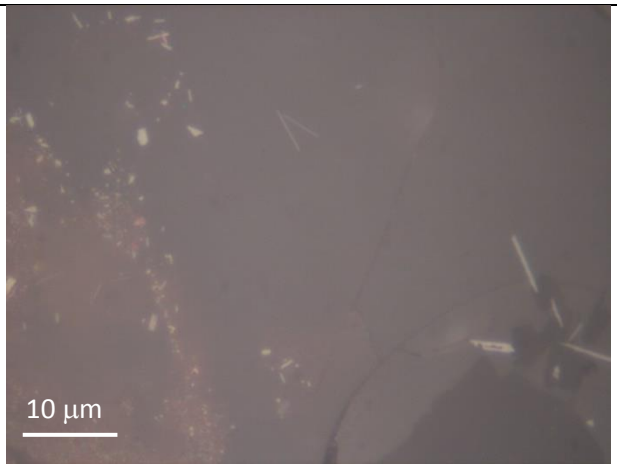

Figure 28. The same area as Figure 27 in RL (reflected light) mode

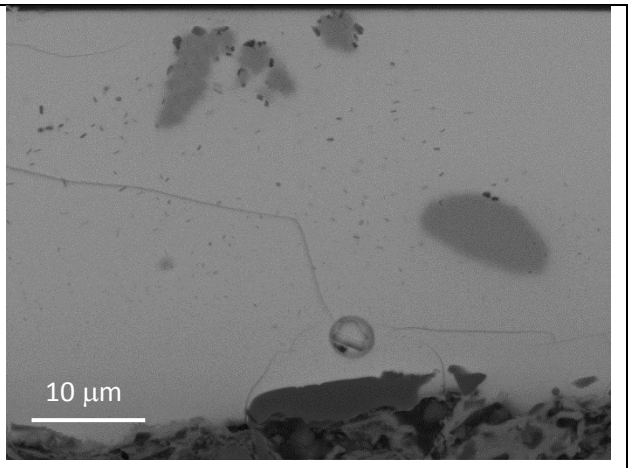

Figure 29. SEM-BSE image. Grey grains of hematite inside lead glaze

<u>Melanotekite,</u> $Pb_2Fe_2Si_2O_9$

Crystal System: Orthorhombic
Space Group: $C2\ 2\ 2_1$
Type: Biaxial (+)
Surface Relief: Very High
RI values: n_α= 2.120 n_β= 2.170 n_γ= 2.310
Max Birefringence: δ = 0.190 δ
Cleavage: Very Good. Two cleavages
Pleochroism: Visible
Optical Extinction: Parallel

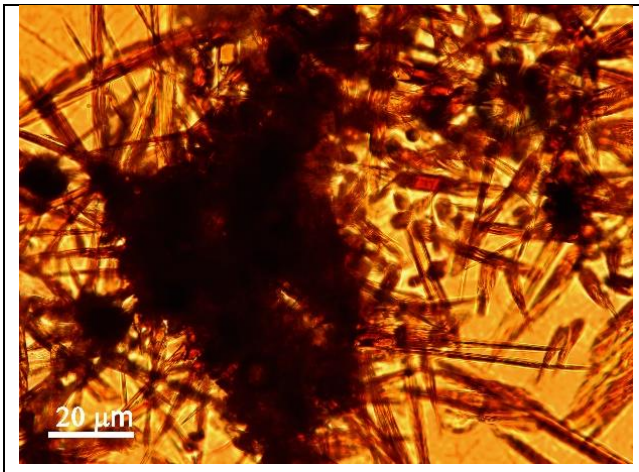

Figure 30. PPL (plane polarized light) mode: honey acicular crystals of melanotekite along with opaque aggregates of hematite

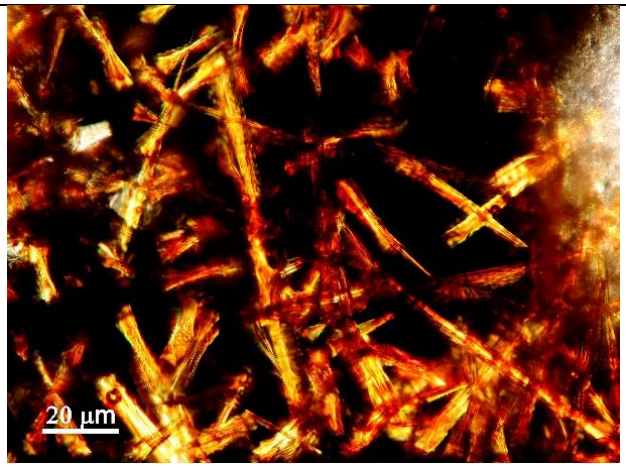

Figure 31. The same image as Figure 30 in XPL (crossed polarized light): melanotekite crystals show yellow/dark orange colours and parallel extinction

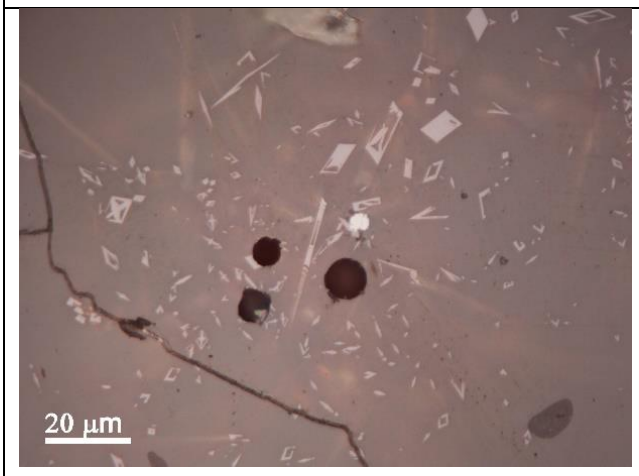

Figure 32. The same area as Figure 30 in RL (reflected light) mode: melanotekite crystals exhibit white to grey-white colours

<u>Kentrolite,</u> $Pb_2Mn_2Si_2O_9$

Crystal System: Orthorhombic
Space Group: *Pbcm*
Type: Biaxial (+)
Surface Relief: Very High
RI values: n_α= 2.100 n_β= 2.200 n_γ= 2.310
Max Birefringence: δ = 0.210
Cleavage: Distinct/Good {110}
Pleochroism: Strong
Optical Extinction: Parallel

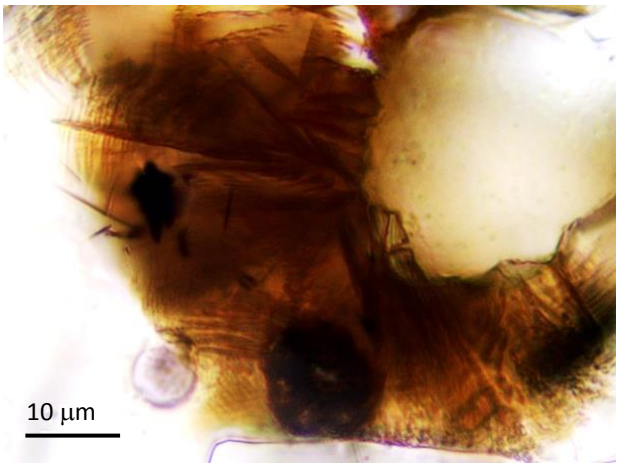

Figure 33. PPL (plane polarized light) mode: brown/ honey acicular crystals of kentrolite

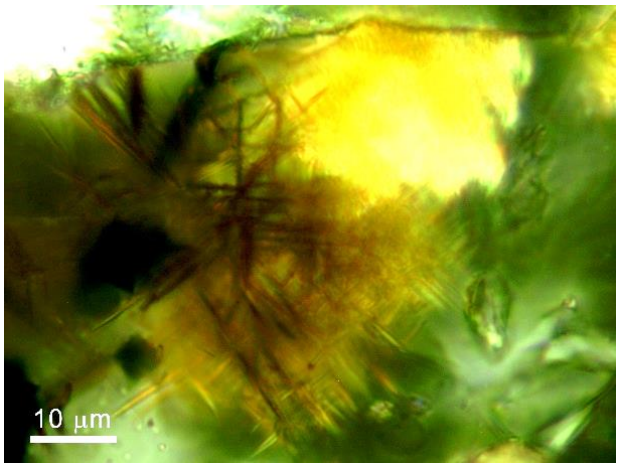

Figure 34. The same area as Figure 33 in XPL (crossed polarized light) mode. Kentrolite crystals show brown/yellowish/honey interference colours and parallel extinction

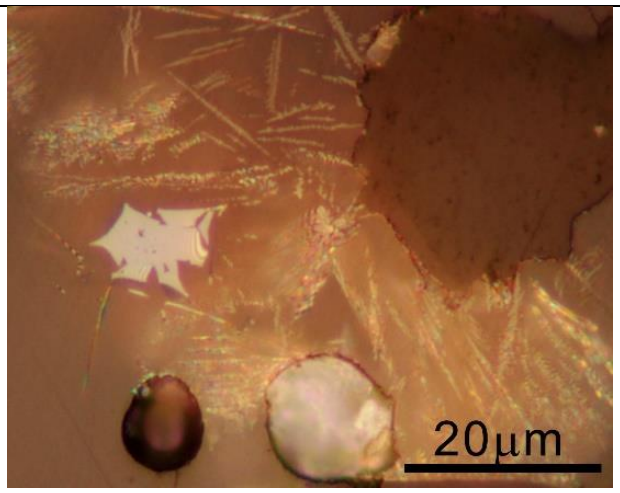

Figure 35. The same area as Figure 33 in RL (reflected light) mode. Kentrolite crystals show greyish colours with many orange and brown internal reflections. White crystal corresponds to braunite

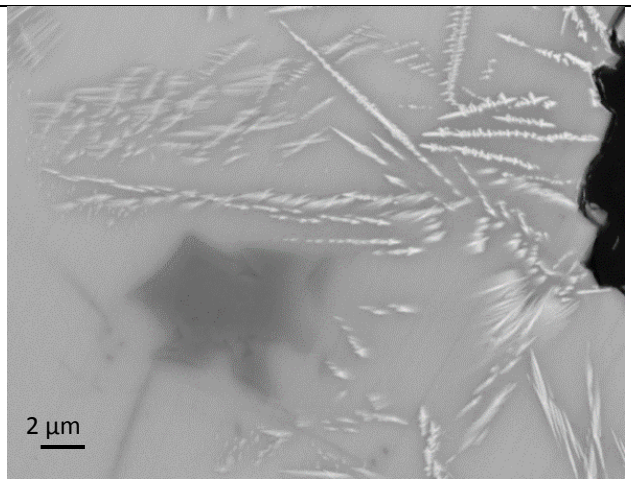

Figure 36. SEM-BSE image. Kentrolite crystals display light colours, while the dark crystal corresponds to braunite

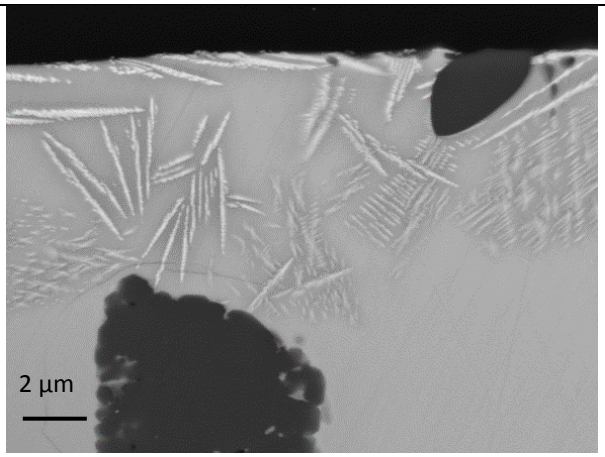

Figure 37. SEM-BSE image of acicular kentrolite crystals near the surface of the glaze

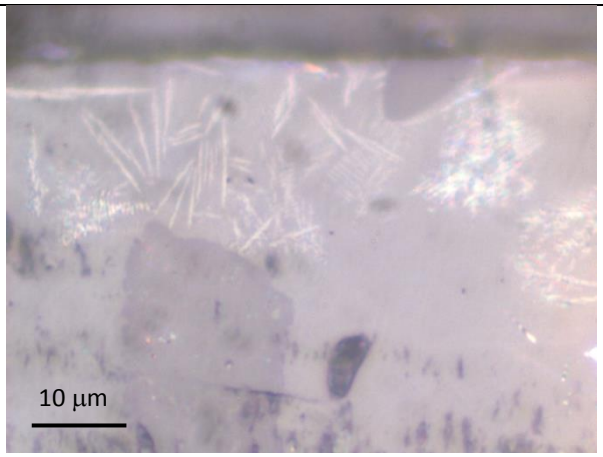

Figure 38. The same area as Figure 37 in RL (reflected light) mode

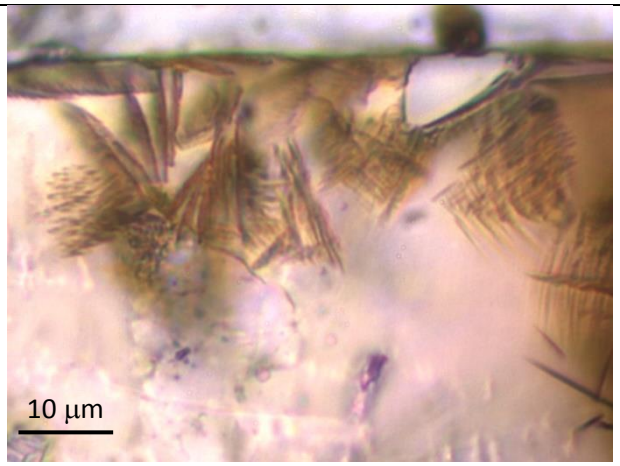

Figure 39. The same area as Figure 37 in PPL (plane polarized light) mode. Kentrolite crystals are light brown

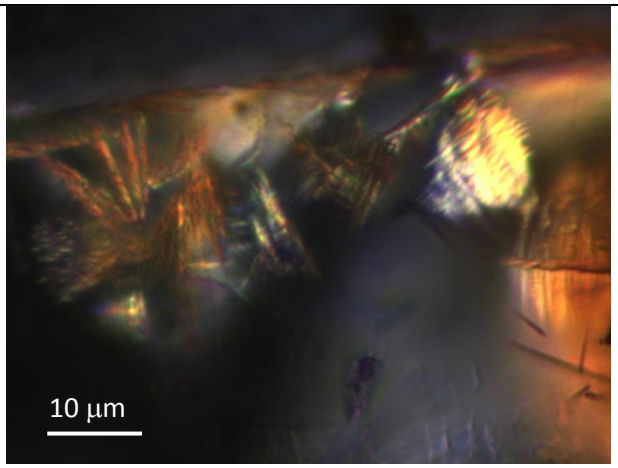

Figure 40. The same area as Figure 39 in XPL (crossed polarized light) mode. Kentrolite crystals exhibit reddish honey interference colours and parallel extinction

Figure 41. Kentrolite crystals in PPL (plane polarized light) mode

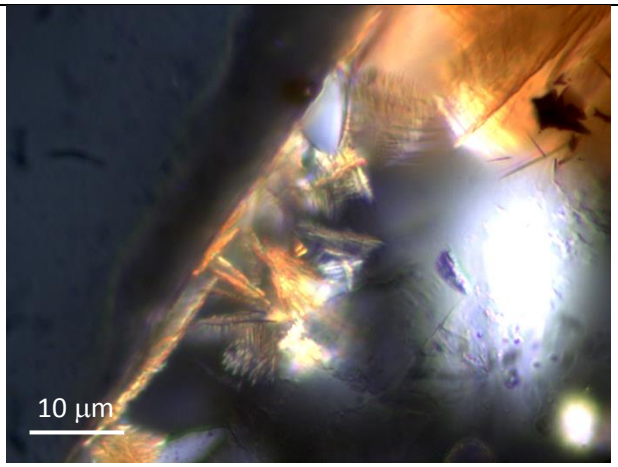

Figure 42. The same area as Figure 41 in XPL (crossed polarized light) mode

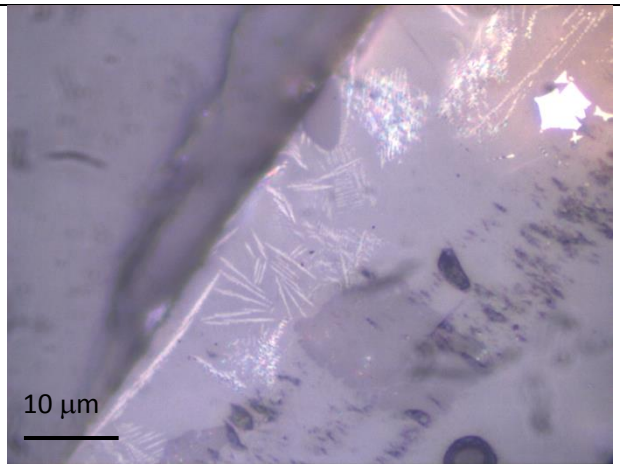

Figure 43. The same area as Figure 41 in RL (reflected light) mode

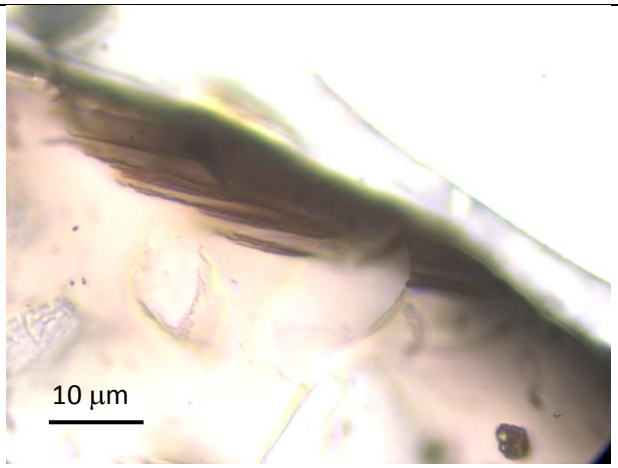

Figure 44. Kentrolite crystals in PPL (plane polarized light) mode

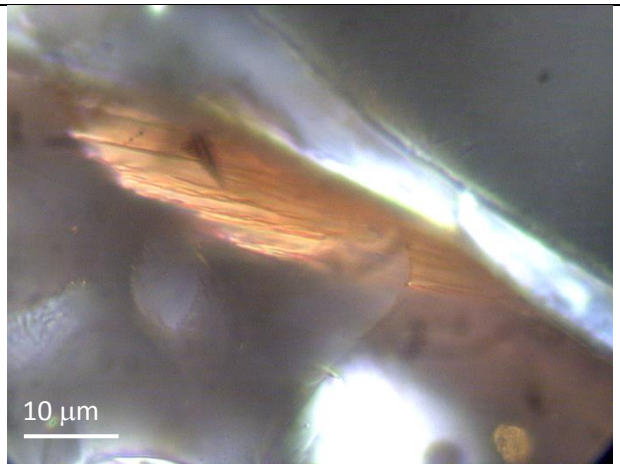

Figure 45. The same area as Figure 44 in XPL (crossed polarized light) mode

Figure 46. The same area as Figure 45 in RL (reflected light) and XPL (crossed polarized light) mode

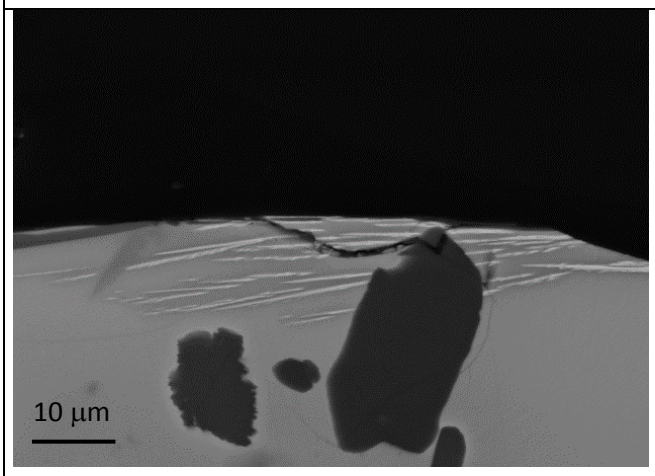

Figure 47. The same area as Figure 45 in SEM-BSE mode

<u>Braunite,</u> $Mn^{2+}Mn^{3+}_6(SiO_4)O_8$

Crystal System*:* Tetragonal
Space Group: $I4_1/acd$
Type: Anisotropic
Cleavage: Perfect
{112} perfect
Colour in reflected light: Grayish white with a brownish tinge
Twinning: On {112} producing a combination with only a small reentrant angle (0°18') on e{011}

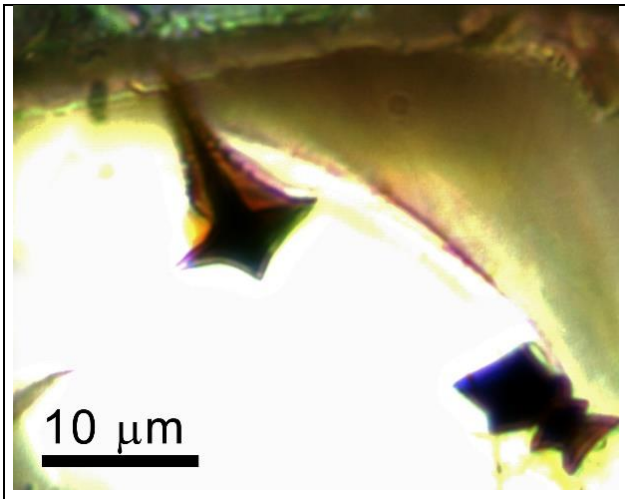

Figure 48. PPL (plane polarized light) mode: dark-brown bipyramidal crystallites of braunite

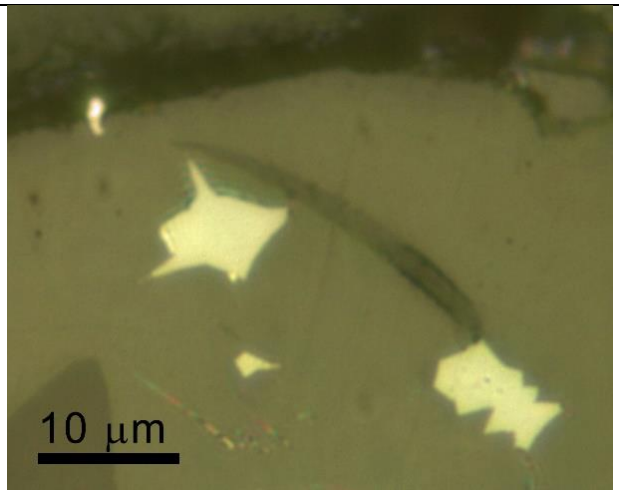

Figure 49. The same area as Figure 48 in RL (reflected light) mode: braunite shows white colours in reflected mode

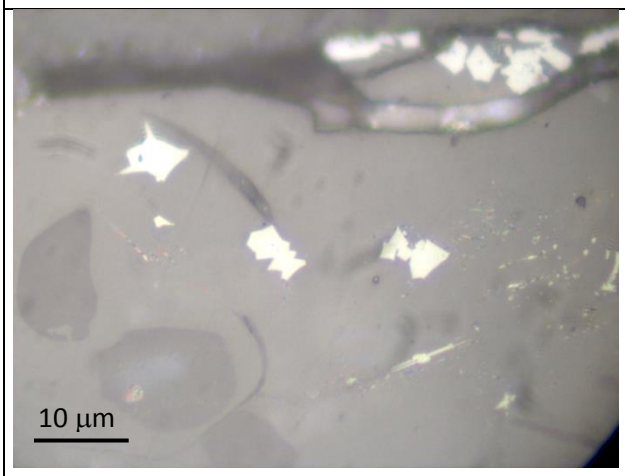

Figure 50. Braunite crystals in RL (reflected light) mode (white crystals)

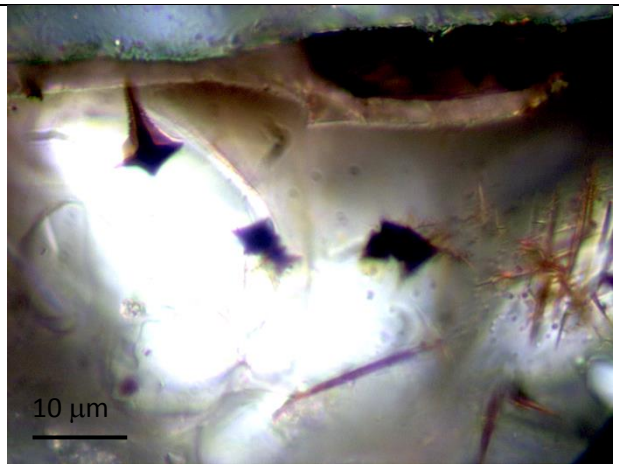

Figure 51. The same area as Figure 50 in XPL (crossed polarized light) mode. Braunite has dark colours in XPL. The illumination has been exagerated in order to show honey acicular crystals of kentrolite and to contrast dark crystals of braunite from dark colour of glass in XPL mode

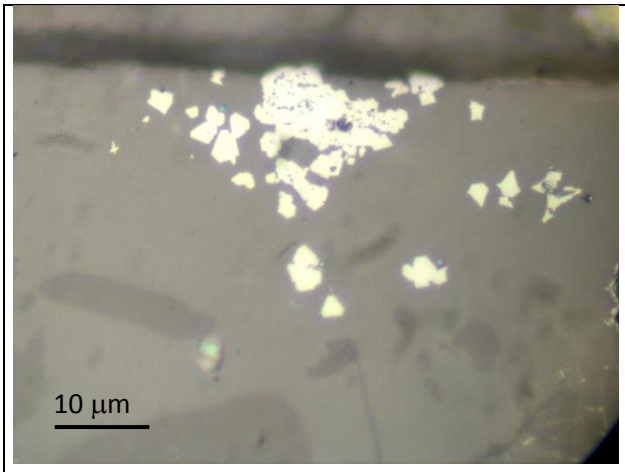

Figure 52. Braunite crystals in RL (reflected light) mode

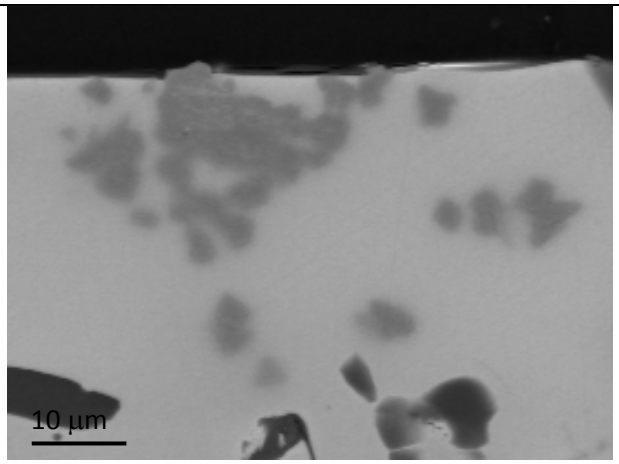

Fig. 53. The same area as Figure 52 in SEM-BSE mode

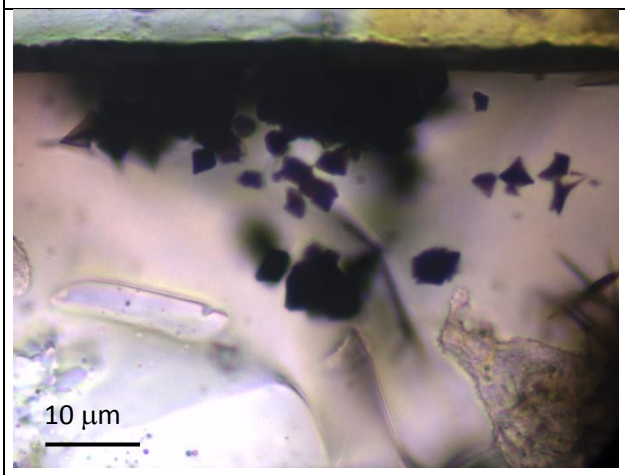

Figure 54. Braunite crystals in PPL (plane polarized light) mode

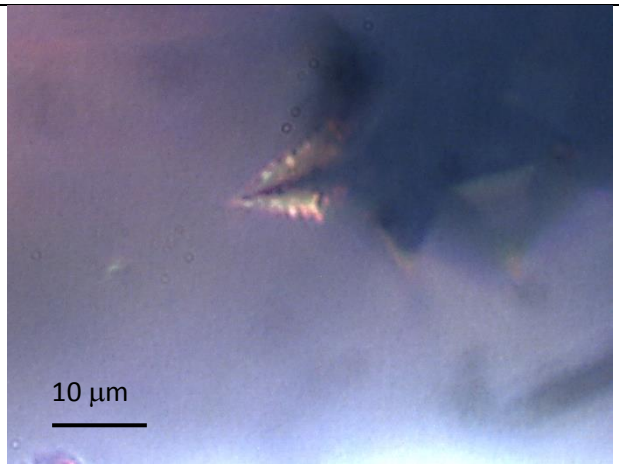

Figure 55. Detail of a dendritic braunite crystal in XPL (crossed polarized light) mode

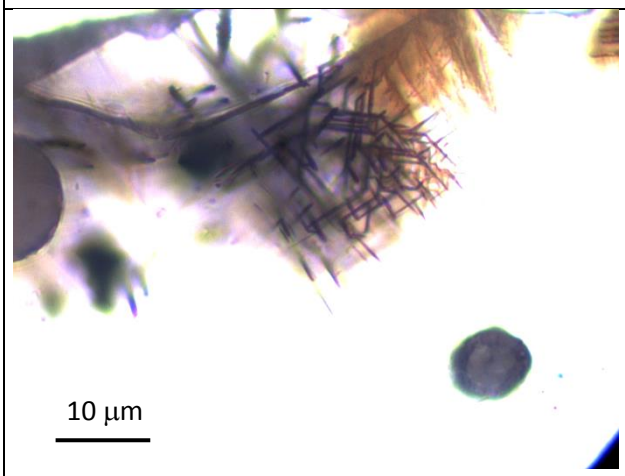

Figure 56. Dendritic braunite crystals in PPL (plane polarized light) mode

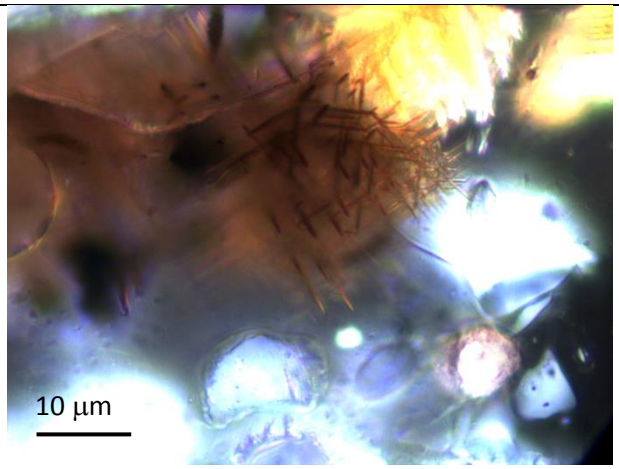

Figure 57. The same area as Figure 56 in XPL (crossed polarized light) mode

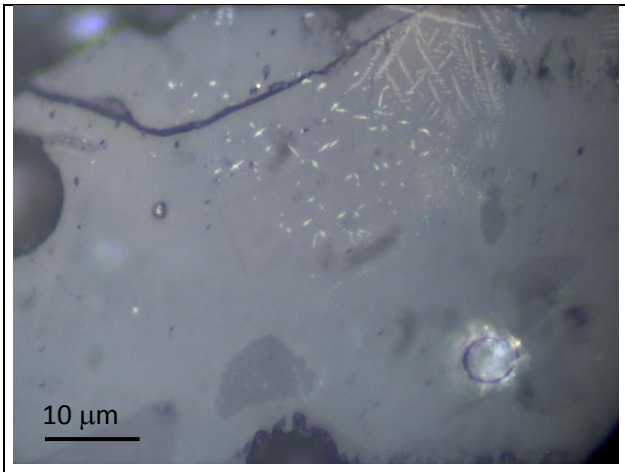

Figure 58. The same area as Figure 57 in RL (reflected light) mode

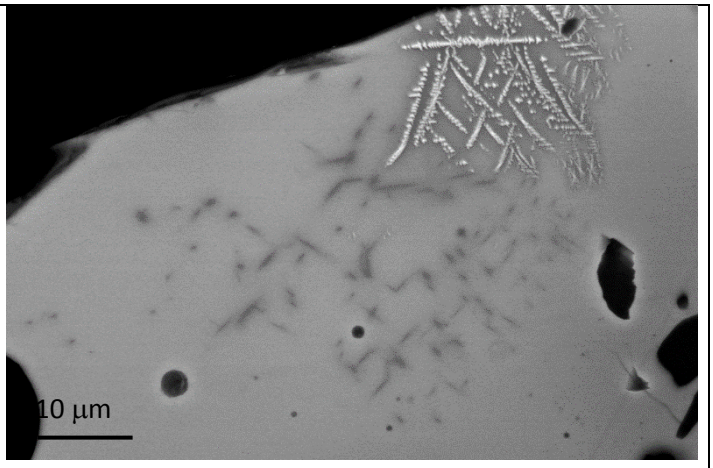

Figure 59. The same area as Figure 58 in SEM-BSE mode

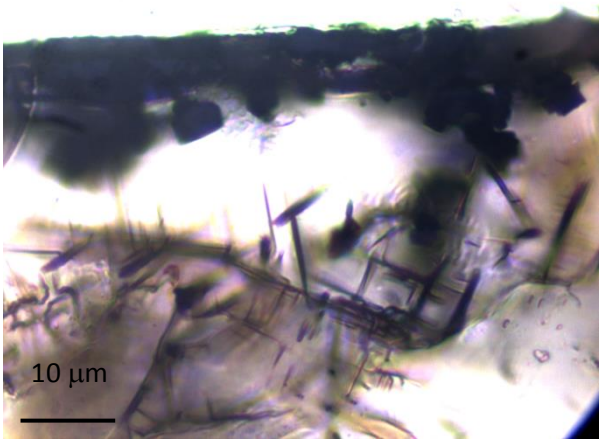

Figure 60. Braunite crystals in PPL (plane polarized light) mode at the top of the glaze and kentrolite crystals at the bottom and central part of the glaze

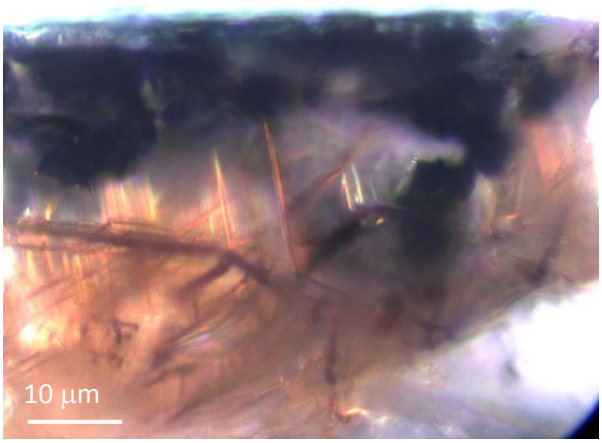

Figure 61. The same area as Figure 61 in XPL (crossed polarized light) mode

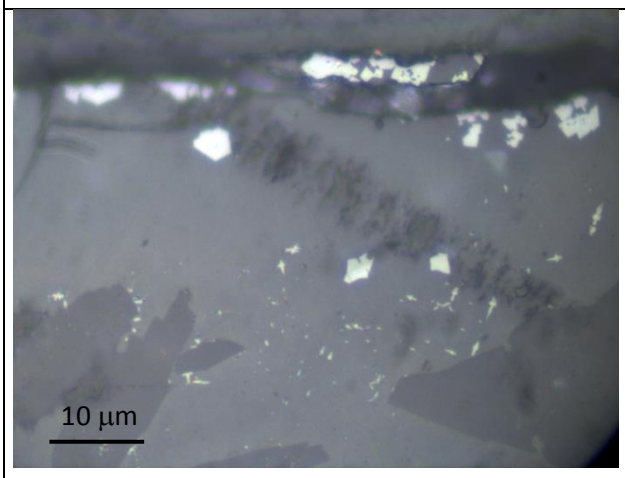

Figure 62. Braunite crystals in RL (reflected light) mode

Annex 3

Other related articles published by R. Di Febo

Anna Gómez, Carles Gil, Roberta Di Febo, Judit Molera (2015). Casa Convalescència (Vic, Osona): Aproximació arqueològica i arqueomètrica a un conjunt de vasos ceràmics del s. XVIII. Actes de les III Jornades d'Arqueologia de la Catalunya Central (2014), pp. 70-81. ISBN 9788439392453.

Jaume Coll Conesa, Josep Pérez Camps, Trinitat Pradell, Judit Molera, Claudio Capelli, Sara Blanes, Marta Caroscio, Roberta Di Febo (2017). La "loza negra" de Manises hallada en el barri dels Obradors. Actas del XIX Congreso de la Asociación de Ceramología, Quart (Girona, 2016), Museo de la terrissa de Quart, Girona, pp.171-196.

Roberta Di Febo, Lluís Casas, Claudio Capelli, Roberto Cabella, Oriol Vallcorba (2018). Catalan imitations of the Ligurian Taches Noires ware in Barcelona (18th -19th century): an example of technical knowledge transfer. *Minerals* **8** (5).